Lead Isotopes and Heavy Metal Concentrations in Galveston Bay Waters, Sediments, and Oysters

---

Final Report

By Dr. Amanda Mulcan Lopez and Dr. Alan Brandon
University of Houston

Jessica Fitzsimmons
Texas A&M University

Frank Ramos
New Mexico State University

Christine Jensen
Texas Parks & Wildlife Department

Submitted to TCEQ September 2021
Contract No. 582-20-10170

Published by the Texas Commission on Environmental Quality, May 2025
AS-511

Prepared for:
Galveston Bay Estuary Program
Texas Commission on Environmental Quality
17041 El Camino Real
Suite 210
Houston, Texas 77058

This project was funded by the Texas Commission on Environmental Quality
and the United States Environmental Protection Agency

By:
Dr. Amanda Mulcan Lopez
Dr. Alan D. Brandon
Department of Earth and Atmospheric Sciences
University of Houston
Houston, TX 77004

In partnership with:
Jessica N. Fitzsimmons
Department of Oceanography
Texas A&M University
College Station, TX 77843

Frank C. Ramos
Department of Geological Sciences
New Mexico State University
Las Cruces, NM 88003

Christine C. Jensen
Coastal Fisheries Division
Texas Parks and Wildlife Department
Dickinson, TX 77539

Suggested citation: Lopez, A. M., Brandon, A. D., Fitzsimmons, J. N., Ramos, F. C., and Jensen, C. C. University of Houston. 2021. Lead (Pb) Isotopes and Heavy Metal Concentrations in Galveston Bay Waters, Sediments and Oysters Final Report. Contract No. 582-20-10170 Galveston Bay Estuary Program. Austin: Texas Commission on Environmental Quality (AS-511).

This project has been funded wholly or in part by the United States Environmental Protection Agency (EPA) under grant number [CE-00655007] to the Texas Commission on Environmental Quality (TCEQ). The contents of this document do not necessarily reflect the views and policies of the EPA, nor does the EPA endorse trade names or recommend the use of commercial products mentioned in this document.

Table of Contents

List of Figures

List of Tables

Abbreviations

Ag	Silver
As	Arsenic
Cd	Cadmium
Cm	Centimeter
cps	Counts per second
Cr	Chromium
Cu	Copper
DL	Detection Limit
EDTriA	Ethylenediaminetriacetic acid
EPA	United States Environmental Protection Agency
Fe	Iron
fg	Femtogram
g	Gram(s)
GBEP	Galveston Bay Estuary Program
HBr	Hydrobromic acid
HDPE	High-density polyethylene
HCl	Hydrochloric acid
Hg	Mercury
HNO3	Nitric acid
HR-ICP-MS	High resolution inductively coupled mass spectrometer
HSC	Houston Ship Channel
IDA	Iminodiacetic acid
In	Indium
kg	Kilogram(s)
km	Kilometer
L	Liter(s)
LCS	Laboratory control standard
m	Meter(s)
MC-ICP-MS	Multi-collector inductively coupled mass spectrometer
µg/g	Micrograms per gram
µL	Microliter
m^3/s	Cubic meters per second -
mg	Milligram
mL	Milliliter
mm	Millimeter(s)
Mn	Manganese
MQ	Milli-Q Ultrapure Water
ng	Nanogram(s)
ng/mL	Nanograms per milliliter
nmol	Nanomole(s)
Ni	Nickel

NIST	National Institute of Standards and Technology
nM	Nanomolar
NMSU	New Mexico State University
NOAA	National Oceanic and Atmospheric Administration
NRCC	National Research Council Canada
Pb	Lead
pg	Picogram(s)
PM	Project manager
ppb	Parts per billion
ppm	Parts per million
ppq	Parts per quadrillion
ppt	Parts per trillion
psu	Practical salinity units
QA	Quality assurance
QAPP	Quality Assurance Project Plan
QAM	Quality assurance manual
QAO	Quality assurance officer
QC	Quality control
QPR	Quarterly Progress Report
RPD	Relative percent difference
RPQ	Retarding Potential Quadrupole Lenses
RSD	Relative standard deviation
Sb	Antimony
SD or σ	Standard deviation
SOP	Standard operating procedure
SOW	Scope of Work
SQuiRTs	Screening Quick Reference Tables
SRM	Standard reference material
TAMU	Texas A&M University
TCEQ	Texas Commission on Environmental Quality
Tl	Thallium
TPWD	Texas Parks and Wildlife Department
UH	University of Houston
µL	Microliter(s)
µg	Microgram(s)
µm	Micron(s)
Zn	Zinc

Executive Summary

The watershed of Galveston Bay encapsulates some of the highest density of petrochemical facilities in the United States. This study investigates heavy metal cycling in Galveston Bay sediments and oysters. The results of this study offer a detailed assessment of Galveston Bay heavy metal geochemistry and provide new insight into heavy metal sources, fluxes, and toxicity in this anthropogenic estuary. Additionally, this study offers the first lead isotope dataset for Galveston Bay and serves as a testbed for future work in this region. This report provides a comprehensive understanding of heavy metal contaminant cycling in Galveston Bay. These data clearly demonstrate that Galveston Bay sediment and water heavy metal concentrations are shaped by riverine input and flocculation dynamics as well as anthropogenic activities. Deeper study of oyster tissue metal contents including biotic and abiotic factors (i.e., age, sex, water temperature, turbidity) is needed to characterize the spatiotemporal controls on oyster tissue heavy metal concentrations in Galveston Bay. Lead isotope tracing reinforces the presence of gasoline-derived and industrial ore-derived lead in Galveston Bay and identifies coal as another anthropogenic metal contaminants source in the bay. Sediments may supply zinc to oysters based on linear correlations between Galveston Bay sediment and oyster tissue metal concentrations. Moreover, Galveston Bay sediment and oyster tissue lead isotope compositions largely overlap, demonstrating that oysters can incorporate metals from ambient sediments. No correlation between water (dissolved fraction) heavy metal contents and oyster tissue heavy metal contents was observed. Future work using oyster tissue, filtered water, and sediment samples collected from the same location and time over multiple sampling events is needed to allow direct spatial and temporal comparison of metal contents between the oysters, waters, and sediments, which would yield a more robust understanding of Galveston Bay oyster tissue metal exchange with ambient waters and sediments. This study highlights the importance of estuaries in regulating heavy metal exchange between terrestrial and marine environments and serves as a testbed for future heavy metal contaminant studies in estuarine systems worldwide as well as a resource for on-going contaminant reduction, remediation, and mitigation efforts in Galveston Bay.

Introduction

The Galveston Bay Estuary Program (GBEP) State of the Bay Report describes the status and trends of the heavy metals cadmium (Cd), copper (Cu), iron (Fe), lead (Pb), manganese (Mn), nickel (Ni), and zinc (Zn) in Galveston Bay (Lester and Gonzalez, 2011). Cd and Pb are biologically non-essential (i.e., not required for metabolism) and toxic even at low concentrations (Wright and Welbourn, 2002). While Cu, Fe, Mn, Zn and possibly Ni are biologically essential, they too become toxic at elevated concentrations (Gomez-Caminero et al., 2001). Exposure to these pollutants has been shown to result in cancer, organ malfunction, cardiovascular disease, reproductive system impairment, neurotoxicity and ultimately death in humans as well as other living organisms (Tchounwou et al., 2012). Marine organisms such as oysters and fish are known to bioaccumulate heavy metals which leads to increased heavy metal exposure levels over time (Boening, 1999; Ip et al., 2007; Shiel et al., 2012). For these reasons, heavy metal contamination of Galveston Bay water and sediments have major potential long-term implications for human and ecosystem health.

The last published study of Galveston Bay heavy metal toxicity is from 1993 (Morse et al. 1993). Significant regulatory and cleanup efforts in Galveston Bay have occurred in the last 25 years, and thus a renewed examination of Galveston Bay water, sediment, and biota heavy metal toxicity is warranted to focus remediation efforts. While heavy metal concentration data highlight areas with elevated pollutant levels, concentration data alone fail to capture the full picture of pollutant sources and mobility (Marcantonio et al., 2000). Pb isotopes provide an efficient fingerprinting method for determining the sources and pathways of pollution because they do not undergo detectable isotope fractionation processes in the natural environment due to their heavy mass (Marcantonio et al., 2000; Komarek et al., 2008; Alyazichi et al., 2016). For this reason, each Pb source possesses its own unique isotopic composition or “fingerprint” by which it can be traced (Komarek et al., 2008). Together the combination of Pb isotopes and heavy metal concentrations are a powerful tool for constraining pollutant sources and fluxes. In this project, heavy metal concentrations were determined for water, sediment, and oyster tissue samples collected in Galveston Bay. Additionally, Pb isotope compositions of the sediment and oyster tissue samples were measured with the goal of determining the current status and potential sources of heavy metal toxins in Galveston Bay. Data generated in this study were compared to the National Oceanic and Atmospheric Administration (NOAA) Screening Quick Reference Tables (SQuiRTs), the TCEQ Texas Surface Water Quality Standards, and the Texas Risk Reduction Program to assess heavy metal toxicity. These data will serve as a guide to regulators and policymakers for ongoing pollution reduction, remediation, and mitigation efforts as well as ecological rehabilitation projects in the area.

Project Significance and Background

Galveston Bay estuary is a mixing zone that exists where terrestrial freshwaters mix with oceanic saltwater from the Gulf of Mexico. Heavy metals (e.g., Cd, Ni, Zn) are emitted into estuaries via atmospheric deposition, direct injection into the bay, and incoming freshwaters. Eventually, these metals can be delivered into the Gulf of Mexico via estuarine outflows. Desorption, dissolution, resuspension, precipitation, flocculation, deposition, and biotransformation processes allow metals to be exchanged between bottom sediments, the water column, and the biota within aqueous environments (Turner and Millward, 2002). Heavy metals are particle reactive and show a strong affinity for the particulate phase (Hem, 1976; Honeyman and Santschi, 1988; Hamelin et al. 1990). Thus, many aqueous heavy metals readily sorb onto particles in the water column and become sequestered in bottom sediments, while a smaller portion of aqueous metals remain in the dissolved phase, either as truly dissolved cations or as colloidal nanoparticles within the water column. Bivalves (i.e., clams, mussels, oysters) are sedentary suspension feeders that largely reside in bottom sediments. Bivalves have been shown to take up metals from the surrounding water column and sediments and store them in their soft tissues (Boening, 1999; Sajwan et al., 2008). Accordingly, bivalves are a widely used bio-indicators for detecting environmental contamination (Otchere, 2019).

Covering 1600 square kilometers, Galveston Bay is the seventh largest estuary in the United States. The greater watershed that drains into Galveston Bay extends roughly 600 kilometers (km) northwest of the bay and includes the Dallas-Fort Worth and Houston metropolitan areas. The majority of freshwater inflow to Galveston Bay comes from the Trinity River (approximately 55%), San Jacinto River (approximately 15%), and local Houston-area waterways, primarily Buffalo Bayou (approximately 10%) (Dorado et al. 2015; Lester and Gonzalez, 2011). The bay's brackish setting hosts multiple habitats including wetlands, oyster reefs, mud flats, and seagrass beds. These habitats are home, nursery, and breeding grounds for marine organisms such as shrimp, crab, oysters, bottlenose dolphins, and numerous fish species (Lester and Gonzalez, 2011; "Galveston Bay Report Card 2017," Houston Advanced Research Center and Galveston Bay Foundation). Economically, Galveston Bay fish, shrimp, oysters and crab are at the center of billion-dollar commercial fishing, recreational fishing and tourism businesses in this region (Lester and Gonzalez, 2011). The Houston Ship Channel (HSC) is the heavily industrialized portion of Buffalo Bayou that flows southeast of Houston into Galveston Bay to become the main shipping lane, which bisects the bay and connects to the Gulf of Mexico at its southernmost end. It is estimated that the HSC shoreline contains 30% to 50% of all oil refineries and chemical manufacturers in the United States (Santschi et al., 2001). After being deemed one of the most polluted waterways in the country, concerted effort has been made to clean up the HSC, which has resulted in the decline of industrial pollutant discharges to Galveston Bay and the HSC over the past two decades (Lester and Gonzalez, 2011). Despite these changes, continued pollutant discharges into the bay are likely since enormous quantities of chemicals and oil are transported across the bay and processed by industry each year (Santschi et al., 2001; Saleh and Wilson, 1999). For example, an estimated 80,000 gallons of oil from over 100 facilities and/or marine vessels spilled into Galveston Bay in 2016 ("Galveston Bay Report Card 2017," Houston Advanced Research Center and Galveston Bay Foundation). Industries bordering Galveston Bay estuary may emit heavy metal pollutants into the estuary via industrial runoff, improper disposal of contaminants at industrial facilities, shipping vessel oil and chemical leaks. Once emitted, heavy metals persist and accumulate in the estuarine environment (Wright and Welbourn, 2001). Datasets constraining metal abundances within estuarine sinks (water, sediments, biota) and the mobility of metals between sources and sinks are necessary to improve our understanding of heavy metal biogeochemical cycles and apply this knowledge to successful estuarine resource management (Morse et al., 1993; Rauch and Pacyna, 2009; Lester and Gonzalez, 2011).

Here, heavy metal concentrations were determined for water, surface and core sediment, and oyster tissue samples collected in Galveston Bay. Pb isotope compositions were measured for the sediment and oyster samples. The concentrations of Cd, Cu, Pb, Ni, and Zn were measured in the sediment samples. Water samples were analyzed for Cd, Cu, Fe, Mn, Pb, Ni, and Zn concentrations. Cd, Pb, and Zn concentrations were measured in oyster tissue samples. The new Pb isotope and heavy metal concentration datasets presented in this study provide new information on the spatial variability of metal concentrations across Galveston Bay sediments and waters from the main bay and source waters entering the bay and provide a seasonally resolved time-series of sedimentary metal loadings. The study assessed metals in differing sediment fractions of surface and core sediments, with an emphasis on readily exchangeable surface-adsorbed metals that may be most harmful to the coastal ecosystem. The oyster tissue datasets in this study shed insight into the spatial variability of Pb isotope and heavy metal concentrations in Galveston Bay oysters from Upper Galveston Bay, Lower Galveston Bay, Trinity Bay, West Bay, and East Bay. Data provided by the waters and sediments (surface and core) served to evaluate heavy metal loadings from source waterways into the bay, assess heavy metal toxicity in bay sediments, and understand the history of heavy metal pollution in the bay. Data provided by the oyster tissues were used as a proxy to evaluate heavy metal toxicity in Galveston Bay biota as well as heavy metal pollution sources to biota in the bay. Collectively, these data highlight toxic hotspots in Galveston Bay and identify potential pollutant sources, which can guide ongoing pollution reduction, remediation, and mitigation efforts as well as ecological rehabilitation projects in the bay.

Methods

Sediment Sampling

Galveston Bay sediment samples analyzed in this study can be divided into three categories: surface sediments collected shipboard from Galveston Bay and incoming tributaries (Fig. 1, black), surface sediments collected by hand along the shores of Galveston Bay (Fig. 1, red), and a sediment core collected shipboard in central Trinity Bay (Fig. 1, blue). Galveston Bay surface sediment samples collected by sea were acquired on 11 trips from June 2017 to June 2019 (Table 1) aboard the R/V *Lithos* (June and September 2017 cruises) and the R/V *Trident* (rest of the cruises). A Van Veen grab sampler was used to collect the upper 10 to 15 centimeters (cm) of bottom sediments. During these sampling events the same general Galveston Bay station locations were sampled (Fig. 1 and Table 1). These locations were selected because they capture the geographic variability of Galveston Bay including Trinity Bay near the Trinity River (Stations 8, 9 and 12), Upper Galveston Bay near the San Jacinto River and Buffalo Bayou (Station 13), Lower Galveston Bay near the Gulf of Mexico outflow (Stations 1, 2, 11, 15), the HSC (Stations 3, 7, 13, and 14) and entrance to East Bay (Stations 5a and 5b). Given the very close proximity of Station 15 to Station 1 and the fact that Station 15 was only sampled once, Station 15 will be considered the same as Station 1 unless the data suggests otherwise. The surface sediments from Stations 1, 3, 5 (A and B), 9, 12, 13, 14, and 15 are collectively referred to as the “bay” stations henceforth. On June 15-16, 2019, surface sediments were also sampled aboard the R/V

Rockport from tributaries that drain into Galveston Bay including the HSC/Buffalo Bayou (Stations 201-203), the San Jacinto River (Stations 301-302), the Trinity River (Stations 501-503), Dickinson Bayou (Stations 101-103), and East Bay/Oyster Bayou (Stations 401-402). These tributary stations 101, 102, 103, 201, 202, 203, 301, 302, 401, 402, 501, 502, and 503 will be referred to as the “endmember” stations.

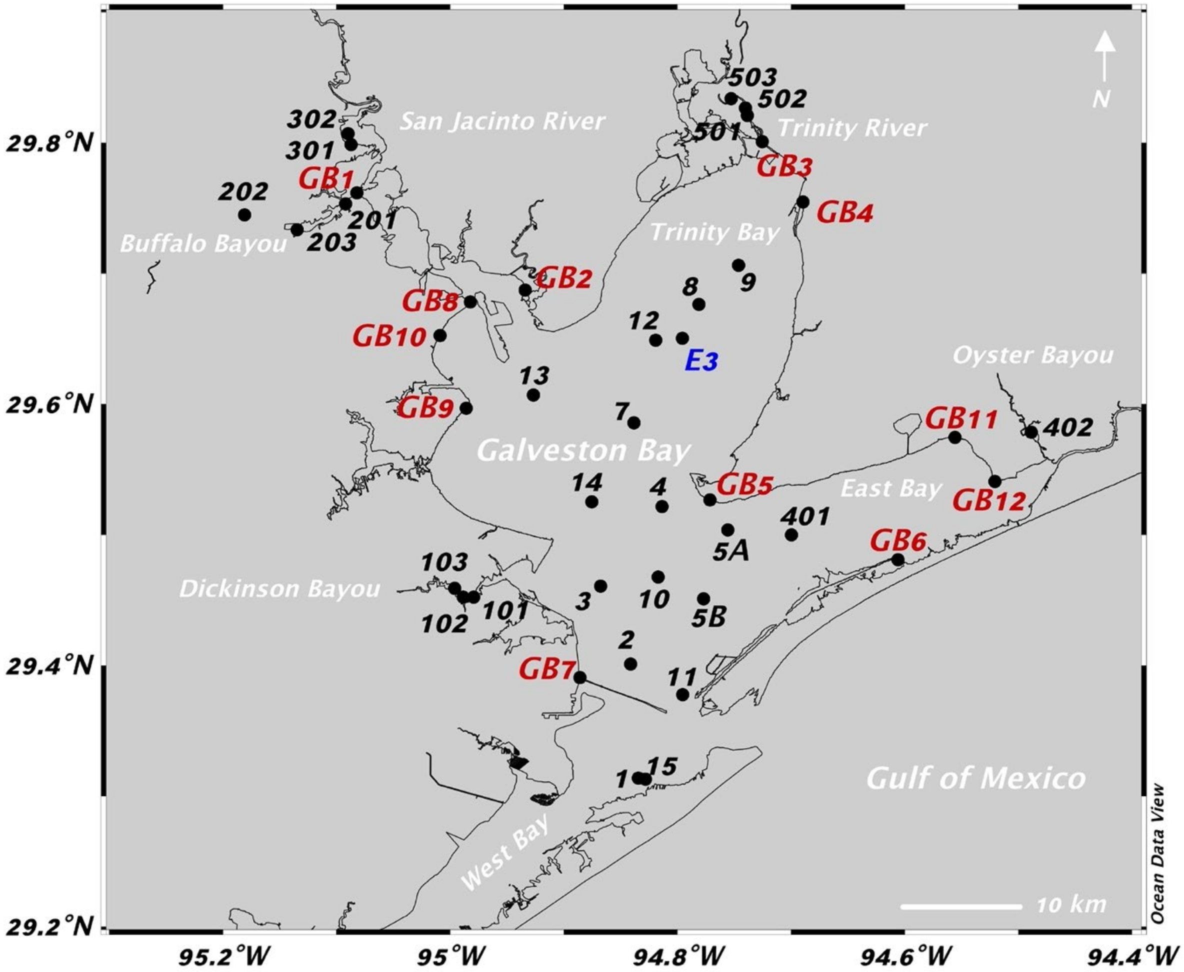

Black labels designate surface sediment and water samples collected during Texas A&M University (TAMU) Galveston Bay cruises. Red labels indicate surface sediment samples that were hand collected from the Galveston Bay shoreline. The dark blue label shows the E3 sediment core location. Five of the main freshwater inflows to Galveston Bay (Trinity River, San Jacinto River, Buffalo Bayou, Dickinson Bayou and Oyster Bayou) are labeled for reference. Different areas with Galveston Bay including Trinity Bay, West Bay and East Bay are noted for reference.

Figure 1. Galveston Bay sediment and water sample location map.

Table 1. Galveston Bay surface sediment collection sampling events

Station	Latitude	Longitude	Jun 5, 2017	Jun 8, 2017	Sept 9, 2017	Sept 16, 2017	Nov 4, 2017	Mar 24, 2018	Jun 16, 2018	Jul 22, 2018	Aug 7, 2018	Sept 22, 2018	Nov 3, 2018	Mar 23, 2019	Jun 9, 2019	Jun 15, 2019	Jun 16, 2019	Jun 19, 2019
1	29.314	-94.835	X		X		X		X				X	X				X
2	29.401	-94.841	X		X													
3	29.461	-94.868			X	X	X					X	X	X				X
4	29.522	-94.814	X															
5A	29.504	-94.756	X			X	X											X
5B	29.451	-94.777						X	X			X	X	X				X
7	29.586	-94.839		X		X												
8	29.676	-94.781		X		X												
9	29.706	-94.746		X		X	X	X	X			X	X	X				X
10	29.468	-94.817		X														
11	29.378	-94.796										X	X					
12	29.649	-94.819					X	X	X			X	X	X				X
13	29.607	-94.927					X	X	X			X	X	X				X
14	29.525	-94.875					X	X	X			X	X	X				
15	29.313	-94.828						X										
101	29.452	-94.979														X		
102	29.452	-94.989														X		

Station	**Latitude**	**Longitude**	**Jun 5, 2017**	**Jun 8, 2017**	**Sept 9, 2017**	**Sept 16, 2017**	**Nov 4, 2017**	**Mar 24, 2018**	**Jun 16, 2018**	**Jul 22, 2018**	**Aug 7, 2018**	**Sept 22, 2018**	**Nov 3, 2018**	**Mar 23, 2019**	**Jun 9, 2019**	**Jun 15, 2019**	**Jun 16, 2019**	**Jun 19, 2019**
103	29.459	-94.996														X		
201	29.753	-95.092														X		
202	29.745	-95.181														X		
203	29.734	-95.135														X		
301	29.799	-95.087														X		
302	29.807	-95.090														X		
401	29.500	-94.700															X	
402	29.579	-94.489															X	
501	29.801	-94.726															X	
502	29.827	-94.740															X	
503	29.834	-94.753															X	
GB1	29.762	-95.082								X								
GB2	29.687	-94.934								X								
GB3	29.821	-94.739								X								
GB4	29.755	-94.690								X								
GB5	29.527	-94.771								X								
GB6	29.481	-94.606								X								
GB7	29.391	-94.886								X								

Station	Latitude	Longitude	Jun 5, 2017	Jun 8, 2017	Sept 9, 2017	Sept 16, 2017	Nov 4, 2017	Mar 24, 2018	Jun 16, 2018	Jul 22, 2018	Aug 7, 2018	Sept 22, 2018	Nov 3, 2018	Mar 23, 2019	Jun 9, 2019	Jun 15, 2019	Jun 16, 2019	Jun 19, 2019
GB8	29.678	-94.982								X								
GB9	29.597	-94.986									X							
GB10	29.653	-95.009									X							
GB11	29.575	-94.556													X			
GB12	29.541	-94.521													X			

A sediment core (Fig. 1, E3) was collected using a PVL-Technologies® submersible vibrating coring head deployed from the bow mounted A-frame on the R/V *Lithos* in July 2016 (Al Mukaimi et al., 2018). The core was stored under refrigeration at 35°C until it was subsampled for this study. Twenty-three E3 core subsamples, referred to as E3-1 thru E3-23, were acquired from the E3 core. The E3 core subsamples represent 5 cm intervals that span the length of the core with E3-1 representing sediment from the very top of the core and E3-23 representing sediment from the base of the core.

In July-August 2018 and June 2019 surface sediment samples were collected by hand from locations along the shoreline of Galveston Bay; these samples are referred to as the "shoreline" samples with the "GB" sample identifier in Fig. 1. The shoreline samples were collected using gloved hands (nitrile, Dot Scientific) to hand-scoop shallow sediments into acid-cleaned 50 mL centrifuge tubes. The sampling locations were areas that could be accessed by personal vehicle and included boat ramps, fishing docks, and public beaches. The GB station samples may contain Pb which is exogenous or largely anthropogenic in nature given the anthropogenic nature of the sample locations. Furthermore, it has been shown that nitrile laboratory gloves may contribute heavy metal blank during sample collection and handling; therefore, it is possible that the GB station samples are subject to more contamination than the shipboard samples (Garcon et al., 2016). After collection, all samples were transported directly to the laboratory and stored under refrigeration until processing was completed.

Water Sampling

Water samples were collected at the bay stations and endmember stations located in Fig. 1 and enumerated in Table 1. An all-plastic air diaphragm pump (Jabsco, Cole-Parmer) fitted with acid-cleaned C-Flex tubing in the pump head was used to collect surface and bottom water samples (Wen et al. 1996; Jiann et al., 2013). Surface samples were taken approximately 30 cm beneath the water surface and bottom water samples were collected approximately 1 m above the water-sediment interface. In the field, all water samples were filtered through 0.2 µm pore size acid-cleaned in-line polypropylene cartridge filters (Acropak 200) and collected directly into acid-cleaned low-density polyethylene (LDPE) bottles. For most sampling events, four 250 mL filtered water samples (a surface filtered water sample, a duplicate surface filtered water sample, a bottom filtered water sample, and a duplicate bottom filtered water sample) were collected. The surface and bottom 250 mL water samples were analyzed for heavy metal concentrations; the duplicate 250 mL water samples were analyzed if and when an anomalous data point was found, to ensure that bottle contamination is not to blame.

Salinity samples were drawn in the field at the time of sampling at each bay and endmember station into 200 mL Kimax high-alumina borosilicate bottles, which were rinsed three times with sample prior to filling to the shoulder. The bottles were sealed with plastic insert thimbles to reduce evaporation. Practical salinity (Lewis and Perkin, 1981) was calculated for each sample from the measured conductivity ratios. Salinity is reported in practical salinity units (psu). In the laboratory, a Guildline Autosal 8400B salinometer was used for salinity/ conductivity measurements. The laboratory salinity analyses were performed after samples had equilibrated to laboratory temperature, usually within 6 weeks after collection. The salinometer was standardized for each group of analyses using Ocean Scientific International Limited standard seawater, with frequent use of a secondary deep-water standard to check for drift during runs.

Following collection, the water samples were transported directly to the laboratory of Dr. Fitzsimmons at TAMU, where the samples for heavy metal analysis were acidified with ultrapure hydrochloric acid (Optima, Fisher) to 0.012 M concentration and stored at room temperature. The acidified water samples were left to sit for a minimum of 12 weeks at room temperature to allow desorption of metals from the inner walls of the sample bottle (Fitzsimmons and Boyle, 2014; Chen et al. 2016).

Oyster Sampling

Oyster sample collection followed the methods and protocols of the Texas Parks and Wildlife Department (TPWD) Coastal Fisheries Division Marine Resource Monitoring Operations Manual (Martinez-Andrade et al., 2018). Galveston Bay oyster tissue samples were collected by TPWD personnel in two batches: Batch 1 in December 2019 - January 2020 and Batch 2 in September 2020. Oyster sampling locations are shown in Fig. 2 and sample details are listed in Table 2. The oysters were collected using a 0.5 m wide Biloxi-style dredge with 76 mm stretched mesh webbing in the bag. The dredge was pulled linearly for 30 seconds at three miles per hour by a skiff or another similar vessel. A geographic positioning system (GPS) was used to collect the geographical coordinates at each sampling location. Six to ten oysters at each site were collected from the following five areas in Galveston Bay: Upper Galveston Bay/Trinity Bay (Area 1), Upper Galveston Bay/San Jacinto (Area 2), Lower Galveston Bay (Area 3), East Bay (Area 4) and West Bay (Area 5). After collection in the field, the oyster specimens were placed in pre-cleaned polyethylene containers, labeled, stored on ice and transported to the TPWD Dickinson Marine Laboratory.

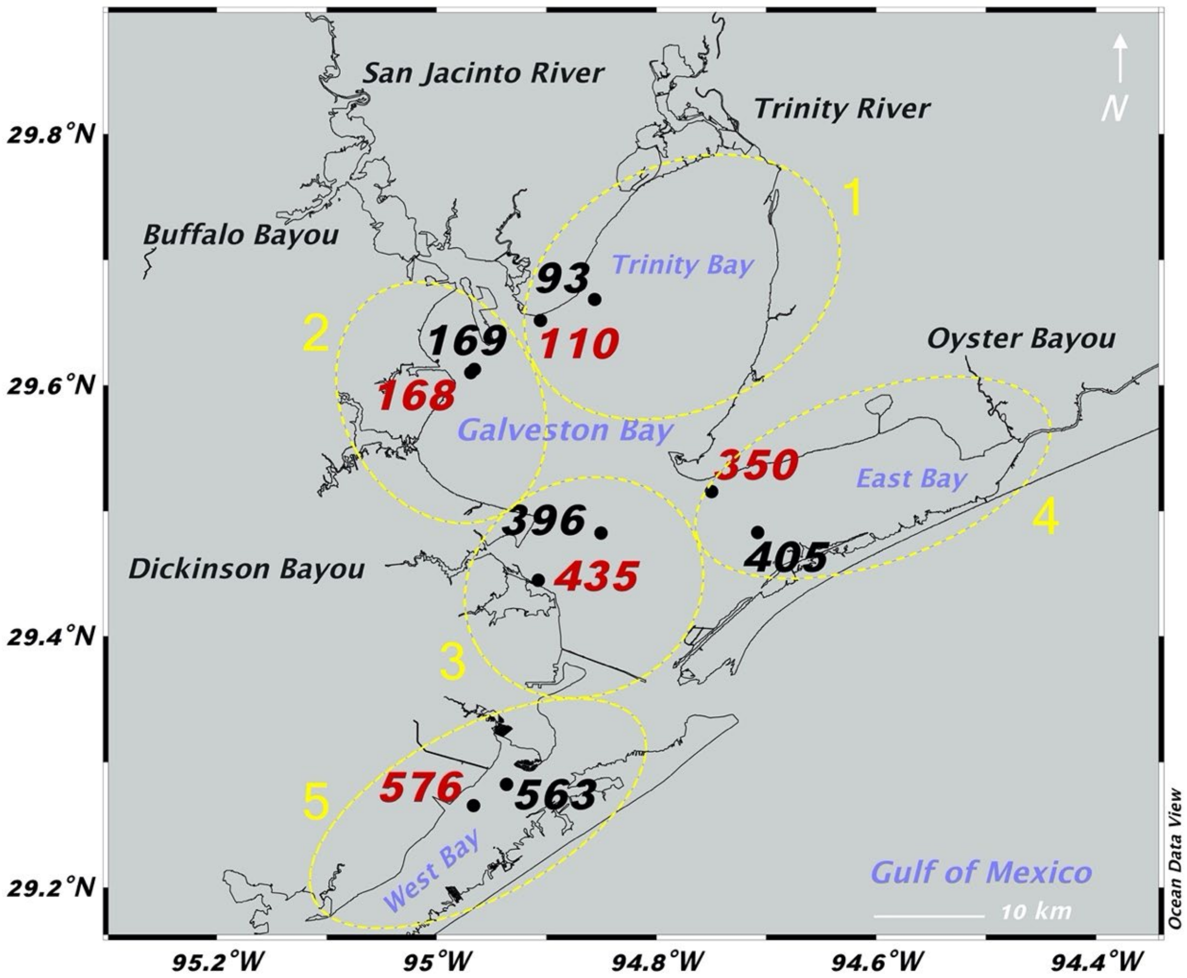

Black sample labels designate oyster samples collected in December 2019 and January 2020. Red labels indicate oyster samples collected in September 2020. Yellow outlines show the five main sampling areas in this study, Area 1 – Upper Galveston Bay/Trinity Bay, Area 2 – Upper Galveston Bay/San Jacinto River, Area 3 – Lower Galveston Bay, Area 4 – East Bay and Area 5 – West Bay.

Figure 2. Galveston Bay oyster sample location map.

Table 2. Galveston Bay oyster sample details

Sample ID	Latitude (˚N)	Longitude (˚E)	n	Area Number	Area Description	Date collected
93	29.6686	-94.8564	8	1	Upper Galveston Bay/Trinity Bay	Jan 23, 2020
169	29.6131	-94.9658	9	2	Upper Galveston Bay/San Jacinto River	Dec 18, 2019
396	29.4825	-94.8506	9	3	Lower Galveston Bay	Dec 4, 2019

Sample ID	Latitude (˚N)	Longitude (˚E)	n	Area Number	Area Description	Date collected
405	29.4831	-94.7078	8	4	East Bay	Jan 28, 2020
563	29.2825	-94.9364	10	5	West Bay	Dec 18, 2019
110	29.5419	-94.9056	6	1	Upper Galveston Bay/Trinity Bay	Sep 25, 2020
168	29.6103	-94.9689	8	2	Upper Galveston Bay/San Jacinto River	Sep 25, 2020
435	29.4450	-94.9075	8	3	Lower Galveston Bay	Sep 11, 2020
350	29.5156	-94.7497	8	4	East Bay	Sep 16, 2020
576	29.2656	-94.9664	8	5	West Bay	Sep 17, 2020

n = number of individual oysters collected at each location and used in composite

Sediment Sample Processing

Previous studies have established that heavy metals can partition into different chemical forms in marine and estuarine sediments; this is referred to as solid phase speciation (Wen et al., 2008, Tessier et al., 1979). There are five general fractions that heavy metals partition into: the surface exchangeable fraction, the carbonate bound fraction, the Fe-Mn bound fraction, the organic matter bound fraction, and the residual fraction (Tessier et al., 1979). Heavy metals complex with sediment carbonates in the carbonate bound fraction, Fe and Mn oxides and hydroxides in the Fe-Mn bound fraction, and a variety of organic matter in the organic matter bound fraction. The surface exchangeable fraction involves heavy metals that are adsorbed to the major constituents of the sediments in which they reside. Heavy metals in this fraction undergo sorption and desorption processes, allowing them to be released into and removed from estuarine waters. The residual fraction is the fraction left after the four other fractions have been removed. It includes primary and secondary minerals that may contain heavy metals in their crystalline structure; these metals are not anticipated to be released in solution. In Galveston Bay, heavy metals are known to be present in the surface exchangeable, carbonate, and Fe-Mn bound fractions (Tang et al., 2002; Wen et al., 2008). Pollutant heavy metals are thought to reside on the surface exchangeable and Fe-Mn bound heavy metal fractions of sediment, while heavy metals in the residual fraction represent crystalline bound, non-pollutant metals (Tang et al., 2002; Ip et al. 2007).

The collected sediments were centrifuged and oven-dried at 60˚C for up to seven days to remove all water. Visible shell material was removed from the dried sediments using clean carbon fiber tweezers. This removed the visible carbonate fractions from each sediment sample. Shell-free dried sediments were homogenized using a mortar and pestle. Heavy metal concentration and Pb isotope analyses were performed using the dried, homogenized sediments. Two smaller samples were taken from each dried, homogenized sediment sample: one subsample was leached, and the residue digested for heavy metal concentration and Pb isotope analyses, and one subsample was fully digested (no leach) and analyzed for bulk heavy metal concentrations and Pb isotope ratios. Procedural blanks and standard reference materials (SRMs) were prepared alongside all samples and measured accordingly.

The leaching procedure used follows the recommendation of recent leaching studies in which 0.02 M hydroxylamine hydrochloride (HH) in 25% acetic acid is used as a reductant (Kryc et al., 2003; Gutjahr et al., 2007; Berger et al., 2008; Basak et al., 2010; Wilson et al., 2013). Approximately 20 mg of dried, homogenized sediment was weighed into acid-cleaned 15 mL centrifuge tubes; two mL of the HH-acetic acid leaching solution was added to each tube. Tubes containing sediment samples in the leaching solution were placed into a hot water bath for two hours; water temperature was approximately 90˚C for the first 10 minutes of the leach after which the hot plate was turned off and the water was allowed to cool gradually. Each sample was centrifuged at 3100 rpm for 20 minutes and the leachate supernatant was transferred into new, acid cleaned Savillex Teflon vials. To ensure that as much of each leached phase was collected as possible, 0.5 mL of ultrapure Milli-Q (MQ) water (1 x distilled) was added to the sediment residue remaining in the tube and centrifuged again. The supernatant of the second centrifuge step was added to the leachate sample vials. Exactly half of each leachate sample was pipetted into a new, acid cleaned Savillex Teflon vial; this resulted in an isotope leachate aliquot and a concentration leachate aliquot of equal volume for each sample. Both the isotope and concentration leachate aliquots were acidified with 100 microliters (µL) of concentrated nitric acid then taken to dryness; this step was repeated once.

The sediment residues remaining in the centrifuge tubes were dried then weighed to calculate the mass lost during the leaching process. Residues were digested using a 2:1 mixture of concentrated hydrofluoric acid and concentrated nitric acid mixture, followed by concentrated hydrochloric acid, and lastly 2N hydrochloric acid (Lopez et al., 2021). Residues were digested on a hot plate for a minimum of one hour between 120˚C -160˚C during each digestion step then taken to dryness. After being digested in 2N hydrochloric acid overnight the samples were transferred into acid-cleaned centrifuge tubes and centrifuged for 15-20 minutes at 6400 rpm to remove undissolved material. For each sample, exactly half of the supernatant was pipetted back into the vial used for digestion and the other half of the supernatant was pipetted into a new, acid cleaned Savillex Teflon vial. This created an isotope residue aliquot and a concentration residue aliquot of equal volume for each sample. Both the isotope and concentration leachate aliquots were taken to dryness. The concentration leachate aliquots were taken up again in 40 µL concentrated nitric acid then dried down; this step was repeated twice. The concentration leachate and residue aliquots were dissolved in 3 mL of 2% concentrated nitric acid spiked with one part per billion (ppb) indium (In) to monitor inductively coupled mass spectrometer (ICP-MS) drift. The samples were volumetrically diluted by a factor of 100 with the same In-spiked nitric acid solution and then analyzed for heavy metal abundances as described below.

Total digests (no leach) of the sediment samples were also completed. Approximately 10 mg of dried, homogenized sediment was weighed into acid cleaned Savillex Teflon vials then digested using a concentrated hydrofluoric acid and concentrated nitric acid mixture followed by concentrated hydrochloric acid, and finally 2N hydrochloric acid. Total digests were digested on a hot plate for a minimum of one hour between 120-160˚C during each digestion step then taken to dryness. After being digested in 2N hydrochloric acid exactly half of the total digest sample was pipetted into an acid cleaned Savillex Teflon vial. This created an isotope total digest aliquot and a concentration total digest aliquot of equal volume for each sample. Both the isotope and concentration total digest aliquots were taken to dryness. The concentration total digest aliquots were taken up again in 40 µL concentrated nitric acid then dried down; this step was repeated twice. The concentration total digest aliquots were taken up in 3 mL of 2% concentrated nitric acid spiked with 1 ppb In to monitor ICP-MS drift. The samples were volumetrically diluted by a factor of 100 with the same In-spiked nitric acid solution and then analyzed for heavy metal abundances as described below.

All isotope aliquots were prepared for Pb isotope measurements following the column chemistry procedure described here. Samples were purified for Pb isotopic measurements using AG-1X8 chloride form, 100-200 mesh anion exchange resin. Once added to the columns, the resin was washed with 6N HCl (hydrochloric acid, 1 x distilled), then MQ (1 x distilled), and conditioned with 0.5N HBr (hydrobromic acid, Optima grade) before sample introduction. Samples were dissolved in 1 mL of 0.5N HBr then loaded onto the resin-bearing columns. Additional 0.5N HBr was washed through each column, then Pb was eluted with 6N HCl. After collection samples were taken to dryness, and the same column chemistry procedure was repeated. Lastly, each sample received 10 µL of 15N HNO_3 (nitric acid) to burn off any remaining organics then each sample was dried down. This step was repeated twice. For the Pb isotope measurements each sample was taken up in 0.45N HNO_3 and spiked with National Bureau of Standards (NBS) 997 Tl (Marcantonio et al., 2000; Ewing et al., 2010; Widory et al., 2010; Zhu et al., 2010; Sun et al., 2011; Cundy and Croudace, 2017). Procedural blanks were prepared alongside all samples and measured accordingly.

Water Sample Processing

Water samples were prepared for heavy metal concentration analysis as described in Jensen et al. 2020 (as modified from Lagerstrom et al. 2013), using the automated SeaFAST system (Elemental Scientific). Briefly, approximately 10 mL of acidified, filtered water sample is weighed and spiked with rare isotope solutions of calibrated concentration and then loaded into the SeaFAST system. The SeaFAST subsequently buffers the solution to about pH 6.5 using an ammonium acetate solution, made from Milli-Q (MQ) water, ultrapure 17 M acetic acid, and ultrapure 11 M ammonium hydroxide. Then, the SeaFAST system pushes the buffered water sampled across a column bed of Nobias PA-1 chelating resin, which has been used to extract heavy metals from seawater in several previous trace metal extraction studies, with low blank contamination (Sohrin et al., 2008; Conway et al. 2013). The resin is made of methacrylate polymer beads that contain ethylenediaminetriacetic acid (EDTriA) and IDA (iminodiacetic acid) functional groups. These functional groups strongly bind to metal ions such that the resin has a stronger affinity for trace metals than major cations such as Mg, Na, and Ca. This resin bed is then rinsed with buffered MQ water to wash away the salts, and then the resin-bound heavy metals are back-eluted from the resin into 10% nitric acid eluent, resulting in 400 uL of eluent, representing a 25-fold pre-concentration factor for each sample.

These samples are analyzed for the heavy metal concentrations on the ThermoScientific Element XR high-resolution inductively coupled plasma mass spectrometer in the R. Ken Williams Radiogenic Lab in the College of Geosciences at TAMU. Cd and Pb isotopes are analyzed in low resolution, while Fe, Mn, Cu, Zn, and Ni are analyzed in medium resolution. Isotope dilution techniques are used to quantify concentrations of Fe, Cu, Zn, Ni, Cd, and Pb, while Mn is quantified using matrix-matched standard curves. In short, low-metal filtered and acidified seawater solutions were spiked with increasing concentrations of Mn up to 60 nanomolar (nM); these Mn-spiked seawater solutions were put through the SeaFAST system as any other sample, and these samples were used to establish the standard curve that was utilized to calculate seawater Mn concentrations. Procedural blanks were analyzed using an injection of a spiked sample of MQ water as a blank, and commonly used seawater consensus samples (Johnson et al. 2007) were prepared alongside samples and measured accordingly.

Oyster Sample Processing

In the TPWD Dickinson Marine Laboratory, oyster samples were lightly rinsed with deionized or MQ and then opened with a stainless-steel knife. The soft tissues were removed and sparingly rinsed with MQ to remove particles before being transferred to clean polyethylene storage bags and weighed. The soft tissue oyster samples were frozen at approximately -18°C until processing was completed. Frozen individual oyster tissues in clean polyethylene storage bags were transferred directly from freezer storage into a freeze dryer (Harvest Right, oil free scroll vacuum pump) and lyophilized. Individual, dry oyster tissues were reweighed to calculate water loss. Dried oyster tissues were powdered and homogenized using a mortar and pestle. Individual oyster tissues from each sample location were compiled into a single composite sample representative of that site (e.g., the eight individual dried, powdered oyster tissues from sampling location 576 were combined into one homogenized sample).

Heavy metal concentration and Pb isotope analyses were performed using the dried, homogenized composite oyster tissue samples.

Concentrated HCl, HF, HNO_3 acids are commonly used to break down organic matter (Tessier et al., 1979; Wen et al., 2008; Zhang et al., 2008; Chen et al., 2017). These digestion steps are widely accepted methods to dissolve organic matter and release associated metals into solution. For heavy metal abundances, approximately 200 mg of each dried, homogenized oyster tissue sample was weighed out into an acid-cleaned Teflon vial and then digested in 3 mL of 15N HNO_3. After the 3 mL of 15N HNO3 was added, the vials were loosely capped and left to sit overnight in a clean laboratory fume hood. The following day the vial caps were tightened, and the vials were heated on a 110˚C hot plate for one hour, two hours, four hours and overnight. In between each heating step the vials were taken off the hot plate to cool and the caps were loosened to release pressure. Following the overnight hot plate digestion, the samples were taken to dryness. Procedural blanks and SRMs were processed alongside the samples. The digested oyster tissue heavy metal subsamples were dissolved in 3 mL mixture of 2% HNO_3 spiked with 1 ng/g In and centrifuged at 3,000 revolutions per minute for 30 minutes. The samples were volumetrically diluted by a factor of 250 with the same In-spiked HNO_3 solution and then analyzed for heavy metal abundances as described below.

For oyster tissue Pb isotope measurements, approximately 100 mg of each dried, homogenized oyster tissue sample was weighed out into an acid-cleaned Teflon vial and then digested in four steps. In the first and second steps 5 mL of 15N nitric acid (2 x distilled) was used, a mixture of 5 mL 15N nitric acid (2 x distilled) and 200 µL 28N hydrofluoric (Optima) was used in the third step, and a mixture of 4.5 mL 15N nitric acid (2 x distilled) and 0.5 mL 30% hydrogen peroxide (Optima) was used in the fourth step. During each step the residues were digested on a 90-110°C hot plate overnight, then taken to dryness. During the fourth digestion step, while each sample was in 4.5 mL 15N nitric acid (2 x distilled) and 0.5 mL 30% hydrogen peroxide (Optima), half of each solution was pipetted into a new, acid-cleaned Teflon vial. The resulting solution was dried and purified for Pb isotope measurements following the same procedure as the sediment samples. Procedural blanks were prepared alongside all samples and measured accordingly.

Heavy Metal Concentration Measurements

Heavy metal concentrations in all samples were analyzed at the R. Ken Williams Radiogenic Isotope Laboratory at TAMU in the College of Geosciences on a ThermoFisher Element XR high resolution inductively coupled mass spectrometer (HR-ICP-MS) in collaboration with the subcontractor Dr. Jessica Fitzsimmons. Quantification was achieved using standard solutions made in the same In-spiked nitric acid solution to match samples. The standard solutions were measured at the start and end of each run and had concentrations bracketing the range of observed natural concentrations. Changes in sensitivity over the course of the run were corrected by normalizing to changes in the In counts. The instrument background signal was determined from acid blanks and removed from the final sample measurements, and reagent/procedure blanks (with reagents and full leach/residue/digestion methods but without any sample) were quantified in moles and subtracted from the measured moles in each sample after dilution-correction.

SRMs were used to assess the recovery and accuracy of the heavy metal concentration measurements. Percent recoveries are calculated as the average measured SRM value divided by the certified SRM value multiplied by 100% (recoveries of 100% indicate that the measured value matches the certified value perfectly). Percent recovery errors are calculated as the standard deviation of the measured SRM values divided by the certified SRM value multiplied by 100. Recovery between 75% – 125% of certified SRM consensus values within error is considered acceptable. The National Research Council Canada (NRCC) MESS-4 (n=3) and PACS-3 (n=3) SRMs in addition to the National Institute of Standards (NIST) 2702 SRM (n=3) were used for the sediment heavy metal concentrations. The sediment data SRM recoveries are shown in Table 3. The SAFe D2 GEOTRACES seawater reference solution (n=2) was used for the water heavy metal concentration measurements (Johnson et al., 2007). The SAFe D2 recoveries are Cd 106.3% ± 0.4%, Cu 120.9% ± 1.1%, Fe 99.2% ± 1.0%, Mn 127.1% ± 5.4%, Ni 104.0% ± 0.5%, Pb 97.5% ± 0.0%, and Zn 99.6% ± 2.2%. The NIST 1566b SRM (n=2) was used for the oyster sample heavy metal concentration measurements. The NIST 1566b SRM recoveries are as follows: Cd 96.4% ± 5.3%, Pb 94.0% ± 3.3%, and Zn 101.6% ± 3.6%.

Table 3. Recovery summary for SRMs NRCC MESS-4, NRCC PACS-3 and NIST 2702.

Metal	PACS-3 % recovery ± % recovery error	NIST 2702 % recovery ± % recovery error	MESS-4 % recovery ± % recovery error
Cd	126% ± 0.5%	118% ± 2.9%	90% ± 15.9%
Cu	100% ± 7.0%	84% ± 3.8%	104% ± 4.9%
Ni	98% ± 10.4%	77% ± 2.3%	85% ± 8.6%
Pb	101% ± 8.9%	93% ± 2.9%	132% ± 53.7%
Zn	95% ± 13.0%	79% ± 3.1%	99% ± 9.6%

Uncertainty (data error) in each heavy metal concentration was evaluated based on the standard deviation of replicate measurements (sediments n=46, waters n=30, oysters n=2) of individual samples. For the sediment data, the error for each metal concentration is as follows: the Pb concentration errors are ±2%, the Zn concentration errors are ±4%, the Cu and Ni concentration errors are ±6%, and the Cd concentration errors are ±14%. For the water data, the error for each metal concentration is as follows: ±2% for Ni and Pb, ±5% for Cu, ±6% for Fe, Zn and Cd, and ±7% for Mn. For the oyster tissue data, the Cd concentration data error is 0.1%, the Pb concentration data error is 9% and the Zn concentration data error is 3%.

Procedural blank concentrations for the sediment data (n=41) were below 23.5 ng with an average blank of 3.1 ng for all elements. Average procedural blank concentrations for the water data were 0.0001 nanograms per milliliter (ng/mL) Cd, 0.0008 ng/mL Cu, 0.0025 ng/mL Fe, 0.0002 ng/mL Mn, 0.0009 ng/mL Ni, 0.00002 ng/mL Pb, and 0.005 ng/mL Zn. For the oyster tissues, procedural blank (n=2) concentrations ranged between 0.02 – 0.06 ng (Cd), 0.25 – 0.35 ng (Pb), and 21.35 – 28.54 ng (Zn). Blank contributions were negligible in comparison to sample metal concentrations indicating no blank contamination occurred during sample processing. Blank contributions were removed from final sample concentrations prior to finalizing the reported concentration values.

Pb Isotope Ratio Measurement

Isotope analysis of ^{204}Pb, ^{206}Pb, ^{207}Pb, and ^{208}Pb for the sediment and oyster tissue samples was performed using a Neptune Plus high-resolution multi-collector inductively coupled mass spectrometer (MC-ICP-MS) at the Johnson Mass Spectrometry Laboratory at New Mexico State University. Before each sample measurement, the instrument on peak baseline was measured and removed from the measured sample signal. Procedural blanks (oysters n=4, sediments n=41) were spiked with 99% pure ^{208}Pb spike and subsequently Pb blank concentrations were calculated. Blank Pb concentrations were less than 1% of the sample Pb concentrations, which is negligible in comparison to sample concentrations and indicates that no blank contamination occurred during sample processing. The measured Pb isotope ratios were blank corrected. The average percent change in each ratio value due to the blank correction for the ^{206}Pb/^{204}Pb, ^{207}Pb/^{204}Pb, ^{208}Pb/^{204}Pb, ^{208}Pb/^{206}Pb, and ^{207}Pb/^{206}Pb ratios respectively, was equal to or less than: 0.024%, 0.009%, 0.004%, 0.025%, and 0.033%. Measured ratios were normalized to the NBS 997 ^{205}Tl/^{203}Tl ratio of 0.4189 (Wolff and Ramos, 2003). The NIST SRM NBS981 was analyzed at the start and end of each analytical session as well as after every third sample during an analytical session. Measured NBS981 Pb isotope ratios were within or nearly within error of certified NBS981 values (observed values matched certified values within 0.1%), therefore samples were not normalized to NBS981. The Pb/Tl ratios ranged from 1.1 to 11.5 in the NBS981 standards and from 0.3 to 20.0 in the samples. Variation of the Pb/Tl ratios in the NBS981 standards did not result in distinguishably different Pb isotope ratio measurements. The ^{202}Hg signal was monitored throughout each run to correct for the potential interference of ^{204}Hg on ^{204}Pb. One hundred Pb isotope ratios were measured and averaged to produce the reported values and their corresponding ±2 standard error (±2SE) for each sample.

Results and Observations

Galveston Bay Sediment Heavy Metal Concentrations

Elemental concentrations measured in Galveston Bay sediment leachates and bulk digests are in Tables 4-6. Sediment leachates are indicated with an "L" identifier and bulk sediment digests are marked with a "D" identifier in subsequent tables and figures. The sediment leachates have lower heavy metal concentrations than bulk digests for all metals measured in the Galveston Bay surface sediments. In the leachates, metal levels range from 0.01 – 0.3 micrograms per gram (µg/g) for Cd, 0.3 – 295.4 µg/g for Cu, 0.2 – 13.3 µg/g for Ni, 0.3 – 14.0 µg/g for Pb, and 3.7 – 302.6 µg/g for Zn. The bulk sediment metal concentrations range as follows, Cd 0.02 – 0.5 µg/g, Cu 0.8 – 351.8 µg/g, Ni 1.1 – 30.3 µg/g, Pb 1.8 – 29.2 µg/g, and Zn 4.3 – 336.6 µg/g.

Table 4. Heavy metal concentrations in Galveston Bay sediment leachates and corresponding salinity measurements at each sample station.

Sample ID	Salinity (*psu)	Cd (*µg/g)	Pb (µg/g)	Ni (µg/g)	Cu (µg/g)	Zn (µg/g)
1L 06-17	22.548	0.01	1.38	0.77	0.66	6.35
2L 06-17	18.954	0.02	1.98	1.01	0.83	7.78
4L 06-17	15.175	0.04	3.10	1.38	0.95	8.12
5L 06-17	15.263	0.04	3.03	1.63	0.84	7.11
7L 06-17	14.117	0.05	4.24	1.87	0.79	10.08
8L 06-17	10.432	0.05	2.87	1.68	0.98	10.57
9L 06-17	7.494	0.07	1.83	4.02	1.01	10.15
10L 06-17	18.863	0.03	2.50	1.08	0.79	7.56
1L 09-17	7.899	0.03	1.88	0.91	0.84	8.18
2L 09-17	3.214	0.02	1.83	1.04	1.09	10.89
3AL 09-17	2.698	0.04	2.12	0.95	1.19	14.17
3BL 09-17	6.103	0.03	1.84	0.92	0.77	7.49
5L 09-17	2.358	0.04	2.79	1.45	0.89	9.64
7L 09-17	1.882	0.05	4.22	1.88	1.00	12.07
8L 09-17	0.661	0.09	3.46	2.31	1.59	22.91

Sample ID	Salinity (*psu)	Cd (*µg/g)	Pb (µg/g)	Ni (µg/g)	Cu (µg/g)	Zn (µg/g)
9L 09-17	0.186	0.07	2.08	1.39	0.97	9.51
1L 11-17	25.476	0.05	3.49	1.69	4.11	35.84
3L 11-17	18.432	0.03	2.12	1.00	0.88	11.62
5L 11-17	9.592	0.03	2.14	1.12	1.26	11.84
9L 11-17	20.304	0.06	2.49	2.00	1.05	8.72
12L 11-17	11.302	0.07	3.57	1.98	1.78	23.04
13L 11-17	12.527	0.02	2.02	0.93	1.02	8.51
14L 11-17	15.888	0.05	3.54	1.77	1.97	21.09
5L 03-18	14.12	0.04	3.09	1.83	0.88	7.85
9L 03-18	0.273	0.07	2.54	1.79	0.93	7.11
12L 03-18	2.533	0.05	3.19	1.55	1.17	12.21
13L 03-18	8.527	0.07	2.45	1.08	1.12	8.46
14L 03-18	14.361	0.02	1.82	0.91	0.69	6.55
15L 03-18	25.155	0.04	4.02	1.90	1.53	12.23
1L 06-18	29	0.03	2.93	1.28	1.48	17.20
5L 06-18	33	0.02	1.72	0.83	0.55	5.32
9L 06-18	9.8	0.06	2.69	2.03	0.98	10.54
12L 06-18	14	0.06	3.73	2.04	1.25	10.54
13L 06-18	18.6	0.03	2.11	0.86	0.88	10.36
14L 06-18	25	0.01	1.27	0.79	0.50	7.34
3L 09-18	17.897	0.02	1.92	1.07	1.04	15.45
5L 09-18	20.2449	0.04	3.96	1.77	1.46	15.67
9L 09-18	12.7436	0.08	3.00	13.26	2.26	24.54
11L 09-18	25.3671	0.02	2.56	2.26	1.14	15.97

Sample ID	Salinity (*psu)	Cd (*µg/g)	Pb (µg/g)	Ni (µg/g)	Cu (µg/g)	Zn (µg/g)
12L 09-18	15.5935	0.06	3.82	1.86	1.89	23.26
13L 09-18	16.0797	0.02	2.81	1.11	4.76	11.61
14L 09-18	16.9239	0.02	1.79	1.14	1.24	17.89
1L 11-18	23.17	0.04	2.10	1.21	1.49	21.56
3L 11-18	10.74	0.04	1.23	0.70	1.04	19.28
5L 11-18	10.75	0.05	3.55	1.32	1.11	13.91
9L 11-18	0.155	0.08	2.78	1.55	1.39	16.39
11L 11-18	23.41	0.03	1.82	0.73	0.33	10.37
12L 11-18	0.198	0.07	3.53	1.60	0.98	11.54
13L 11-18	5.218	0.03	1.92	0.66	0.73	6.16
14L 11-18	8.384	0.03	1.55	0.80	0.65	6.99
1L 03-19	18.102	0.02	3.61	1.84	1.57	14.73
3L 03-19	12.946	0.02	2.57	1.38	1.02	39.44
5L 03-19	12.977	0.03	3.52	1.69	1.14	16.63
9L 03-19	1.148	0.06	3.33	1.97	1.52	9.87
12L 03-19	7.604	0.06	4.55	2.19	1.61	16.62
13L 03-19	10.188	0.03	2.68	1.66	1.42	17.93
14L 03-19	12.587	0.02	2.10	1.60	0.89	8.85
1L 06-19	13.7	0.02	2.27	1.40	0.96	13.57
3L 06-19	8.4	0.03	3.22	1.59	1.32	15.46
5AL 06-19	4.5	0.05	3.75	2.20	1.42	15.49
5BL 06-19	10.5	0.05	4.42	2.19	1.79	16.00
9L 06-19	0.16	0.07	3.51	2.62	2.18	20.86
12L 06-19	0.4	0.06	4.19	1.97	1.40	17.52

Sample ID	**Salinity (*psu)**	**Cd (*µg/g)**	**Pb (µg/g)**	**Ni (µg/g)**	**Cu (µg/g)**	**Zn (µg/g)**
13L 06-19	1.85	0.04	3.68	1.86	1.26	12.69
101L	1.3	0.06	3.61	1.69	2.66	22.60
102L	0.8	0.09	4.24	2.35	3.56	40.79
103L	0.3	0.07	3.14	1.48	1.42	27.58
201L	6.15	0.17	8.43	2.02	3.86	62.81
202L	3.6	0.25	12.58	3.31	8.81	86.74
203L	4.85	0.12	13.01	2.06	19.77	42.10
301L	3.2	0.06	3.94	1.74	2.09	23.68
302L	2.7	0.10	5.48	11.62	7.19	302.55
401L	6.5	0.04	4.50	2.79	1.67	19.16
402L	3.3	0.02	2.51	1.85	0.73	6.03
501L	0.15	0.01	0.29	0.57	0.27	5.80
502L	0.15	0.01	0.38	1.07	0.52	9.29
503L	0.15	0.01	0.38	0.90	0.41	31.87
GB1L	n/a	0.04	12.21	1.02	4.94	36.32
GB2L	n/a	0.04	7.82	1.12	2.14	17.11
GB3L	n/a	0.04	1.92	0.71	0.88	6.86
GB4L	n/a	0.06	2.34	1.19	2.76	12.99
GB5L	n/a	0.02	1.14	0.52	1.15	7.26
GB6L	n/a	0.03	2.67	1.16	1.45	15.41
GB7L	n/a	0.02	1.39	0.67	0.95	7.72
GB8L	n/a	0.03	2.09	0.68	3.18	16.45
GB9L	n/a	0.01	0.45	0.31	0.68	6.73
GB10L	n/a	0.01	0.28	0.21	0.50	3.72

Sample ID	Salinity (*psu)	Cd (*µg/g)	Pb (µg/g)	Ni (µg/g)	Cu (µg/g)	Zn (µg/g)
GB11L	n/a	0.01	2.03	1.58	0.71	5.35
GB12L	n/a	0.02	1.46	2.23	1.26	8.02
E31L	n/a	0.08	4.58	2.95	10.18	29.72
E32L	n/a	0.07	4.99	3.14	2.29	18.86
E33L	n/a	0.07	4.43	2.55	1.27	7.19
E34L	n/a	0.06	3.87	2.48	1.64	21.35
E35L	n/a	0.26	14.03	8.50	5.76	37.69
E36L	n/a	0.05	3.95	2.43	1.61	11.00
E37L	n/a	0.06	2.69	2.32	1.44	12.44
E38L	n/a	0.07	3.38	3.44	3.69	30.64
E39L	n/a	0.05	2.76	2.19	1.58	11.21
E310L	n/a	0.04	2.88	2.06	0.98	5.99
E311L	n/a	0.04	3.01	2.05	1.03	4.89
E312L	n/a	0.04	2.68	2.15	1.06	5.00
E313L	n/a	0.04	2.47	2.34	1.21	7.12
E314L	n/a	0.04	2.80	2.49	1.09	6.24
E315L	n/a	0.03	2.26	2.07	0.76	4.60
E316L	n/a	0.03	2.34	2.06	1.11	5.30
E317L	n/a	0.03	2.44	2.36	1.48	10.79
E318L	n/a	0.03	2.64	1.74	1.13	6.19
E319L	n/a	0.02	2.59	1.93	1.03	6.98
E320L	n/a	0.03	1.86	2.43	2.83	24.24
E321L	n/a	0.04	3.16	2.66	295.42	211.29
E322L	n/a	0.02	2.65	2.02	112.80	81.88

Sample ID	Salinity (*psu)	Cd (*µg/g)	Pb (µg/g)	Ni (µg/g)	Cu (µg/g)	Zn (µg/g)
E323L	n/a	0.04	2.99	2.29	21.12	23.71

*psu = practical salinity unit; µg/g = micrograms per gram

Table 5. Heavy metal concentrations in Galveston Bay bulk sediments and corresponding salinity measurements at each sample station.

Sample ID	Salinity (*psu)	Cd (*µg/g)	Pb (µg/g)	Ni (µg/g)	Cu (µg/g)	Zn (µg/g)
1D 06-17	22.548	0.06	6.60	6.38	4.54	35.29
2D 06-17	18.954	0.06	6.36	6.07	4.21	31.28
4D 06-17	15.175	0.09	10.66	11.43	6.84	50.42
5D 06-17	15.263	0.10	12.45	12.20	8.36	55.97
7D 06-17	14.117	0.11	13.95	13.70	8.96	64.50
8D 06-17	10.432	0.12	13.70	14.51	10.01	68.96
9D 06-17	7.494	0.11	8.99	8.92	7.10	52.88
10D 06-17	18.863	0.09	10.86	11.42	7.87	64.19
1D 09-17	7.899	0.05	5.62	5.63	4.07	42.30
2D 09-17	3.214	0.05	6.21	6.50	4.51	44.99
3AD 09-17	2.698	0.05	6.56	6.52	4.39	34.55
3BD 09-17	6.103	0.05	6.21	5.88	3.45	32.01
5D 09-17	2.358	0.08	10.06	10.59	6.68	46.92
7D 09-17	1.882	0.13	15.42	16.85	11.85	95.18
8D 09-17	0.661	0.14	12.50	12.35	9.15	78.51
9D 09-17	0.186	0.10	10.26	9.29	6.54	50.98
1D 11-17	25.476	0.07	10.47	10.97	7.54	61.56
3D 11-17	18.432	0.04	5.98	5.27	3.44	31.67
5D 11-17	9.592	0.08	8.64	9.36	6.87	64.58

Sample ID	**Salinity (*psu)**	**Cd (*µg/g)**	**Pb (µg/g)**	**Ni (µg/g)**	**Cu (µg/g)**	**Zn (µg/g)**
9D 11-17	20.304	0.12	10.42	10.20	6.48	45.49
12D 11-17	11.302	0.11	12.10	11.98	7.96	57.89
13D 11-17	12.527	0.06	6.44	5.52	4.50	59.02
14D 11-17	15.888	0.10	12.06	12.78	8.34	69.93
5D 03-18	14.12	0.09	11.56	13.00	8.20	66.14
9D 03-18	0.273	0.22	16.82	19.31	14.11	194.49
12D 03-18	2.533	0.11	10.84	9.91	7.47	49.39
13D 03-18	8.527	0.08	6.82	4.83	3.99	33.55
14D 03-18	14.361	0.05	6.57	4.71	3.27	28.57
15D 03-18	25.155	0.11	14.43	14.37	11.53	67.27
1D 06-18	29	0.09	10.00	8.92	8.33	67.52
5D 06-18	33	0.12	10.32	9.90	7.08	53.85
9D 06-18	9.8	0.05	7.18	6.36	3.99	42.57
12D 06-18	14	0.10	12.17	11.60	8.51	56.70
13D 06-18	18.6	0.04	6.59	5.19	4.44	34.05
14D 06-18	25	0.04	5.44	3.88	2.34	35.30
3D 09-18	17.897	0.07	6.56	5.96	5.59	33.21
5D 09-18	20.2449	0.13	12.72	13.67	10.13	56.81
9D 09-18	12.7436	0.13	11.21	10.93	8.72	43.52
11D 09-18	25.3671	0.06	7.26	9.00	5.14	32.55
12D 09-18	15.5935	0.12	12.22	12.40	9.31	49.85
13D 09-18	16.0797	0.02	1.95	1.79	1.69	8.64
14D 09-18	16.9239	0.04	6.18	4.67	3.49	20.69
1D 11-18	23.17	0.05	7.61	7.82	5.88	31.91

Sample ID	Salinity (*psu)	Cd (*µg/g)	Pb (µg/g)	Ni (µg/g)	Cu (µg/g)	Zn (µg/g)
3D 11-18	10.74	0.07	6.70	5.60	5.67	35.78
5D 11-18	10.75	0.12	13.28	14.89	10.73	64.22
9D 11-18	0.155	0.18	12.78	12.39	12.20	85.23
11D 11-18	23.41	0.06	5.95	5.07	3.52	27.65
12D 11-18	0.198	0.14	12.98	12.84	9.74	52.83
13D 11-18	5.218	0.05	4.53	3.74	3.70	18.40
14D 11-18	8.384	0.05	5.75	4.79	3.58	31.72
1D 03-19	18.102	0.08	11.36	11.50	9.25	51.09
3D 03-19	12.946	0.05	6.22	5.97	3.97	25.93
5D 03-19	12.977	0.14	13.58	14.55	9.73	54.32
9D 03-19	1.148	0.14	12.49	11.76	9.93	57.72
12D 03-19	7.604	0.12	13.81	13.81	10.19	51.03
13D 03-19	10.188	0.03	6.41	6.27	3.80	16.79
14D 03-19	12.587	0.04	6.12	5.53	4.22	28.10
1D 06-19	13.7	0.06	8.20	9.00	5.82	55.75
3D 06-19	8.4	0.05	6.64	9.21	5.71	26.10
5AD 06-19	4.5	0.12	13.29	14.00	9.97	52.12
5BD 06-19	10.5	0.09	13.42	16.84	9.60	65.08
9D 06-19	0.16	0.14	13.69	13.89	9.72	57.97
12D 06-19	0.4	0.18	13.72	14.05	10.90	56.56
13D 06-19	1.85	0.13	14.65	15.14	12.35	64.98
101D	1.3	0.16	13.31	13.70	19.18	93.81
102D	0.8	0.16	14.16	19.49	19.26	114.94
103D	0.3	0.14	13.97	12.84	16.37	94.77

Sample ID	Salinity (*psu)	Cd (*µg/g)	Pb (µg/g)	Ni (µg/g)	Cu (µg/g)	Zn (µg/g)
201D	6.15	0.23	16.19	12.22	18.10	100.10
202D	3.6	0.46	26.25	14.51	28.07	132.04
203D	4.85	0.17	21.02	7.14	76.96	61.14
301D	3.2	0.14	13.41	9.74	13.75	64.63
302D	2.7	0.07	7.82	6.14	7.54	32.05
401D	6.5	0.07	11.40	11.82	7.43	44.14
402D	3.3	0.12	29.19	30.25	16.77	92.71
501D	0.15	0.02	3.18	2.69	1.29	9.57
502D	0.15	0.02	2.33	1.07	0.76	4.31
503D	0.15	0.03	3.27	2.52	2.38	12.99
GB1D	n/a	0.08	15.83	3.09	6.92	41.03
GB2D	n/a	0.07	15.51	5.37	6.98	23.82
GB3D	n/a	0.07	8.09	4.94	4.29	19.73
GB4D	n/a	0.11	9.42	12.34	8.35	33.92
GB5D	n/a	0.07	4.07	2.08	3.29	19.98
GB6D	n/a	0.08	10.99	5.54	5.19	43.07
GB7D	n/a	0.06	5.07	3.71	4.92	34.72
GB8D	n/a	0.06	5.44	3.48	25.47	25.14
GB9D	n/a	0.04	4.69	3.08	3.49	15.91
GB10D	n/a	0.03	1.76	1.94	2.14	15.49
GB11D	n/a	0.09	7.27	4.93	5.08	32.40
GB12D	n/a	0.11	11.55	13.56	9.77	71.51
E31D	n/a	0.14	14.00	12.31	29.34	82.79
E32D	n/a	0.16	16.21	14.49	11.94	63.84

Sample ID	Salinity (*psu)	Cd (*µg/g)	Pb (µg/g)	Ni (µg/g)	Cu (µg/g)	Zn (µg/g)
E33D	n/a	0.12	13.59	12.73	9.95	52.91
E34D	n/a	0.14	16.11	15.89	12.40	72.19
E35D	n/a	0.13	14.20	13.36	10.14	54.61
E36D	n/a	0.15	17.95	15.97	12.41	65.82
E37D	n/a	0.15	14.50	14.90	13.71	63.35
E38D	n/a	0.12	13.82	14.99	11.48	66.00
E39D	n/a	0.06	9.17	10.93	8.53	44.19
E310D	n/a	0.10	13.61	14.18	10.65	51.22
E311D	n/a	0.09	10.48	11.65	8.93	49.83
E312D	n/a	0.12	10.88	12.48	11.42	73.36
E313D	n/a	0.09	12.00	14.66	11.30	49.94
E314D	n/a	0.09	11.44	12.88	9.98	50.31
E315D	n/a	0.08	11.41	12.36	9.70	50.43
E316D	n/a	0.12	12.17	14.23	12.40	68.57
E317D	n/a	0.08	10.07	11.07	7.31	47.04
E318D	n/a	0.07	10.04	11.89	8.21	37.79
E319D	n/a	0.15	16.18	18.18	17.43	62.48
E320D	n/a	0.07	10.42	13.75	9.72	56.13
E321D	n/a	0.07	8.89	10.60	351.84	244.47
E322D	n/a	0.08	9.86	11.26	167.71	128.65
E323D	n/a	0.10	10.53	12.25	45.77	336.65

*psu = practical salinity unit; µg/g = micrograms per gram

Table 6. Galveston Bay sediment heavy metal concentration summary.

Metal (*µg/g)	Sediment type	Leachates	Bulk sediments
Cd	Surface (average, *SD) *Core (average, SD)*	0.01 – 0.3 (0.05, 0.03) *0.02 – 0.3 (0.1, 0.05)*	0.02 – 0.5 (0.1, 0.1) *0.06 – 0.2 (0.1, 0.03)*
Cu	Surface (average, SD) *Core (average, SD)*	0.3 – 19.8 (1.7, 2.4) *0.8 – 295.4 (20.5, 64.3)*	0.8 – 77.0 (8.6, 8.8) *7.3 – 351.8 (34.9, 76.6)*
Ni	Surface (average, SD) *Core (average, SD)*	0.2 – 13.3 (1.7, 1.8) *1.7 – 8.5 (2.6, 1.3)*	1.1 – 30.3 (9.3, 4.9) *10.6 – 18.1 (13.3, 1.9)*
Pb	Surface (average, SD) *Core (average, SD)*	0.3 – 13.0 (3.1, 2.2) *1.9 – 14.0 (3.5, 2.4)*	1.8 – 29.2 (10.1, 4.7) *8.9 – 18.0 (12.5, 2.6)*
Zn	Surface (average, SD) *Core (average, SD)*	3.7 – 302.6 (19.0, 32.8) *4.6 – 211.3 (25.4, 44.0)*	4.3 – 194.5 (50.1, 28.5) *37.8 – 336.6 (81.4, 69.8)*

µg/g = micrograms per gram; SD = Standard Deviation

Heavy metal concentrations in sediment leachates

Leachates represent metals adsorbed to sediment grain surfaces, which may be bioavailable to organisms depending on metal speciation within the system (Berger et al., 2008). The percentages of each element in the leachable fraction of Galveston Bay sediments range as follows: Cd 15% – 87% (average of 46%), Cu 4.4% – 95% (average of 22%), Ni 6% – 100% (average of 19%), Pb 9% – 99% (average of 29%), and Zn 1% – 89% (average of 31%). These percentages indicate that metal lability in Galveston Bay sediments follows the order of Cd > Zn > Pb > Cu, Ni. Individual metal concentrations were assessed as a function of Al, Fe and Mn concentrations for the Galveston Bay sediment samples. Aluminum is a tracer for lithogenic phases in estuarine sediments; thus, strong linear relationships with Al ($R^2 > 0.89$) indicate predominantly natural (lithogenic) metal sources (Lam et al., 2015; Ohnemus and Lam, 2015). Likewise, metal correlations with Fe and Mn concentrations can be used as proxies for the Fe-Mn oxide phases estuarine sediments, which are typically authigenic (Lam et al., 2015; Koschinsky and Hein, 2003). Nonlinear relationships between metals and Al, Fe, and Mn concentrations can indicate anthropogenically sourced metals or reflect estuarine sediment processes like resuspension and flocculation (Wen et al., 2008; Sharma et al., 1999). No metals in the leachate fraction display linear relationships with the leachate Al, Fe, or Mn concentrations (R^2 between 0.004 – 0.49). This makes sense given that leachates represent surface-adsorbed metals, which are often associated with contaminant releases. Bulk sediment Ni and Cr are strongly correlated with both Al and Fe concentrations ($R^2 = 0.89 – 0.94$) indicating that these metals reside in the lithogenic or Fe oxide sediment fraction. The strong linear correlation between Al and

Fe ($R^2 = 0.96$) indicates that the Fe-Mn oxide phases in Galveston Bay sediments covary with the lithogenic phases; thus, metal to Al and metal to Fe linear correlations cannot be used to distinguish metal associations with Fe-Mn oxide versus lithogenic phases. Subsequently, the strong correlations (R^2 between 0.89 – 0.94) between the Ni and Cr concentrations and Al and Fe concentrations in the bulk sediments indicates that these metals are associated with the Fe (oxyhydr) oxide phase or that these metals are predominantly naturally sourced. Weak correlations (R^2 between 0.04 – 0.77) exist between the Pb, Sb, As, Zn, Cd, Cu and Hg concentrations and Al, Fe and Mn concentrations in the bulk sediments indicating that these metals may be anthropogenically sourced and influenced by processes such as flocculation, resuspension, and diagenesis. No clear assessment of metal speciation in Galveston Bay sediments can be made based on metal concentration correlation data alone.

Previous work has shown that artifacts result from the 0.02M HH-acetic acid leach method (Graney et al. 1995; Sholkovitz, 1989; Chester and Hughes, 1967). For example, Graney et al. (1995) demonstrated that different Pb concentrations and isotope ratios were measured in the same sediments when leached with acetic acid versus HCl, HNO_3, and HCl and HNO_3 leaching solutions. Several studies have found that re-adsorption of leached metals back onto sediment grains often occurs during sequential leaching procedures, including the 0.02M HH-acetic acid leach method (Piper and Wandless, 1992; Nirel and Morel, 1990; Sholkovitz, 1989). Furthermore, there are no SRMs with certified leachate metal concentrations by which the accuracy of leached metal concentrations can be evaluated. Considering these issues, the sediment leachate data presented here is interpreted only for potential lability within the system and anthropogenic versus natural metal sourcing in Galveston Bay. Data from the bulk sediment digests will be used to evaluate the spatiotemporal trends, toxicity, heavy metal enrichment and heavy metal sourcing in Galveston Bay sediments.

Spatial variability in bulk surface sediment heavy metal concentrations

The primary control on sediment metal concentrations in Galveston Bay is their spatial location across all sampling time points, namely their location east or west of the HSC. Heavy metal concentrations were highest to the east of the HSC in Trinity Bay and near the entrance of East Bay (Figs. 3-5). Stations 4, 5, 7, 8, 9, and 12 are located to the east of the HSC and possessed mean ± standard deviation (SD) metal concentrations of Cd 0.12 ± 0.03 µg/g, Pb 12.17 ± 1.96 µg/g, Ni 12.55 ± 2.61 µg/g, Cu 8.93 ± 1.97 µg/g, and Zn 62.59 ± 26.24 µg/g. Stations 2, 3, 11, 13, and 14 are located to the west of the HSC and have mean ± SD metal concentrations of Cd 0.06 ± 0.02 µg/g, Pb 7.33 ± 2.68 µg/g, Ni 7.02 ± 3.10 µg/g, Cu 5.20 ± 2.45 µg/g, and Zn 38.07 ± 15.98 µg/g. Shoreline station metal concentrations mimicked the east/west divide seen in the bay stations metal concentrations such that shoreline stations on the Galveston Bay eastern border possessed higher metal concentrations than stations on the western border (Fig. 3). Shoreline station GB1 is located north of Galveston Bay proper near the convergence of the San Jacinto River and Buffalo Bayou/HSC, for this reason it is not considered indicative of the main bay, and it is not included in the eastern versus western bay metal distribution assessment. Endmember Stations 101, 102, 103, 201, 202, 203, 301, 302, 401 and 402 bulk sediment metal concentrations were within the range of concentrations observed at bay stations east of the HSC. Stations 501-503 (Trinity River endmember stations) bulk sediment metal concentrations were substantially lower than the other endmember stations with Cd of 0.02 – 0.03 µg/g, Pb of 2.33 – 3.27 µg/g, Ni of 1.07 – 2.69 µg/g, Cu of 0.76 – 2.38 µg/g, and Zn of 4.31 – 12.99 µg/g.

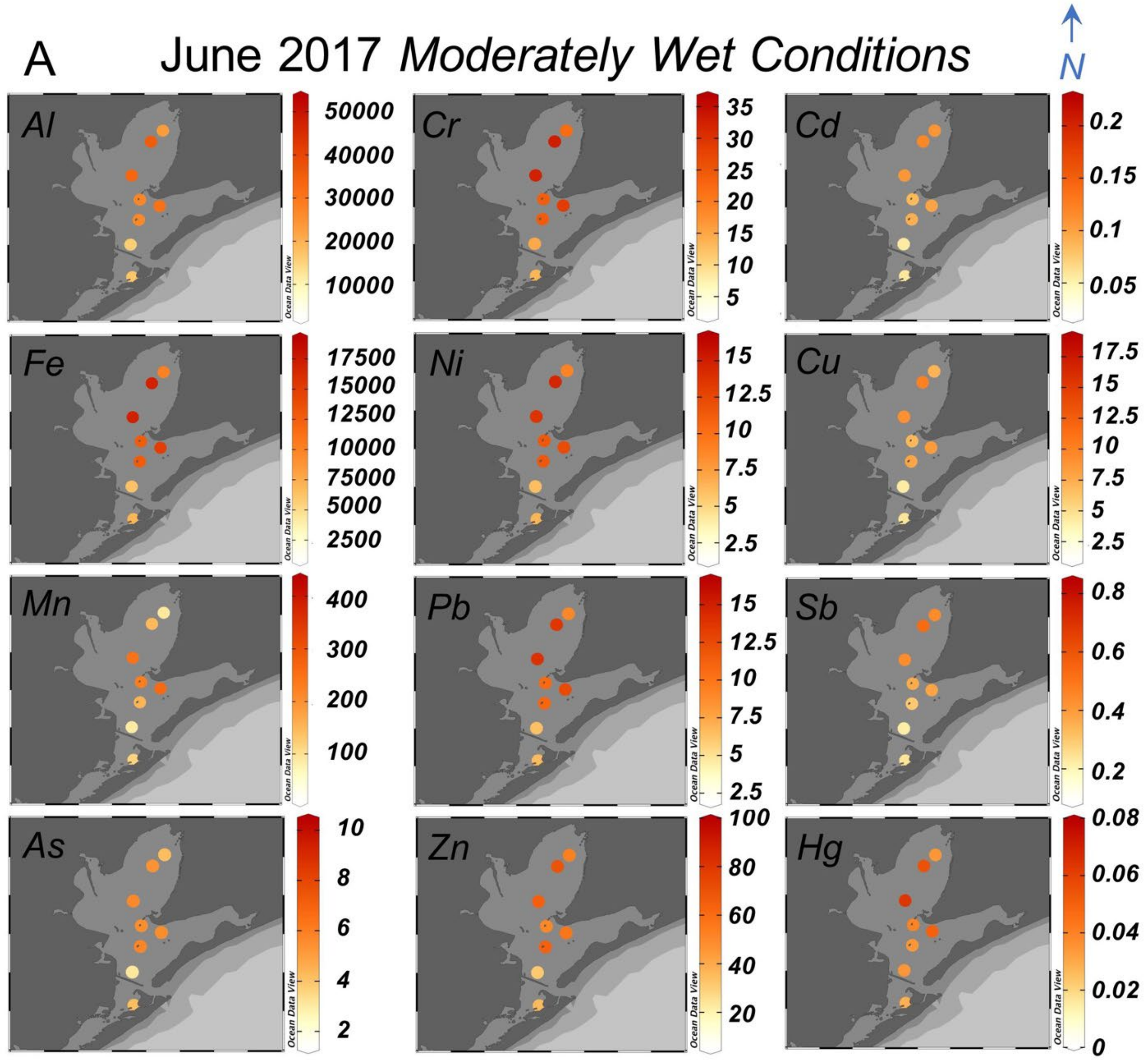

The June 2017 bay station samples were collected during moderately wet conditions, which correspond with medium levels of Trinity River discharge (170 – 340 m^3/s). m^3/s = Cubic meters per second.

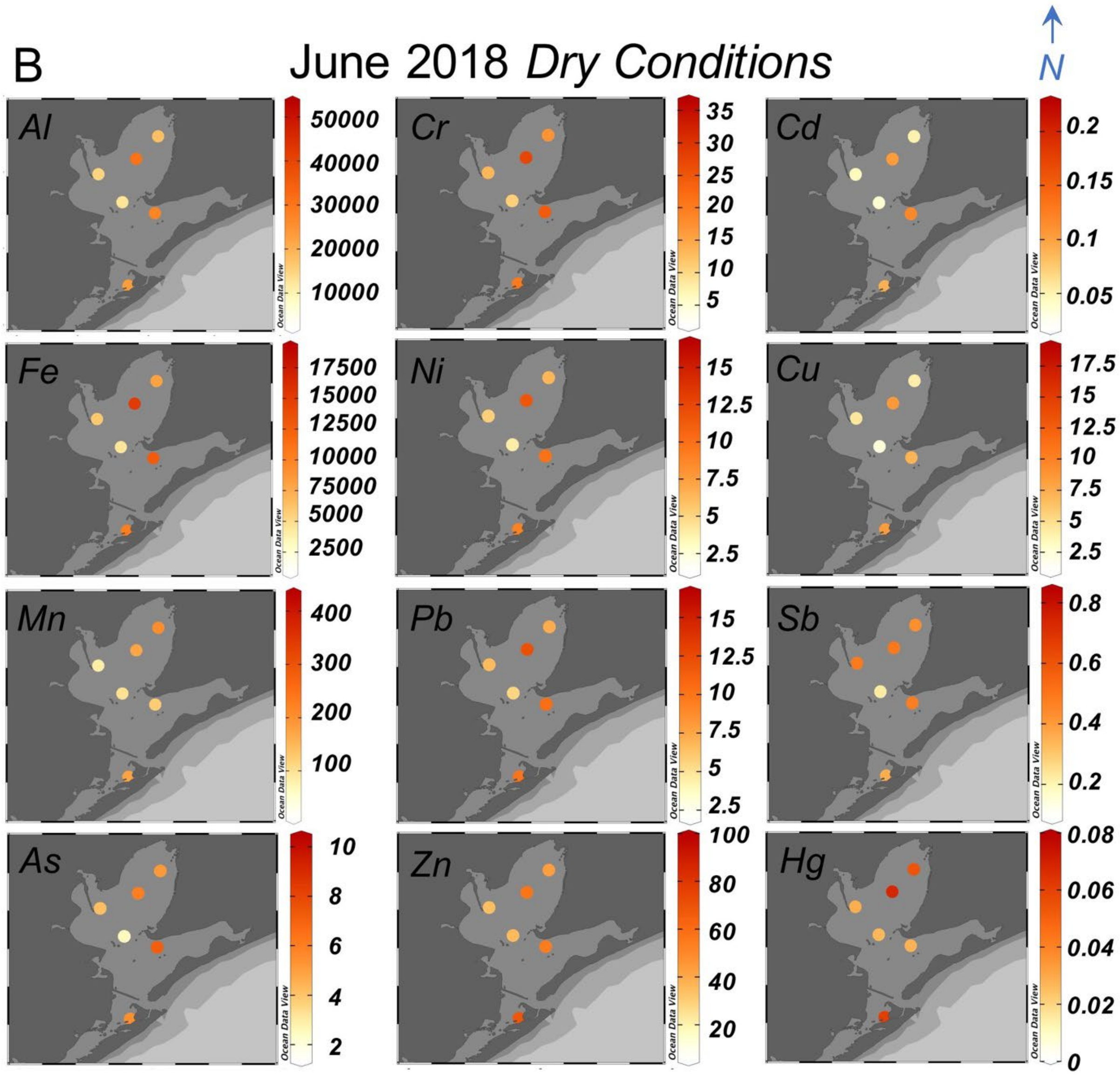

The June 2018 bay station samples were collected during dry conditions, which correspond with low levels of Trinity River discharge (0 – 170 m^3/s). m^3/s = Cubic meters per second.

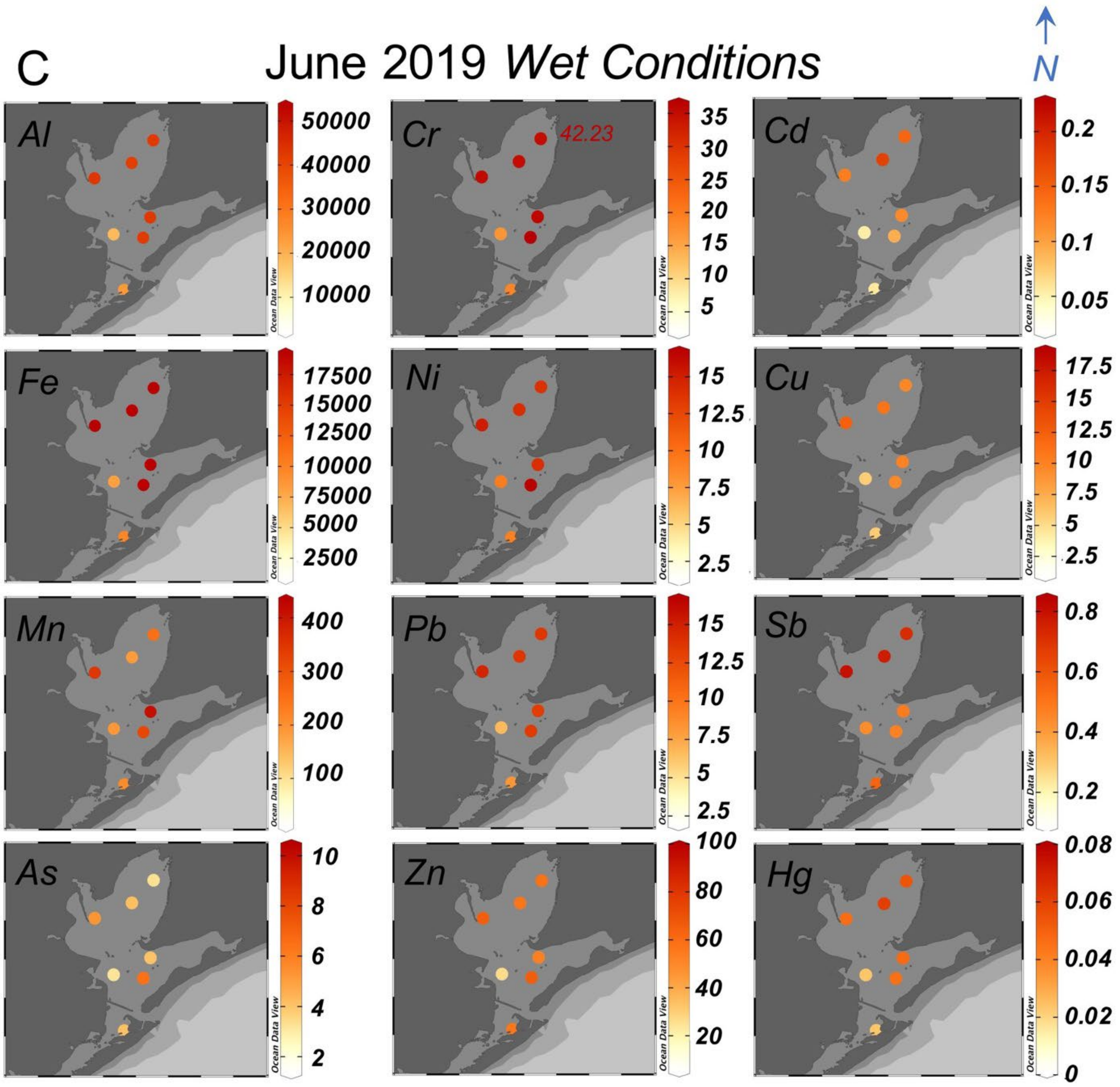

The June 2019 bay station samples were collected during wet conditions, which correspond with high levels of Trinity River discharge (340+ m^3/s). These three timepoints highlight the spatiotemporal trends in sediment heavy metal concentration variation in Galveston Bay. Spatially, eastern bay stations have higher metal concentrations than western bay stations. Temporally, metal concentrations are higher during wet conditions (high riverine discharge) and lower during dry conditions (low riverine discharge). m^3/s = Cubic meters per second.

Figure 3. Spatiotemporal variation in Galveston Bay bulk sediment heavy metal concentrations (µg/g) at bay stations during the June sampling events in this study from 2017 (A), 2018 (B), and 2019 (C).

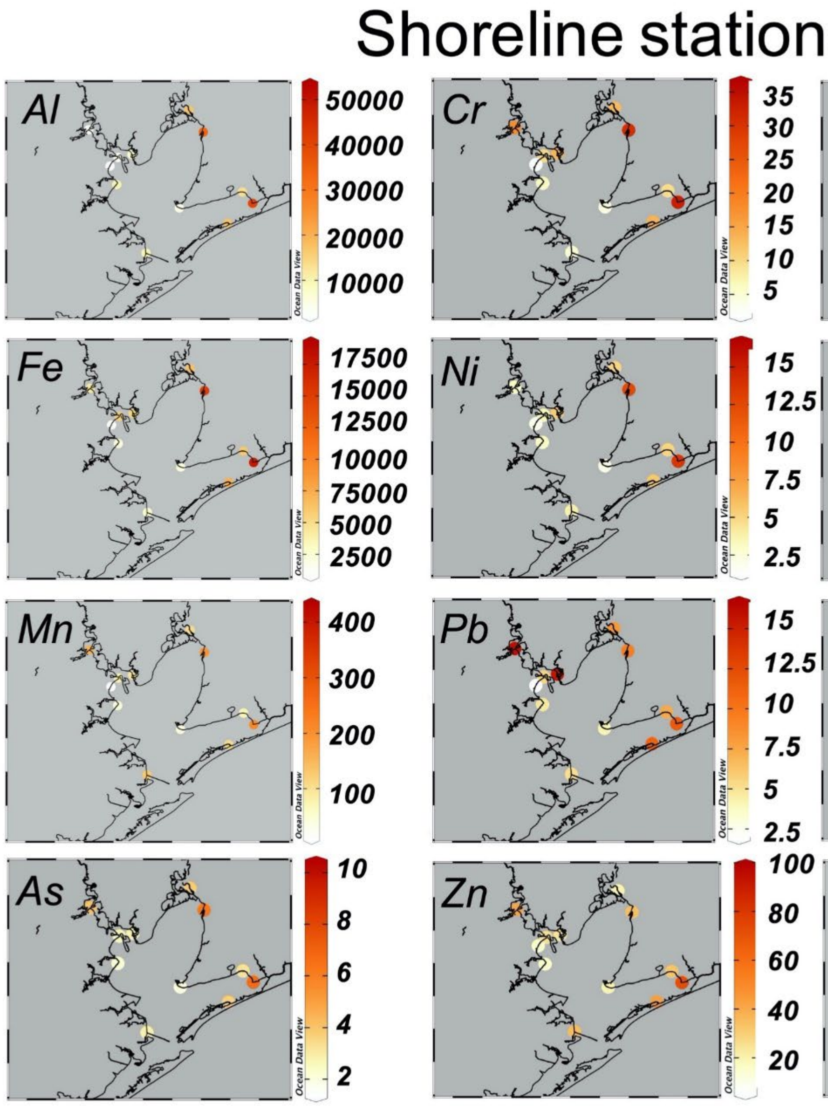

These stations were sampled once during the study period; thus they are considered for spatial variation only.

Figure 4. Galveston Bay bulk sediment heavy metal concentrations (µg/g) at shoreline stations.

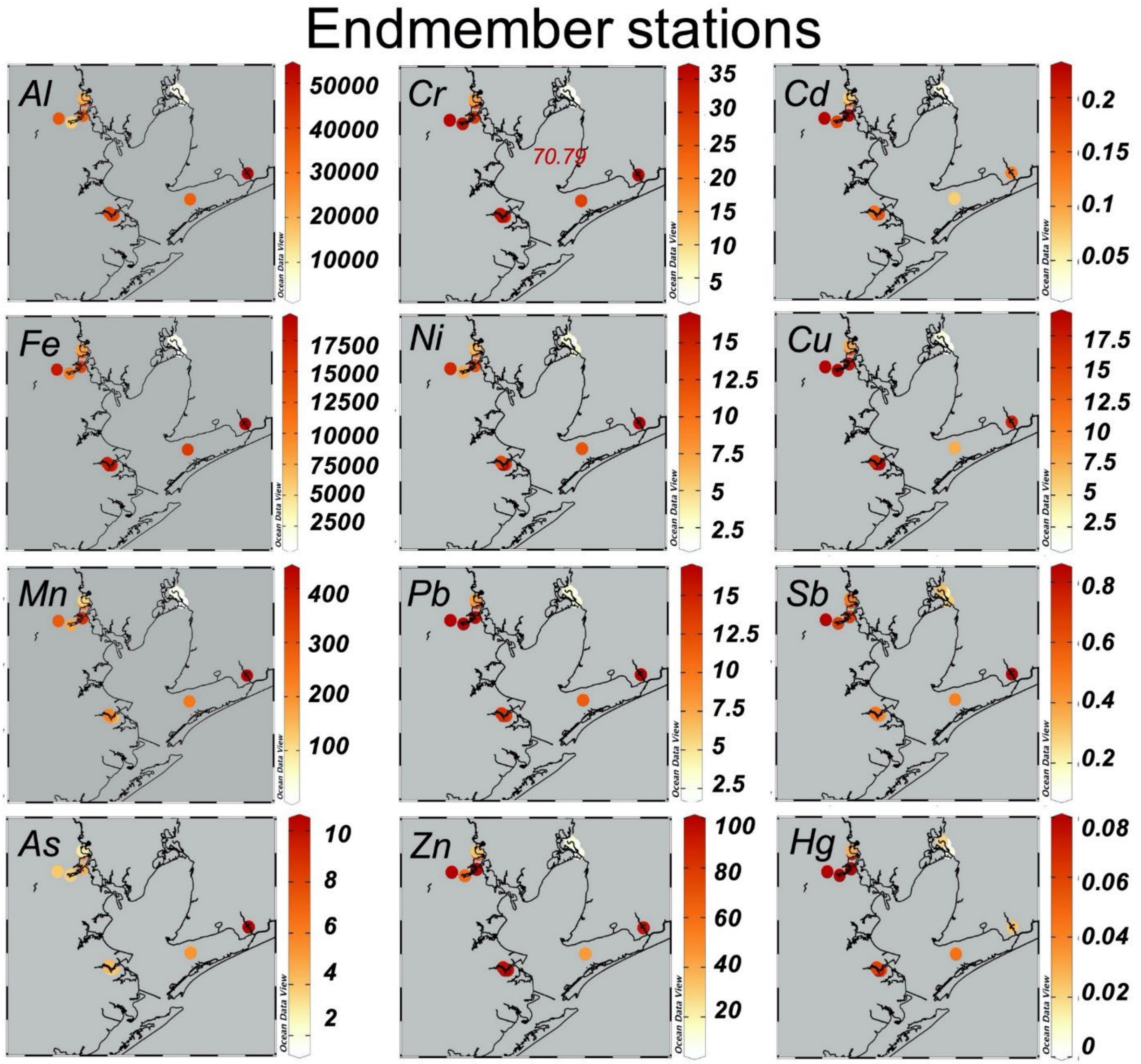

b.d. = below detection.

Figure 5. Galveston Bay bulk sediment heavy metal concentrations (µg/g) at endmember stations. These stations were sampled once during study period; thus they are considered for spatial variation only.

Temporal variability in bulk surface sediment heavy metal concentrations

A secondary control on the variability of metal concentrations in Galveston Bay sediments is temporal variability in freshwater discharge to the bay, which can carry sediments into the bay directly as well as move the flocculation boundary closer (under dry conditions) or farther (under wet conditions) from the river mouth. Metal concentrations were lower during periods of low Trinity River discharge and higher when Trinity River discharge was high (Fig. 3; Table 7). The Trinity River is the largest inflow to Galveston Bay contributing an estimated 55%-77% of the freshwater to the bay (Du et al., 2019a-b; Guthrie et al., 2012). The San Jacinto River and Buffalo Bayou are the second and third largest freshwater inflows supplying a collected 20%-28% of the Galveston Bay freshwater input (Du et al., 2019a-b; Guthrie et al., 2012). Table 7 summarizes Trinity River discharge over the study period based on river gage data from the U.S. Geological Survey (USGS). Trinity River discharge <250 cubic meters per second (m^3/s) constitutes dry conditions and Trinity River discharge >250 m^3/s indicates wet conditions. Using this categorization, dry conditions occur during the November 2017, June 2018, and September 2018 sampling events and wet conditions prevail during June 2017, September 2017, March 2018, November 2018, March 2019, and June 2019. From Aug. 26 through Aug. 30 Hurricane Harvey moved across southeast Texas depositing record-breaking rainfall totals which resulted in massive freshwater fluxes through Galveston Bay (Steichen et al., 2020). Consequently, the typical flocculation of dissolved metals did not occur (bay freshening due to high freshwater flux), and the September 2017 bulk sediment metal concentrations resemble metal concentrations for samples collected during dry conditions.

Table 7. Study period Trinity River discharge summary.

Sampling event	Average Trinity River discharge (m^3/s)	Discharge conditions	Bay conditions
June 2017	257	Medium	Moderate wet
September 2017*	387 / 85	High / Low	Wet
November 2017	28	Low	Dry
March 2018	298	Medium	Moderate wet
June 2018	3	Low	Dry
August 2018	4	Low	Dry
September 2018	35	Low	Dry
November 2018	602	High	Wet
March 2019	331	Medium	Moderate wet
June 2019	514	High	Wet

Low discharge is between 0 – 170 m^3/s, medium discharge is between 170 – 340 m^3/s and high discharge is 340+ m^3/s.*Two sampling dates have different conditions; the September 2017 sampling event is classified as “wet” following the passage of Hurricane Harvey. m^3/s = Cubic meters per second.

Temporal variability in bulk core sediment heavy metal concentrations

The E3 core, sampled from Trinity Bay, presents an opportunity to study the longer-term temporal variability of metal concentrations at a single location in Galveston Bay. Previous ^{210}Pb dating of the E3 core established the year 1968 at a depth of 37 cm and estimated an age model using an average sedimentation rate of 0.41 cm/year for this site and bulk density correction for depth based off of sediment water content (Pekowski, 2017). Accordingly, the E3-23 subsample approximately represents the year ~1880 and the E3-1 subsample represents the year 2016. The highest Cu (167.71 – 351.84 µg/g) and Zn (128.65 – 244.47 µg/g) concentrations of all sediments measured in this study are between ~1880-1914 (core depths 100-111 cm). These concentrations are anomalously high and may be the result of unique historical pollution or sample contamination. These data points are thus omitted from further discussion as their validity cannot be confirmed. The long-term trends in sediment heavy metal concentrations in the E3 core can be used to approximate whether Galveston Bay sediments are getting cleaner with respect to metals over time. Between 1920 and the 1990s Zn concentrations increase, while Cu is generally consistent (Fig. 6b). Aside from E3-19 (year ~1927), Pb, Ni, and Cd concentrations generally increase from the late 1800s into the 1990s (Fig. 6), in line with industrialization increasing their fluxes to bay sediments. Importantly, Pb, Ni, and Cd concentrations level off from the 1990s to present day, whereas the Cu and Zn concentrations increase, particularly since 2009 (Fig. 6b).

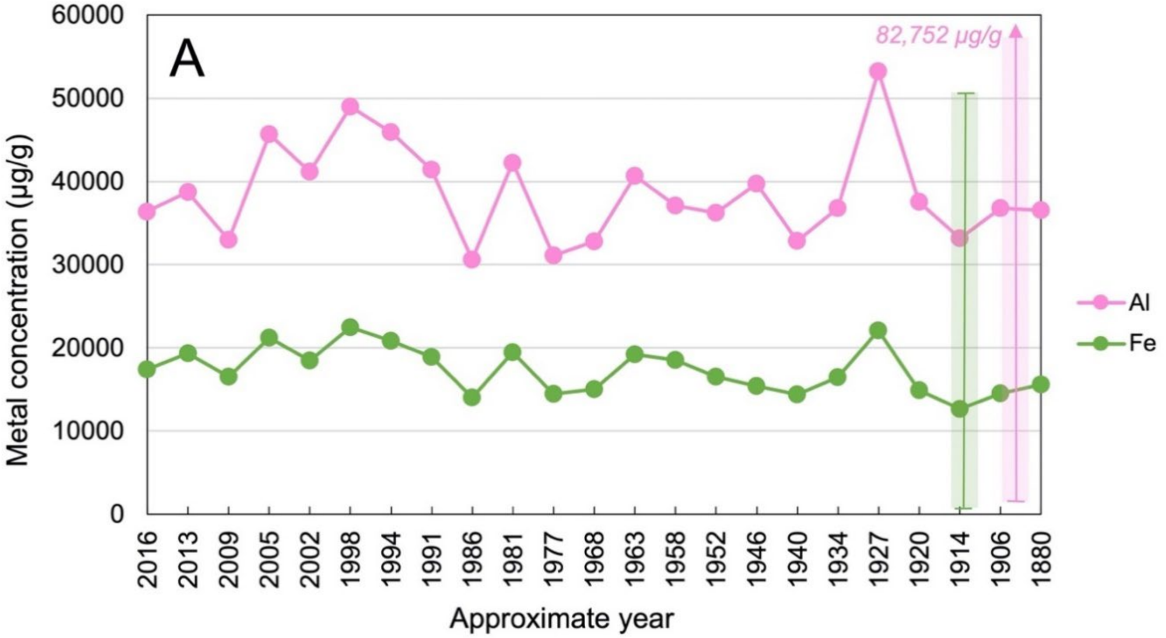

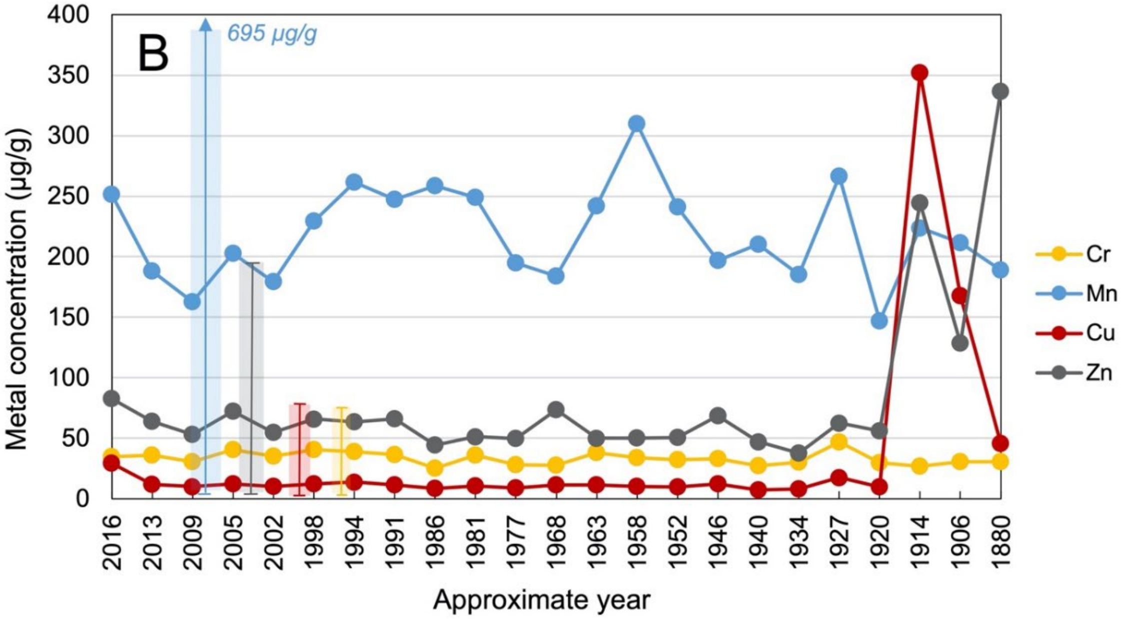
B
695 µg/g
Metal concentration (µg/g)
0
50
100
150
200
250
300
350
400
2016
2013
2009
2005
2002
1998
1994
1991
1986
1981
1977
1968
1963
1958
1952
1946
1940
1934
1927
1920
1914
1906
1880
Approximate year
Cr
Mn
Cu
Zn

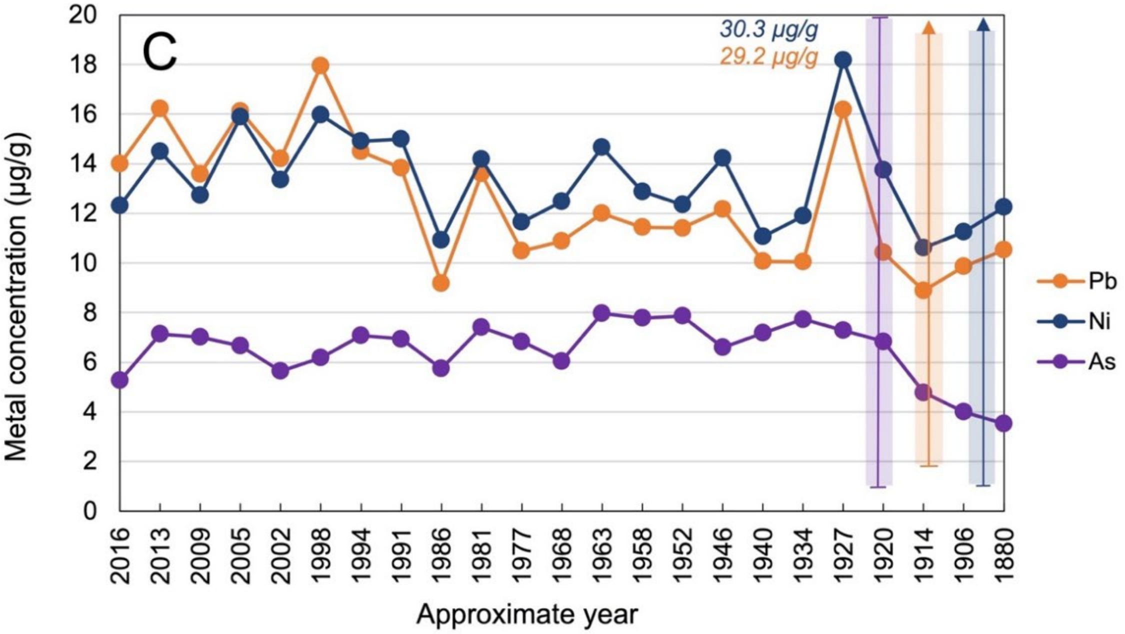
C
30.3 µg/g
29.2 µg/g
Metal concentration (µg/g)
0
2
4
6
8
10
12
14
16
18
20
2016
2013
2009
2005
2002
1998
1994
1991
1986
1981
1977
1968
1963
1958
1952
1946
1940
1934
1927
1920
1914
1906
1880
Approximate year
Pb
Ni
As

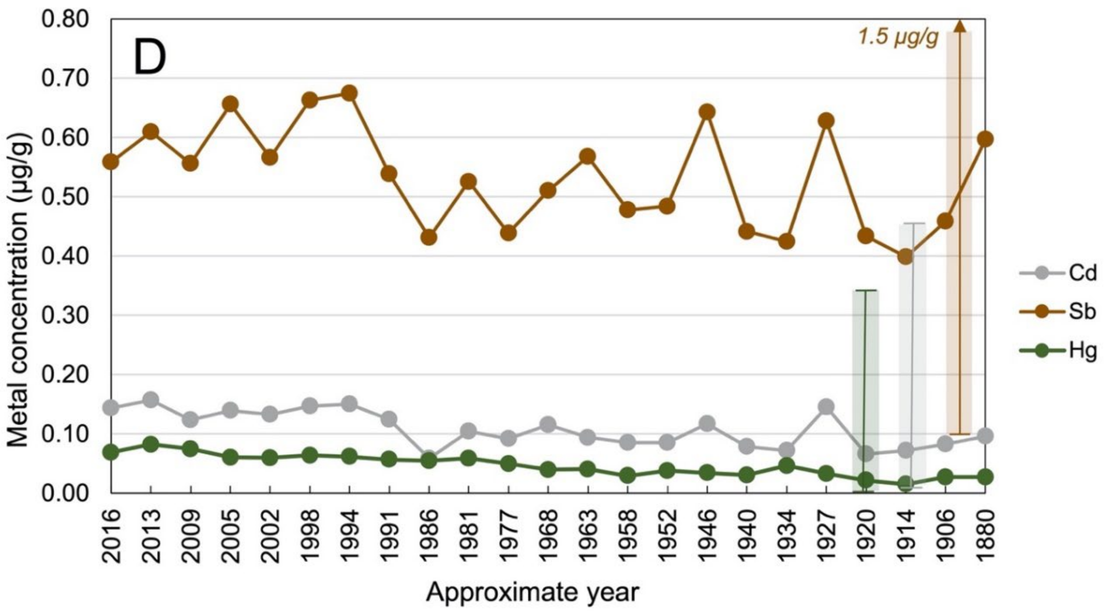

Corresponding surface sediment metal concentration ranges shown for reference using colored, shaded bars. In cases where the surface sediment metal concentration range upper limit is larger than figure scale, the upper limit range value is listed.

Figure 6. Temporal variation in bulk sediment E3 core subsamples. The E3 core sediments represent the years 1880 to 2016. Temporal variation in Al and Fe (A), Cr, Mn, Cu and Zn (B), Pb Ni and As (C) and Cd, Sb and Hg (D) concentrations are shown in each panel.

Galveston Bay Sediment Pb Isotope Ratios

The Pb isotope ratios and concentrations determined in this study are presented in Tables 8, 9, and 10. Sediment leachates are indicated with an "L" identifier, sediment residues are labelled with an "R" identifier, and bulk sediment digests are marked with a "D" identifier in all subsequent tables and figures.

Table 8. Lead isotope ratios and concentrations for Galveston Bay sediment leachates.

Sample ID	Station Type	Pb (µg/g)	^{206}Pb/^{204}Pb	error	^{207}Pb/^{204}Pb	error	^{208}Pb/^{204}Pb	error	^{208}Pb/^{206}Pb	error	^{207}Pb/^{206}Pb	error
1L 06-17	Bay	1.4	19.050	0.004	15.665	0.003	38.811	0.008	2.03739	0.00009	0.82234	0.00003
2L 06-17	Bay	2.0	19.207	0.003	15.673	0.003	38.892	0.008	2.02489	0.00010	0.81601	0.00003
4L 06-17	Bay	3.1	19.103	0.002	15.661	0.002	38.814	0.005	2.03177	0.00006	0.81983	0.00002
5L 06-17	Bay	3.0	19.043	0.001	15.654	0.001	38.789	0.003	2.03698	0.00007	0.82205	0.00002
7L 06-17	Bay	4.2	19.020	0.002	15.655	0.002	38.759	0.004	2.03776	0.00007	0.82304	0.00002
8L 06-17	Bay	2.9	18.996	0.002	15.644	0.002	38.740	0.004	2.03935	0.00007	0.82353	0.00002
9L 06-17	Bay	1.8	18.972	0.004	15.626	0.003	38.716	0.008	2.04065	0.00009	0.82365	0.00003
10L 06-17	Bay	2.5	19.106	0.002	15.661	0.002	38.816	0.006	2.03165	0.00006	0.81973	0.00002
1L 09-17	Bay	1.9	19.062	0.004	15.662	0.003	38.822	0.008	2.03660	0.00008	0.82165	0.00003
2L 09-17	Bay	1.8	19.051	0.005	15.650	0.006	38.788	0.01	2.03601	0.00014	0.82146	0.00007
3AL 09-17	Bay	2.1	19.028	0.003	15.643	0.002	38.746	0.006	2.03627	0.00009	0.82212	0.00003
3BL 09-17	Bay	1.8	19.077	0.003	15.668	0.002	38.807	0.007	2.03419	0.00009	0.82130	0.00002
5L 09-17	Bay	2.8	19.138	0.002	15.636	0.002	38.805	0.005	2.02759	0.00009	0.81698	0.00002
7L 09-17	Bay	4.2	19.002	0.002	15.648	0.002	38.751	0.004	2.03938	0.00005	0.82352	0.00002

Sample ID	**Station Type**	**Pb (µg/g)**	**^{206}Pb/^{204}Pb**	**error**	**^{207}Pb/^{204}Pb**	**error**	**^{208}Pb/^{204}Pb**	**error**	**^{208}Pb/^{206}Pb**	**error**	**^{207}Pb/^{206}Pb**	**error**
8L 09-17	Bay	3.5	18.964	0.001	15.648	0.001	38.738	0.003	2.04274	0.00005	0.82514	0.00002
9L 09-17	Bay	2.1	18.963	0.003	15.627	0.002	38.710	0.006	2.04135	0.00006	0.82410	0.00002
1L 11-17	Bay	3.5	18.989	0.002	15.653	0.002	38.737	0.004	2.03998	0.00005	0.82433	0.00002
3L 11-17	Bay	2.1	18.929	0.003	15.649	0.003	38.672	0.007	2.04294	0.00008	0.82672	0.00003
5L 11-17	Bay	2.1	18.946	0.003	15.636	0.002	38.721	0.006	2.04380	0.00008	0.82532	0.00003
9L 11-17	Bay	2.5	18.959	0.003	15.654	0.002	38.727	0.006	2.04271	0.00005	0.82571	0.00002
12L 11-17	Bay	3.6	18.988	0.003	15.662	0.002	38.762	0.006	2.04137	0.00006	0.82482	0.00002
13L 11-17	Bay	2.0	18.894	0.003	15.641	0.002	38.635	0.006	2.04484	0.00007	0.82784	0.00002
14L 11-17	Bay	3.5	19.037	0.002	15.663	0.002	38.801	0.004	2.03818	0.00005	0.82275	0.00002
5L 03-18	Bay	3.1	19.082	0.002	15.662	0.002	38.832	0.004	2.03504	0.00005	0.82078	0.00002
9L 03-18	Bay	2.5	18.963	0.002	15.642	0.002	38.741	0.005	2.04298	0.00005	0.82486	0.00002
12L 03-18	Bay	3.2	18.963	0.002	15.652	0.002	38.726	0.004	2.04222	0.00005	0.82541	0.00002
13L 03-18	Bay	2.4	18.813	0.002	15.645	0.002	38.569	0.005	2.05012	0.00005	0.83159	0.00002
14L 03-18	Bay	1.8	18.858	0.003	15.646	0.004	38.616	0.006	2.04776	0.00007	0.82970	0.00002

Sample ID	**Station Type**	**Pb (µg/g)**	**^{206}Pb/^{204}Pb**	**error**	**^{207}Pb/^{204}Pb**	**error**	**^{208}Pb/^{204}Pb**	**error**	**^{208}Pb/^{206}Pb**	**error**	**^{207}Pb/^{206}Pb**	**error**
15L 03-18	Bay	4.0	19.035	0.002	15.656	0.002	38.772	0.004	2.03686	0.00004	0.82250	0.00002
1L 06-18	Bay	2.9	19.039	0.003	15.651	0.002	38.788	0.005	2.03729	0.00006	0.82204	0.00002
5L 06-18	Bay	1.7	19.058	0.003	15.666	0.003	38.810	0.007	2.03645	0.00007	0.82202	0.00003
9L 06-18	Bay	2.7	18.938	0.002	15.642	0.002	38.720	0.005	2.04458	0.00006	0.82595	0.00002
12L 06-18	Bay	3.7	18.976	0.002	15.650	0.002	38.736	0.004	2.04127	0.00005	0.82469	0.00002
13L 06-18	Bay	2.1	18.896	0.003	15.649	0.002	38.650	0.006	2.04537	0.00007	0.82813	0.00002
14L 06-18	Bay	1.3	19.020	0.005	15.652	0.004	38.758	0.01	2.03770	0.00006	0.82289	0.00003
3L 09-18	Bay	1.9	19.080	0.004	15.664	0.003	38.827	0.008	2.03490	0.00007	0.82095	0.00002
5L 09-18	Bay	4.0	19.055	0.002	15.653	0.002	38.801	0.006	2.03631	0.00008	0.82148	0.00002
9L 09-18	Bay	3.0	18.966	0.003	15.639	0.003	38.744	0.007	2.04284	0.00007	0.82462	0.00002
11L 09-18	Bay	2.6	19.198	0.004	15.661	0.004	38.952	0.009	2.02901	0.00008	0.81576	0.00003
12L 09-18	Bay	3.8	19.005	0.003	15.659	0.002	38.778	0.006	2.04043	0.00006	0.82396	0.00002
13L 09-18	Bay	2.8	18.980	0.002	15.659	0.002	38.742	0.005	2.04118	0.00008	0.82503	0.00003
14L 09-18	Bay	1.8	19.048	0.006	15.646	0.005	38.777	0.012	2.03579	0.00010	0.82144	0.00003

Sample ID	**Station Type**	**Pb (µg/g)**	**$^{206}Pb/^{204}Pb$**	**error**	**$^{207}Pb/^{204}Pb$**	**error**	**$^{208}Pb/^{204}Pb$**	**error**	**$^{208}Pb/^{206}Pb$**	**error**	**$^{207}Pb/^{206}Pb$**	**error**
1L 11-18	Bay	2.1	19.082	0.003	15.666	0.003	38.838	0.007	2.03530	0.00006	0.82095	0.00002
3L 11-18	Bay	1.2	19.039	0.004	15.657	0.003	38.776	0.008	2.03668	0.00008	0.82239	0.00003
5L 11-18	Bay	3.5	19.070	0.002	15.652	0.002	38.808	0.005	2.03502	0.00007	0.82078	0.00002
9L 11-18	Bay	2.8	18.954	0.002	15.631	0.002	38.719	0.006	2.04281	0.00007	0.82470	0.00002
11L 11-18	Bay	1.8	19.143	0.003	15.667	0.002	38.894	0.006	2.03173	0.00006	0.81841	0.00002
12L 11-18	Bay	3.5	18.986	0.002	15.649	0.002	38.741	0.004	2.04057	0.00007	0.82428	0.00002
13L 11-18	Bay	1.9	18.945	0.003	15.640	0.002	38.668	0.006	2.04107	0.00008	0.82557	0.00002
14L 11-18	Bay	1.5	19.083	0.003	15.667	0.002	38.832	0.006	2.03497	0.00008	0.82100	0.00002
1L 03-19	Bay	3.6	19.096	0.002	15.653	0.002	38.831	0.004	2.03343	0.00005	0.81967	0.00002
3L 03-19	Bay	2.6	19.062	0.002	15.656	0.002	38.800	0.004	2.03545	0.00005	0.82130	0.00002
5L 03-19	Bay	3.5	19.059	0.001	15.658	0.001	38.810	0.003	2.03636	0.00005	0.82158	0.00002
9L 03-19	Bay	3.3	18.866	0.002	15.639	0.001	38.738	0.004	2.05333	0.00004	0.82893	0.00002
12L 03-19	Bay	4.5	18.990	0.001	15.649	0.001	38.750	0.003	2.04053	0.00005	0.82404	0.00001
13L 03-19	Bay	2.7	18.987	0.002	15.647	0.002	38.736	0.004	2.04013	0.00005	0.82409	0.00002

Sample ID	**Station Type**	**Pb (µg/g)**	$^{206}\text{Pb}/^{204}\text{Pb}$	**error**	$^{207}\text{Pb}/^{204}\text{Pb}$	**error**	$^{208}\text{Pb}/^{204}\text{Pb}$	**error**	$^{208}\text{Pb}/^{206}\text{Pb}$	**error**	$^{207}\text{Pb}/^{206}\text{Pb}$	**error**
14L 03-19	Bay	2.1	19.048	0.003	15.652	0.002	38.782	0.006	2.03599	0.00006	0.82171	0.00002
1L 06-19	Bay	2.3	19.090	0.003	15.666	0.002	38.851	0.005	2.03519	0.00006	0.82064	0.00002
3L 06-19	Bay	3.2	19.069	0.002	15.666	0.002	38.832	0.004	2.03641	0.00006	0.82154	0.00002
5AL 06-19	Bay	3.8	19.034	0.001	15.656	0.001	38.806	0.003	2.03881	0.00004	0.82253	0.00001
5BL 06-19	Bay	4.4	19.054	0.001	15.657	0.001	38.809	0.003	2.03683	0.00006	0.82172	0.00002
9L 06-19	Bay	3.5	18.966	0.001	15.649	0.001	38.759	0.003	2.04359	0.00004	0.82508	0.00001
12L 06-19	Bay	4.2	18.991	0.001	15.654	0.001	38.763	0.003	2.04117	0.00005	0.82430	0.00001
13L 06-19	Bay	3.7	18.989	0.001	15.658	0.001	38.753	0.003	2.04086	0.00004	0.82459	0.00001
101L	Endmember	3.6	18.896	0.002	15.654	0.002	38.654	0.004	2.04562	0.00009	0.82841	0.00002
102L	Endmember	4.2	18.876	0.001	15.644	0.001	38.626	0.003	2.04634	0.00007	0.82880	0.00002
103L	Endmember	3.1	18.881	0.002	15.646	0.002	38.629	0.004	2.04590	0.00006	0.82864	0.00002
201L	Endmember	8.4	18.834	0.001	15.644	0.001	38.516	0.002	2.04500	0.00006	0.83061	0.00002
202L	Endmember	12.6	18.767	0.001	15.642	0.001	38.432	0.002	2.04785	0.00007	0.83348	0.00002
203L	Endmember	13.0	19.129	0.001	15.665	0.001	38.689	0.003	2.02246	0.00007	0.81888	0.00002
301L	Endmember	3.9	18.870	0.002	15.641	0.001	38.593	0.004	2.04520	0.00006	0.82890	0.00001

Sample ID	**Station Type**	**Pb (µg/g)**	**^{206}Pb/^{204}Pb**	**error**	**^{207}Pb/^{204}Pb**	**error**	**^{208}Pb/^{204}Pb**	**error**	**^{208}Pb/^{206}Pb**	**error**	**^{207}Pb/^{206}Pb**	**error**
302L	Endmember	5.5	18.905	0.002	15.648	0.002	38.645	0.004	2.04415	0.00007	0.82774	0.00002
401L	Endmember	4.5	19.046	0.002	15.654	0.002	38.795	0.004	2.03695	0.00007	0.82194	0.00002
402L	Endmember	2.5	19.025	0.002	15.657	0.001	38.823	0.004	2.04057	0.00007	0.82297	0.00002
501L	Endmember	0.3	18.930	0.011	15.600	0.008	38.721	0.021	2.04548	0.00020	0.82410	0.00010
502L	Endmember	0.4	18.985	0.01	15.616	0.008	38.769	0.02	2.04213	0.00013	0.82256	0.00005
503L	Endmember	0.4	19.024	0.096	15.567	0.08	38.616	0.196	2.02989	0.00080	0.81830	0.00034
GB1L	Shoreline	12.2	18.971	0.001	15.665	0.001	38.535	0.002	2.03124	0.00004	0.82571	0.00001
GB2L	Shoreline	7.8	18.996	0.001	15.677	0.001	38.572	0.003	2.03059	0.00001	0.82529	0.00001
GB3L	Shoreline	1.9	18.811	0.004	15.638	0.003	38.624	0.008	2.05327	0.00008	0.83131	0.00003
GB4L	Shoreline	2.3	19.009	0.003	15.648	0.003	38.812	0.008	2.04173	0.00008	0.82319	0.00002
GB5L	Shoreline	1.1	18.845	0.001	15.641	0.001	38.636	0.005	2.05020	0.00005	0.83000	0.00002
GB6L	Shoreline	2.7	18.986	0.002	15.650	0.002	38.705	0.005	2.03865	0.00008	0.82433	0.00002
GB7L	Shoreline	1.4	18.907	0.001	15.649	0.001	38.634	0.003	2.04335	0.00006	0.82767	0.00002
GB8L	Shoreline	2.1	18.868	0.003	15.656	0.003	38.565	0.008	2.04395	0.00007	0.82978	0.00002
GB9L	Shoreline	0.5	18.972	0.005	15.653	0.003	38.735	0.007	2.04166	0.00006	0.82505	0.00002
GB10L	Shoreline	0.3	19.523	0.005	15.699	0.003	38.710	0.01	1.98280	0.00005	0.80412	0.00003
GB11L	Shoreline	2.0	18.859	0.002	15.634	0.002	38.589	0.003	2.04621	0.00004	0.82900	0.00002
GB12L	Shoreline	1.5	19.198	0.002	15.660	0.002	38.951	0.005	2.02895	0.00005	0.81573	0.00002

Sample ID	**Station Type**	**Pb (µg/g)**	**^{206}Pb/^{204}Pb**	**error**	**^{207}Pb/^{204}Pb**	**error**	**^{208}Pb/^{204}Pb**	**error**	**^{208}Pb/^{206}Pb**	**error**	**^{207}Pb/^{206}Pb**	**error**
E3-1L	E3 core	4.6	18.985	0.002	15.633	0.001	38.734	0.003	2.04019	0.00008	0.82343	0.00003
E3-2L	E3 core	5.0	18.956	0.001	15.646	0.001	38.702	0.002	2.04172	0.00004	0.82542	0.00001
E3-3L	E3 core	4.4	18.989	0.001	15.617	0.001	38.652	0.002	2.03543	0.00005	0.82239	0.00001
E3-4L	E3 core	3.9	19.090	0.002	15.635	0.002	38.774	0.004	2.03108	0.00008	0.81898	0.00002
E3-5L	E3 core	14.0	19.012	0.001	15.636	0.001	38.976	0.002	2.05010	0.00004	0.82244	0.00001
E3-6L	E3 core	4.0	19.009	0.001	15.640	0.001	38.775	0.002	2.03987	0.00006	0.82275	0.00002
E3-7L	E3 core	2.7	19.211	0.002	15.557	0.002	38.768	0.004	2.01807	0.00008	0.80982	0.00002
E3-8L	E3 core	3.4	19.060	0.002	15.654	0.001	38.853	0.004	2.03843	0.00006	0.82128	0.00002
E3-9L	E3 core	2.8	18.977	0.001	15.630	0.001	38.769	0.002	2.04294	0.00400	0.82360	0.00001
E3-10L	E3 core	2.9	19.064	0.001	15.645	0.001	38.858	0.003	2.03831	0.00005	0.82064	0.00002
E3-11L	E3 core	3.0	19.001	0.001	15.635	0.001	38.809	0.003	2.04245	0.00004	0.82286	0.00001
E3-12L	E3 core	2.7	19.024	0.001	15.642	0.001	38.830	0.003	2.04104	0.00005	0.82219	0.00001
E3-13L	E3 core	2.5	19.033	0.001	15.640	0.001	38.833	0.003	2.04026	0.00005	0.82172	0.00002
E3-14L	E3 core	2.8	19.155	0.002	15.656	0.001	38.928	0.004	2.03220	0.00005	0.81729	0.00001
E3-15L	E3 core	2.3	19.034	0.002	15.633	0.001	38.829	0.004	2.03994	0.00004	0.82132	0.00001
E3-16L	E3 core	2.3	19.072	0.001	15.625	0.001	38.824	0.003	2.03570	0.00005	0.81928	0.00001
E3-17L	E3 core	2.4	19.167	0.002	15.652	0.002	38.930	0.005	2.03114	0.00006	0.81664	0.00002
E3-18L	E3 core	2.6	19.137	0.001	15.652	0.001	38.917	0.003	2.03357	0.00004	0.81790	0.00001

Sample ID	Station Type	Pb (µg/g)	^{206}Pb/^{204}Pb	error	^{207}Pb/^{204}Pb	error	^{208}Pb/^{204}Pb	error	^{208}Pb/^{206}Pb	error	^{207}Pb/^{206}Pb	error
E3-19L	E3 core	2.6	19.184	0.001	15.649	0.001	38.939	0.003	2.02979	0.00005	0.81575	0.00002
E3-20L	E3 core	1.9	19.141	0.004	15.642	0.003	38.897	0.007	2.03212	0.00006	0.81721	0.00003
E3-21L	E3 core	3.2	19.083	0.002	15.651	0.002	38.875	0.005	2.03716	0.00008	0.82015	0.00002
E3-22L	E3 core	2.6	19.118	0.002	15.649	0.002	38.900	0.003	2.03476	0.00006	0.81858	0.00003
E3-23L	E3 core	3.0	19.057	0.001	15.639	0.001	38.847	0.003	2.03851	0.00004	0.82065	0.00002

Table 9. Lead isotope ratios and concentrations for Galveston Bay sediment residues.

Sample ID	Station Type	Pb (µg/g)	^{206}Pb/^{204}Pb	error	^{207}Pb/^{204}Pb	error	^{208}Pb/^{204}Pb	error	^{208}Pb/^{206}Pb	error	^{207}Pb/^{206}Pb	error
1R 06-17	Bay	3.7	18.662	0.002	15.627	0.002	38.268	0.004	2.05058	0.00007	0.83737	0.00002
2R 06-17	Bay	5.4	19.286	0.001	15.676	0.001	38.693	0.003	2.00626	0.00003	0.81281	0.00001
4R 06-17	Bay	6.6	19.217	0.001	15.669	0.001	39.191	0.009	2.03939	0.00005	0.81537	0.00001
5R 06-17	Bay	8.6	19.103	0.002	15.661	0.001	38.878	0.004	2.03517	0.00006	0.81982	0.00002
7R 06-17	Bay	9.3	19.088	0.001	15.660	0.001	38.860	0.002	2.03583	0.00003	0.82041	0.00001

Sample ID	**Station Type**	**Pb (µg/g)**	**^{206}Pb/^{204}Pb**	**error**	**^{207}Pb/^{204}Pb**	**error**	**^{208}Pb/^{204}Pb**	**error**	**^{208}Pb/^{206}Pb**	**error**	**^{207}Pb/^{206}Pb**	**error**
8R 06-17	Bay	8.7	19.074	0.001	15.654	0.001	38.862	0.003	2.03743	0.00005	0.82070	0.00002
9R 06-17	Bay	6.4	19.063	0.001	15.653	0.001	38.974	0.003	2.04448	0.00004	0.82112	0.00001
10R 06-17	Bay	5.6	19.064	0.001	15.652	0.001	38.796	0.002	2.03503	0.00005	0.82102	0.00001
1R 09-17	Bay	4.4	18.670	0.002	15.626	0.002	38.543	0.004	2.06443	0.00005	0.83696	0.00002
2R 09-17	Bay	4.7	19.067	0.001	15.657	0.001	38.888	0.004	2.03954	0.00004	0.82115	0.00002
3AR 09-17	Bay	4.4	18.983	0.002	15.646	0.002	38.934	0.004	2.05099	0.00003	0.82421	0.00002
3BR 09-17	Bay	4.1	18.966	0.002	15.653	0.002	39.079	0.004	2.06048	0.00004	0.82532	0.00002
5R 09-17	Bay	6.1	19.088	0.001	15.661	0.001	38.830	0.003	2.03426	0.00005	0.82046	0.00002
7R 09-17	Bay	10.2	19.056	0.001	15.654	0.001	38.857	0.003	2.03909	0.00004	0.82147	0.00001
8R 09-17	Bay	7.2	19.049	0.001	15.653	0.001	38.855	0.003	2.03974	0.00004	0.82172	0.00001
9R 09-17	Bay	5.9	19.042	0.001	15.653	0.001	38.856	0.003	2.04054	0.00005	0.82202	0.00001
1R 11-17	Bay	9.4	18.972	0.001	15.652	0.001	38.723	0.002	2.04106	0.00003	0.82500	0.00001

Sample ID	**Station Type**	**Pb (µg/g)**	**^{206}Pb/^{204}Pb**	**error**	**^{207}Pb/^{204}Pb**	**error**	**^{208}Pb/^{204}Pb**	**error**	**^{208}Pb/^{206}Pb**	**error**	**^{207}Pb/^{206}Pb**	**error**
3R 11-17	Bay	5.2	19.056	0.001	15.653	0.001	38.898	0.003	2.04124	0.00003	0.82142	0.00002
5R 11-17	Bay	7.4	19.008	0.001	15.648	0.001	38.838	0.002	2.04324	0.00003	0.82323	0.00001
9R 11-17	Bay	8.9	19.069	0.002	15.657	0.001	39.040	0.003	2.04730	0.00003	0.82107	0.00001
12R 11-17	Bay	10.3	19.054	0.001	15.653	0.001	38.891	0.002	2.04109	0.00003	0.82150	0.00001
13R 11-17	Bay	4.5	19.362	0.002	15.685	0.001	39.400	0.003	2.03490	0.00004	0.81008	0.00002
14R 11-17	Bay	8.2	19.153	0.001	15.663	0.001	39.111	0.003	2.04202	0.00003	0.81778	0.00001
5R 03-18	Bay	4.8	19.141	0.001	15.660	0.001	38.887	0.002	2.03158	0.00003	0.81813	0.00001
9R 03-18	Bay	10.4	19.025	0.001	15.650	0.001	38.836	0.002	2.04131	0.00003	0.82260	0.00001
12R 03-18	Bay	7.1	19.125	0.001	15.660	0.001	38.993	0.003	2.03884	0.00004	0.81882	0.00001
13R 03-18	Bay	4.5	18.899	0.002	15.641	0.001	38.601	0.003	2.04247	0.00004	0.82760	0.00001
14R 03-18	Bay	4.1	19.137	0.002	15.661	0.001	39.182	0.004	2.04743	0.00004	0.81835	0.00002
15R 03-18	Bay	7.0	19.021	0.001	15.653	0.001	38.825	0.001	2.04116	0.00004	0.82293	0.00002

Sample ID	**Station Type**	**Pb (µg/g)**	**^{206}Pb/^{204}Pb**	**error**	**^{207}Pb/^{204}Pb**	**error**	**^{208}Pb/^{204}Pb**	**error**	**^{208}Pb/^{206}Pb**	**error**	**^{207}Pb/^{206}Pb**	**error**
1R 06-18	Bay	5.1	19.014	0.002	15.656	0.002	38.771	0.004	2.03906	0.00005	0.82339	0.00002
5R 06-18	Bay	3.2	18.815	0.002	15.634	0.002	39.062	0.005	2.07612	0.00006	0.83093	0.00002
9R 06-18	Bay	6.7	19.048	0.001	15.656	0.001	38.920	0.004	2.04325	0.00006	0.82192	0.00002
12R 06-18	Bay	7.9	19.080	0.001	15.658	0.001	38.895	0.003	2.03851	0.00004	0.82064	0.00001
13R 06-18	Bay	3.2	19.179	0.002	15.666	0.002	38.966	0.004	2.03167	0.00007	0.81682	0.00002
14R 06-18	Bay	3.3	19.234	0.002	15.667	0.002	38.996	0.005	2.02742	0.00005	0.81453	0.00002
3R 09-18	Bay	2.7	19.673	0.004	15.719	0.003	40.165	0.009	2.04164	0.00009	0.79901	0.00003
5R 09-18	Bay	7.4	19.112	0.003	15.659	0.002	38.890	0.006	2.03482	0.00006	0.81932	0.00002
9R 09-18	Bay	7.5	19.076	0.001	15.653	0.001	38.892	0.003	2.03877	0.00006	0.82055	0.00002
11R 09-18	Bay	4.7	18.966	0.001	15.637	0.001	38.621	0.003	2.03629	0.00006	0.82446	0.00002
12R 09-18	Bay	8.0	19.087	0.001	15.653	0.001	38.884	0.004	2.03718	0.00007	0.82008	0.00001
13R 09-18	Bay	4.7	19.296	0.002	15.679	0.002	39.326	0.004	2.03806	0.00008	0.81256	0.00002

Sample ID	Station Type	Pb (µg/g)	$^{206}Pb/^{204}Pb$	error	$^{207}Pb/^{204}Pb$	error	$^{208}Pb/^{204}Pb$	error	$^{208}Pb/^{206}Pb$	error	$^{207}Pb/^{206}Pb$	error
14R 09-18	Bay	3.2	19.459	0.003	15.700	0.002	40.459	0.006	2.07917	0.00007	0.80681	0.00002
1R 11-18	Bay	4.2	18.790	0.002	15.632	0.001	38.495	0.003	2.04869	0.00006	0.83193	0.00002
3R 11-18	Bay	4.3	19.292	0.002	15.695	0.001	39.007	0.004	2.02192	0.00007	0.81354	0.00002
5R 11-18	Bay	8.1	19.169	0.001	15.665	0.001	38.974	0.002	2.03317	0.00004	0.81720	0.00001
9R 11-18	Bay	7.2	19.088	0.001	15.653	0.001	38.930	0.003	2.03950	0.00006	0.82004	0.00002
11R 11-18	Bay	2.8	18.773	0.003	15.627	0.002	38.773	0.006	2.06536	0.00008	0.83242	0.00002
12R 11-18	Bay	10.6	19.731	0.001	15.721	0.001	39.383	0.002	1.99599	0.00004	0.79676	0.00001
13R 11-18	Bay	2.9	19.173	0.002	15.665	0.002	39.200	0.005	2.04453	0.00005	0.81703	0.00002
14R 11-18	Bay	3.7	19.424	0.002	15.689	0.002	39.186	0.005	2.01739	0.00007	0.80770	0.00002
1R 03-19	Bay	5.7	19.053	0.001	15.652	0.001	38.819	0.004	2.03741	0.00005	0.82149	0.00001
3R 03-19	Bay	2.9	18.988	0.002	15.653	0.002	38.579	0.004	2.03172	0.00006	0.82435	0.00002
5R 03-19	Bay	7.9	19.107	0.001	15.654	0.001	38.924	0.002	2.03715	0.00005	0.81927	0.00001

Sample ID	Station Type	Pb (µg/g)	^{206}Pb/^{204}Pb	error	^{207}Pb/^{204}Pb	error	^{208}Pb/^{204}Pb	error	^{208}Pb/^{206}Pb	error	^{207}Pb/^{206}Pb	error
9R 03-19	Bay	7.0	19.046	0.001	15.644	0.001	38.914	0.002	2.04315	0.00004	0.82137	0.00001
12R 03-19	Bay	5.7	19.077	0.001	15.648	0.001	38.929	0.003	2.04061	0.00005	0.82024	0.00001
13R 03-19	Bay	3.1	19.143	0.002	15.655	0.001	39.224	0.005	2.04898	0.00006	0.81777	0.00002
14R 03-19	Bay	2.0	18.731	0.002	15.614	0.002	38.383	0.005	2.04920	0.00006	0.83359	0.00002
1R 06-19	Bay	3.5	18.854	0.001	15.636	0.001	38.625	0.003	2.04865	0.00004	0.82930	0.00002
3R 06-19	Bay	4.1	19.020	0.001	15.656	0.001	38.688	0.002	2.03410	0.00004	0.82315	0.00001
5AR 06-19	Bay	7.5	19.088	0.001	15.660	0.001	38.892	0.002	2.03747	0.00004	0.82039	0.00001
5BR 06-19	Bay	7.4	19.123	0.001	15.661	0.001	38.914	0.002	2.03489	0.00004	0.81894	0.00001
9R 06-19	Bay	6.7	19.055	0.001	15.654	0.001	38.879	0.002	2.04032	0.00004	0.82150	0.00001
12R 06-19	Bay	8.1	19.078	0.001	15.660	0.001	38.922	0.002	2.04012	0.00005	0.82082	0.00001
13R 06-19	Bay	6.5	19.123	0.001	15.661	0.001	38.959	0.002	2.03735	0.00005	0.81898	0.00001
101R	Endmember	8.6	18.990	0.001	15.655	0.001	38.872	0.002	2.04697	0.00004	0.82438	0.00001
102R	Endmember	7.8	19.028	0.001	15.660	0.001	38.857	0.002	2.04209	0.00005	0.82299	0.00001

Sample ID	Station Type	Pb (µg/g)	^{206}Pb/^{204}Pb	error	^{207}Pb/^{204}Pb	error	^{208}Pb/^{204}Pb	error	^{208}Pb/^{206}Pb	error	^{207}Pb/^{206}Pb	error
103R	Endmember	9.2	19.002	0.001	15.662	0.001	38.831	0.002	2.04352	0.00005	0.82423	0.00001
201R	Endmember	10.9	18.945	0.001	15.652	0.001	38.722	0.003	2.04391	0.00007	0.82618	0.00002
202R	Endmember	10.5	18.884	0.001	15.648	0.001	38.629	0.002	2.04559	0.00005	0.82864	0.00001
203R	Endmember	8.6	19.160	0.001	15.669	0.001	38.770	0.002	2.02348	0.00005	0.81779	0.00001
301R	Endmember	7.1	18.948	0.001	15.645	0.001	38.711	0.002	2.04301	0.00005	0.82568	0.00001
302R	Endmember	5.5	18.941	0.001	15.642	0.001	38.774	0.003	2.04709	0.00006	0.82582	0.00002
401R	Endmember	7.0	19.158	0.001	15.663	0.001	38.890	0.003	2.02995	0.00005	0.81756	0.00002
402R	Endmember	7.7	19.135	0.001	15.663	0.001	38.952	0.002	2.03563	0.00005	0.81855	0.00002
501R	Endmember	1.0	18.552	0.004	15.648	0.003	38.035	0.007	2.05022	0.00011	0.84348	0.00005
502R	Endmember	0.2	18.558	0.024	15.618	0.020	38.608	0.052	2.08045	0.00026	0.84160	0.00014
503R	Endmember	1.6	18.602	0.001	15.626	0.001	38.320	0.005	2.06004	0.00007	0.84002	0.00002
GB1R	Shoreline	4.2	18.652	0.002	15.608	0.001	38.295	0.004	2.05312	0.00008	0.83680	0.00002
GB2R	Shoreline	1.7	18.881	0.003	15.638	0.003	38.425	0.007	2.03512	0.00008	0.82823	0.00003
GB3R	Shoreline	3.8	18.905	0.002	15.633	0.002	38.562	0.004	2.03976	0.00007	0.82692	0.00002
GB4R	Shoreline	6.5	19.091	0.001	15.660	0.001	38.951	0.003	2.04027	0.00005	0.82028	0.00001
GB5R	Shoreline	0.7	19.181	0.003	15.673	0.002	38.774	0.006	2.02143	0.00007	0.81708	0.00002
GB6R	Shoreline	5.6	18.872	0.001	15.630	0.001	38.604	0.003	2.04556	0.00005	0.82821	0.00001
GB7R	Shoreline	2.2	18.609	0.028	15.629	0.022	38.257	0.060	2.05588	0.00074	0.83987	0.00024
GB8R	Shoreline	1.6	18.380	0.004	15.601	0.004	37.919	0.010	2.06305	0.00010	0.84878	0.00003

Sample ID	**Station Type**	**Pb (µg/g)**	**^{206}Pb/^{204}Pb**	**error**	**^{207}Pb/^{204}Pb**	**error**	**^{208}Pb/^{204}Pb**	**error**	**^{208}Pb/^{206}Pb**	**error**	**^{207}Pb/^{206}Pb**	**error**
GB9R	Shoreline	1.8	19.274	0.003	15.694	0.005	40.704	0.007	2.11188	0.00008	0.81427	0.00003
GB10R	Shoreline	1.3	18.746	0.004	15.708	0.003	37.929	0.008	2.02334	0.00008	0.83794	0.00003
GB11R	Shoreline	3.9	18.858	0.001	15.637	0.001	38.640	0.003	2.04899	0.00005	0.82919	0.00002
GB12R	Shoreline	6.1	19.104	0.001	15.658	0.001	38.932	0.002	2.03789	0.00003	0.81961	0.00001
E3-1R	E3 core	10.0	19.077	0.001	15.656	0.001	38.896	0.003	2.03885	0.00005	0.82065	0.00001
E3-2R	E3 core	10.6	19.081	0.001	15.662	0.001	39.333	0.003	2.06131	0.00005	0.82079	0.00001
E3-3R	E3 core	10.5	19.018	0.001	15.653	0.001	38.804	0.003	2.04035	0.00006	0.82304	0.00002
E3-4R	E3 core	11.8	19.058	0.001	15.654	0.001	38.866	0.003	2.03932	0.00006	0.82137	0.00001
E3-5R	E3 core	18.5	19.074	0.001	15.655	0.001	38.879	0.004	2.03830	0.00001	0.82074	0.00002
E3-6R	E3 core	22.5	19.074	0.001	15.656	0.001	38.877	0.002	2.03820	0.00004	0.82079	0.00001
E3-7R	E3 core	11.8	19.084	0.001	15.656	0.001	38.908	0.003	2.03874	0.00005	0.82035	0.00001
E3-8R	E3 core	10.5	19.092	0.001	15.657	0.001	38.897	0.003	2.03741	0.00005	0.82010	0.00001
E3-9R	E3 core	12.7	19.062	0.001	15.654	0.001	38.907	0.002	2.04105	0.00005	0.82120	0.00001
E3-10R	E3 core	10.8	19.083	0.001	15.655	0.001	38.933	0.002	2.04015	0.00005	0.82034	0.00001
E3-11R	E3 core	10.9	19.168	0.001	15.664	0.001	38.990	0.003	2.03417	0.00007	0.81721	0.00004
E3-12R	E3 core	7.6	19.181	0.001	15.666	0.001	39.027	0.003	2.03465	0.00005	0.81674	0.00001
E3-13R	E3 core	9.1	19.137	0.001	15.658	0.001	38.872	0.003	2.03128	0.00004	0.81821	0.00001
E3-14R	E3 core	9.4	19.156	0.001	15.662	0.001	38.984	0.003	2.03514	0.00005	0.81761	0.00001
E3-15R	E3 core	7.7	19.165	0.001	15.666	0.001	39.093	0.002	2.03981	0.00004	0.81743	0.00001

Sample ID	**Station Type**	**Pb (µg/g)**	**$^{206}\text{Pb}/^{204}\text{Pb}$**	**error**	**$^{207}\text{Pb}/^{204}\text{Pb}$**	**error**	**$^{208}\text{Pb}/^{204}\text{Pb}$**	**error**	**$^{208}\text{Pb}/^{206}\text{Pb}$**	**error**	**$^{207}\text{Pb}/^{206}\text{Pb}$**	**error**
E3-16R	E3 core	8.8	19.208	0.001	15.669	0.001	39.127	0.002	2.03702	0.00005	0.81576	0.00001
E3-17R	E3 core	5.2	19.309	0.002	15.681	0.001	39.304	0.004	2.03554	0.00005	0.81212	0.00002
E3-18R	E3 core	7.3	19.146	0.001	15.658	0.001	38.956	0.003	2.03471	0.00005	0.81781	0.00002
E3-19R	E3 core	7.1	19.149	0.001	15.659	0.001	38.959	0.003	2.03456	0.00005	0.81775	0.00001
E3-20R	E3 core	6.2	19.230	0.001	15.668	0.001	38.935	0.003	2.02470	0.00005	0.81475	0.00001
E3-21R	E3 core	5.0	19.293	0.002	15.684	0.001	39.415	0.004	2.04299	0.00005	0.81293	0.00002
E3-22R	E3 core	5.9	19.232	0.002	15.669	0.002	38.970	0.003	2.02631	0.00005	0.81472	0.00001
E3-23R	E3 core	6.4	19.108	0.001	15.658	0.001	39.074	0.003	2.04491	0.00005	0.81945	0.00001

*µg/g = micrograms per gram

Table 10. Lead isotope ratios and concentrations for Galveston Bay bulk sediments.

Sample ID	**Station Type**	**Pb (µg/g)**	**$^{206}\text{Pb}/^{204}\text{Pb}$**	**error**	**$^{207}\text{Pb}/^{204}\text{Pb}$**	**error**	**$^{208}\text{Pb}/^{204}\text{Pb}$**	**error**	**$^{208}\text{Pb}/^{206}\text{Pb}$**	**error**	**$^{207}\text{Pb}/^{206}\text{Pb}$**	**error**
1D 06-17	Bay	6.6	18.856	0.001	15.636	0.001	38.588	0.003	2.04644	0.00006	0.82923	0.00002
2D 06-17	Bay	6.4	19.385	0.001	15.687	0.001	39.144	0.003	2.01926	0.00005	0.80921	0.00002
4D 06-17	Bay	10.7	19.213	0.001	15.668	0.001	39.052	0.002	2.03257	0.00006	0.81548	0.00002
5D 06-17	Bay	12.5	19.068	0.001	15.659	0.001	38.879	0.003	2.03895	0.00006	0.82121	0.00002

Sample ID	Station Type	Pb (µg/g)	$^{206}Pb/^{204}Pb$	error	$^{207}Pb/^{204}Pb$	error	$^{208}Pb/^{204}Pb$	error	$^{208}Pb/^{206}Pb$	error	$^{207}Pb/^{206}Pb$	error
7D 06-17	Bay	14.0	19.060	0.002	15.653	0.002	38.829	0.004	2.03719	0.00010	0.82124	0.00003
8D 06-17	Bay	13.7	19.032	0.001	15.655	0.001	38.837	0.004	2.04061	0.00007	0.82256	0.00002
9D 06-17	Bay	9.0	19.026	0.002	15.650	0.001	38.845	0.004	2.04167	0.00009	0.82255	0.00002
10D 06-17	Bay	10.9	19.020	0.001	15.654	0.001	38.789	0.003	2.03937	0.00007	0.82302	0.00002
1D 09-17	Bay	5.6	18.837	0.004	15.638	0.003	38.550	0.008	2.04649	0.00011	0.83017	0.00003
2D 09-17	Bay	6.2	18.961	0.002	15.645	0.001	38.604	0.004	2.03594	0.00007	0.82510	0.00002
3AD 09-17	Bay	6.6	19.171	0.002	15.667	0.002	39.480	0.005	2.05930	0.00009	0.81721	0.00002
3BD 09-17	Bay	6.2	19.016	0.002	15.656	0.002	38.655	0.006	2.03273	0.00008	0.82330	0.00002
5D 09-17	Bay	10.1	19.144	0.001	15.668	0.001	38.887	0.004	2.03127	0.00007	0.81842	0.00002
7D 09-17	Bay	15.4	19.044	0.001	15.658	0.001	38.826	0.003	2.03874	0.00007	0.82220	0.00002
8D 09-17	Bay	12.5	19.013	0.001	15.662	0.001	38.813	0.004	2.04138	0.00007	0.82375	0.00002
9D 09-17	Bay	10.3	18.923	0.001	15.645	0.001	38.746	0.002	2.04755	0.00002	0.82677	0.00002

Sample ID	**Station Type**	**Pb (µg/g)**	**^{206}Pb/^{204}Pb**	**error**	**^{207}Pb/^{204}Pb**	**error**	**^{208}Pb/^{204}Pb**	**error**	**^{208}Pb/^{206}Pb**	**error**	**^{207}Pb/^{206}Pb**	**error**
1D 11-17	Bay	10.5	18.975	0.001	15.650	0.001	38.725	0.003	2.04083	0.00007	0.82476	0.00002
3D 11-17	Bay	6.0	18.895	0.002	15.639	0.001	39.419	0.004	2.08618	0.00006	0.82767	0.00002
5D 11-17	Bay	8.6	19.012	0.001	15.644	0.001	38.802	0.002	2.04091	0.00005	0.82284	0.00001
9D 11-17	Bay	10.4	19.076	0.001	15.655	0.001	38.852	0.003	2.03668	0.00006	0.82066	0.00002
12D 11-17	Bay	12.1	18.926	0.001	15.649	0.001	38.729	0.003	2.04633	0.00005	0.82685	0.00002
13D 11-17	Bay	6.4	19.157	0.001	15.670	0.001	39.066	0.003	2.03923	0.00004	0.81796	0.00001
14D 11-17	Bay	12.1	19.123	0.001	15.661	0.001	38.814	0.003	2.02969	0.00005	0.81895	0.00002
5D 03-18	Bay	11.6	19.138	0.001	15.664	0.001	38.947	0.002	2.03505	0.00004	0.81847	0.00001
9D 03-18	Bay	16.8	19.029	0.001	15.652	0.001	38.853	0.002	2.04177	0.00003	0.82253	0.00001
12D 03-18	Bay	10.8	18.991	0.001	15.649	0.001	38.768	0.002	2.04138	0.00005	0.82402	0.00001
13D 03-18	Bay	6.8	19.061	0.001	15.659	0.001	38.780	0.002	2.03450	0.00004	0.82151	0.00001
14D 03-18	Bay	6.6	19.052	0.001	15.655	0.001	38.950	0.002	2.04439	0.00003	0.82169	0.00001

Sample ID	Station Type	Pb (µg/g)	^{206}Pb/^{204}Pb	error	^{207}Pb/^{204}Pb	error	^{208}Pb/^{204}Pb	error	^{208}Pb/^{206}Pb	error	^{207}Pb/^{206}Pb	error
15D 03-18	Bay	14.4	18.928	0.001	15.649	0.001	38.714	0.002	2.04532	0.00004	0.82676	0.00001
1D 06-18	Bay	10.0	18.939	0.001	15.646	0.001	38.691	0.003	2.04292	0.00005	0.82612	0.00001
5D 06-18	Bay	10.3	18.988	0.001	15.650	0.001	38.736	0.003	2.04001	0.00005	0.82420	0.00001
9D 06-18	Bay	7.2	18.993	0.001	15.650	0.001	38.839	0.002	2.04490	0.00004	0.82398	0.00001
12D 06-18	Bay	12.2	19.037	0.001	15.654	0.001	38.812	0.002	2.03876	0.00005	0.82229	0.00001
13D 06-18	Bay	6.6	19.105	0.001	15.656	0.001	39.280	0.002	2.05600	0.00004	0.81946	0.00001
14D 06-18	Bay	5.4	19.169	0.001	15.664	0.001	38.861	0.002	2.02725	0.00004	0.81713	0.00001
3D 09-18	Bay	6.6	19.042	0.002	15.656	0.001	38.673	0.003	2.03090	0.00006	0.82217	0.00003
5D 09-18	Bay	12.7	19.091	0.001	15.659	0.001	38.884	0.002	2.03676	0.00005	0.82022	0.00001
9D 09-18	Bay	11.2	19.029	0.001	15.651	0.001	38.861	0.002	2.04219	0.00005	0.82247	0.00001
11D 09-18	Bay	7.3	19.011	0.002	15.644	0.001	38.752	0.004	2.03838	0.00006	0.82288	0.00002
12D 09-18	Bay	12.2	19.065	0.001	15.658	0.001	38.929	0.003	2.04190	0.00005	0.82129	0.00002

Sample ID	Station Type	Pb (µg/g)	^{206}Pb/^{204}Pb	error	^{207}Pb/^{204}Pb	error	^{208}Pb/^{204}Pb	error	^{208}Pb/^{206}Pb	error	^{207}Pb/^{206}Pb	error
13D 09-18	Bay	2.0	18.996	0.001	15.652	0.001	38.768	0.003	2.04089	0.00006	0.82397	0.00001
14D 09-18	Bay	6.2	19.026	0.002	15.651	0.002	38.732	0.004	2.03571	0.00005	0.82260	0.00002
1D 11-18	Bay	7.6	19.039	0.005	15.671	0.004	39.022	0.011	2.04957	0.00013	0.82309	0.00004
3D 11-18	Bay	6.7	19.051	0.002	15.652	0.001	38.869	0.004	2.04024	0.00012	0.82157	0.00001
5D 11-18	Bay	13.3	19.104	0.001	15.656	0.001	38.889	0.002	2.03563	0.00004	0.81951	0.00001
9D 11-18	Bay	12.8	19.000	0.003	15.648	0.003	38.823	0.008	2.04331	0.00013	0.82357	0.00004
11D 11-18	Bay	6.0	18.833	0.006	15.616	0.005	38.503	0.014	2.04442	0.00012	0.82918	0.00004
12D 11-18	Bay	13.0	19.052	0.001	15.655	0.001	38.830	0.002	2.03809	0.00004	0.82169	0.00009
13D 11-18	Bay	4.5	19.041	0.002	15.646	0.001	38.758	0.003	2.03547	0.00005	0.82168	0.00002
14D 11-18	Bay	5.8	19.514	0.001	15.755	0.001	39.350	0.003	2.01651	0.00006	0.80738	0.00002
1D 03-19	Bay	11.4	19.048	0.001	15.650	0.001	38.812	0.003	2.03758	0.00008	0.82160	0.00002
3D 03-19	Bay	6.2	19.153	0.001	15.666	0.001	39.005	0.003	2.03647	0.00006	0.81792	0.00002

Sample ID	**Station Type**	**Pb (µg/g)**	**^{206}Pb/^{204}Pb**	**error**	**^{207}Pb/^{204}Pb**	**error**	**^{208}Pb/^{204}Pb**	**error**	**^{208}Pb/^{206}Pb**	**error**	**^{207}Pb/^{206}Pb**	**error**
5D 03-19	Bay	13.6	19.086	0.001	15.657	0.001	38.861	0.002	2.03609	0.00004	0.82033	0.00002
9D 03-19	Bay	12.5	18.979	0.001	15.645	0.001	38.801	0.003	2.04441	0.00006	0.82433	0.00002
12D 03-19	Bay	13.8	19.048	0.001	15.656	0.001	38.938	0.002	2.04420	0.00004	0.82192	0.00001
13D 03-19	Bay	6.4	19.187	0.001	15.664	0.001	39.214	0.003	2.04376	0.00005	0.81637	0.00002
14D 03-19	Bay	6.1	18.894	0.001	15.639	0.001	38.532	0.003	2.03935	0.00005	0.82772	0.00001
1D 06-19	Bay	8.2	18.910	0.001	15.645	0.001	38.591	0.003	2.04076	0.00006	0.82733	0.00002
3D 06-19	Bay	6.6	19.042	0.002	15.659	0.001	38.952	0.004	2.04557	0.00008	0.82233	0.00002
5AD 06-19	Bay	13.3	19.061	0.001	15.654	0.001	38.857	0.003	2.03855	0.00005	0.82125	0.00002
5BD 06-19	Bay	13.4	19.021	0.001	15.658	0.001	38.854	0.002	2.04268	0.00005	0.82319	0.00002
9D 06-19	Bay	13.7	18.999	0.001	15.645	0.001	38.829	0.003	2.04373	0.00010	0.82346	0.00002
12D 06-19	Bay	13.7	19.040	0.001	15.650	0.001	38.883	0.002	2.04217	0.00004	0.82195	0.00001
13D 06-19	Bay	14.7	19.028	0.001	15.655	0.001	38.815	0.003	2.03988	0.00007	0.82273	0.00002

Sample ID	Station Type	Pb (µg/g)	^{206}Pb/^{204}Pb	error	^{207}Pb/^{204}Pb	error	^{208}Pb/^{204}Pb	error	^{208}Pb/^{206}Pb	error	^{207}Pb/^{206}Pb	error
101D	Endmember	13.3	18.955	0.001	15.649	0.001	38.835	0.003	2.04879	0.00006	0.82558	0.00001
102D	Endmember	14.2	18.974	0.001	15.659	0.001	38.807	0.002	2.04526	0.00004	0.82528	0.00001
103D	Endmember	14.0	18.969	0.001	15.660	0.001	38.791	0.003	2.04496	0.00007	0.82555	0.00002
201D	Endmember	16.2	18.897	0.001	15.648	0.001	38.624	0.003	2.04391	0.00005	0.82807	0.00001
202D	Endmember	26.3	18.828	0.001	15.647	0.001	38.540	0.002	2.04695	0.00005	0.83105	0.00001
203D	Endmember	21.0	19.146	0.001	15.676	0.001	38.726	0.002	2.02266	0.00005	0.81876	0.00001
301D	Endmember	13.4	18.930	0.001	15.652	0.001	38.698	0.002	2.04426	0.00005	0.82683	0.00001
302D	Endmember	7.8	18.941	0.001	15.647	0.001	38.705	0.003	2.04344	0.00007	0.82608	0.00002
401D	Endmember	11.4	19.106	0.001	15.661	0.001	38.977	0.002	2.04003	0.00005	0.81968	0.00001
402D	Endmember	29.2	19.086	0.001	15.656	0.001	38.888	0.003	2.03751	0.00005	0.82028	0.00001
501D	Endmember	3.2	18.338	0.002	15.598	0.002	38.101	0.004	2.07767	0.00008	0.85056	0.00002
502D	Endmember	2.3	18.604	0.004	15.620	0.003	37.913	0.008	2.03794	0.00012	0.83961	0.00004
503D	Endmember	3.3	18.678	0.002	15.639	0.002	38.121	0.004	2.04097	0.00010	0.83730	0.00003
GB1D	Shoreline	15.8	19.248	0.001	15.681	0.001	38.678	0.002	2.00944	0.00004	0.81467	0.00001
GB2D	Shoreline	15.5	18.440	0.001	15.612	0.001	38.133	0.003	2.06795	0.00005	0.84664	0.00002
GB3D	Shoreline	8.1	18.881	0.001	15.628	0.001	38.834	0.004	2.05677	0.00010	0.82770	0.00002
GB4D	Shoreline	9.4	19.057	0.001	15.650	0.001	38.969	0.003	2.04485	0.00006	0.82121	0.00002
GB5D	Shoreline	4.1	19.349	0.002	15.680	0.002	40.352	0.005	2.08552	0.00007	0.81038	0.00002

Sample ID	Station Type	Pb (µg/g)	^{206}Pb/^{204}Pb	error	^{207}Pb/^{204}Pb	error	^{208}Pb/^{204}Pb	error	^{208}Pb/^{206}Pb	error	^{207}Pb/^{206}Pb	error
GB6D	Shoreline	11.0	18.835	0.001	15.632	0.001	38.464	0.002	2.04214	0.00006	0.82994	0.00001
GB7D	Shoreline	5.1	18.635	0.002	15.619	0.002	38.348	0.006	2.05789	0.00011	0.83816	0.00002
GB8D	Shoreline	5.4	19.233	0.002	15.669	0.002	38.505	0.004	2.00196	0.00005	0.81467	0.00002
GB9D	Shoreline	4.7	19.068	0.004	15.655	0.003	38.350	0.007	2.01121	0.00006	0.82099	0.00002
GB10D	Shoreline	1.8	19.181	0.005	15.662	0.004	38.271	0.010	1.99524	0.00010	0.81652	0.00003
GB11D	Shoreline	7.3	19.777	0.002	15.736	0.001	43.340	0.004	2.19145	0.00008	0.79568	0.00002
GB12D	Shoreline	11.5	19.088	0.002	15.657	0.001	38.797	0.003	2.03252	0.00006	0.82025	0.00002
E3-1D	E3 core	14.0	19.039	0.001	15.659	0.001	38.857	0.003	2.04095	0.00005	0.82247	0.00001
E3-2D	E3 core	16.2	19.001	0.001	15.651	0.001	38.807	0.003	2.04242	0.00005	0.82370	0.00001
E3-3D	E3 core	13.6	19.082	0.001	15.655	0.001	39.015	0.003	2.04460	0.00005	0.82041	0.00001
E3-4D	E3 core	16.1	19.046	0.001	15.652	0.001	38.836	0.002	2.03911	0.00005	0.82181	0.00001
E3-5D	E3 core	14.2	19.052	0.001	15.650	0.001	38.841	0.002	2.03872	0.00004	0.82144	0.00001
E3-6D	E3 core	18.0	19.038	0.001	15.651	0.001	38.848	0.002	2.04061	0.00005	0.82211	0.00001
E3-7D	E3 core	14.5	19.060	0.001	15.654	0.001	38.883	0.003	2.04006	0.00004	0.82130	0.00001
E3-8D	E3 core	13.8	19.066	0.001	15.654	0.001	38.881	0.003	2.03931	0.00005	0.82104	0.00002
E3-9D	E3 core	9.2	19.201	0.001	15.665	0.001	38.990	0.003	2.03065	0.00005	0.81585	0.00001
E3-10D	E3 core	13.6	19.050	0.001	15.650	0.001	38.886	0.002	2.04129	0.00004	0.82152	0.00001
E3-11D	E3 core	10.5	19.089	0.001	15.654	0.001	38.948	0.002	2.04029	0.00005	0.82003	0.00002

Sample ID	**Station Type**	**Pb (µg/g)**	**^{206}Pb/^{204}Pb**	**error**	**^{207}Pb/^{204}Pb**	**error**	**^{208}Pb/^{204}Pb**	**error**	**^{208}Pb/^{206}Pb**	**error**	**^{207}Pb/^{206}Pb**	**error**
E3-12D	E3 core	10.9	19.159	0.001	15.659	0.001	39.049	0.003	2.03811	0.00004	0.81729	0.00001
E3-13D	E3 core	12.0	19.100	0.001	15.660	0.001	38.931	0.003	2.03829	0.00005	0.81988	0.00002
E3-14D	E3 core	11.4	19.114	0.001	15.657	0.001	38.911	0.003	2.03573	0.00004	0.81911	0.00001
E3-15D	E3 core	11.4	19.210	0.002	15.666	0.001	39.037	0.003	2.03207	0.00006	0.81549	0.00002
E3-16D	E3 core	12.2	19.313	0.001	15.681	0.001	39.468	0.003	2.04363	0.00005	0.81194	0.00002
E3-17D	E3 core	10.1	19.272	0.002	15.674	0.001	39.207	0.003	2.03439	0.00005	0.81330	0.00002
E3-18D	E3 core	10.0	19.239	0.001	15.663	0.001	39.111	0.003	2.03293	0.00005	0.81412	0.00001
E3-19D	E3 core	16.2	19.027	0.001	15.649	0.001	38.859	0.002	2.04236	0.00005	0.82247	0.00002
E3-20D	E3 core	10.4	19.140	0.001	15.664	0.001	38.914	0.003	2.03310	0.00005	0.81836	0.00002
E3-21D	E3 core	8.9	19.155	0.001	15.662	0.001	39.009	0.003	2.03652	0.00005	0.81764	0.00001
E3-22D	E3 core	9.9	19.129	0.001	15.657	0.001	38.831	0.002	2.02991	0.00005	0.81846	0.00001
E3-23D	E3 core	10.5	19.077	0.001	15.652	0.001	38.863	0.003	2.03716	0.00007	0.82045	0.00002

*µg/g = micrograms per gram

Galveston Bay surface sediment Pb isotope ratios

Leachate Pb isotope ratios in surface (shoreline, bay, and endmember) sediments are ^{206}Pb/^{204}Pb = 18.417 – 19.523 ± 0.004, ^{207}Pb/^{204}Pb = 15.567 – 15.778 ± 0.003, ^{208}Pb/^{204}Pb = 38.432 – 38.952 ± 0.008, ^{208}Pb/^{206}Pb = 1.98280 – 2.10426 ± 0.00008 and ^{207}Pb/^{206}Pb = 0.80412 – 0.85672 ± 0.00003. The shoreline, bay, and endmember residues ^{206}Pb/^{204}Pb, ^{207}Pb/^{204}Pb, ^{208}Pb/^{204}Pb, ^{208}Pb/^{206}Pb and ^{207}Pb/^{206}Pb ratios range between 18.380 – 19.731 ±0.002, 15.601 – 15.721 ± 0.002, 37.919 – 40.704 ± 0.005, 1.99599 – 2.11188 ± 0.00006 and 0.79676 – 0.84878 ± 0.00002, respectively. The shoreline, bay, and endmember bulk sediments have ^{206}Pb/^{204}Pb between 18.338 – 19.777 ± 0.001, ^{207}Pb/^{204}Pb between 15.598 – 15.755 ± 0.001, ^{208}Pb/^{204}Pb between 37.913 – 43.340 ± 0.003, ^{208}Pb/^{206}Pb between 1.9524 – 2.19145 ± 0.00006 and ^{207}Pb/^{206}Pb between 0.79568 – 0.85056 ± 0.00002.

Three isotope plots displaying the relationships between the Pb isotope ratios of bay, shoreline and endmember sediment leachates, residues and bulk digests are shown in Fig. 7. In ^{207}Pb/^{204}Pb versus ^{206}Pb/^{204}Pb space the leachate, residue, and bulk digest R^2 values are 0.26, 0.73, and 0.82 respectively. Leachates, residues, and bulk digests in the ^{208}Pb/^{204}Pb versus ^{206}Pb/^{204}Pb diagram have R^2 values of 0.51, 0.61, and 0.49. The ^{208}Pb/^{206}Pb versus ^{207}Pb/^{206}Pb diagram yields the clearest distinction between leachable Pb and non-leachable Pb, in this case the leachates $R^2 = 0.8055$, residues $R^2 = 0.2007$, and bulk digest $R^2 = 0.0006$. The lack of consistent linear correlations in ^{204}Pb space indicates that the leachates, residues, and bulk sediments do not fit into a single binary mixing model with two main Pb sources. Rather it is likely that more than two Pb sources contribute to both sediment leachates and residues. In all diagrams, it is clear that the leachates form tighter clusters as compared to the residues and digests, which show larger ranges of values. This pattern indicates that leachate Pb sources are better constrained than Pb sources influencing the residues.

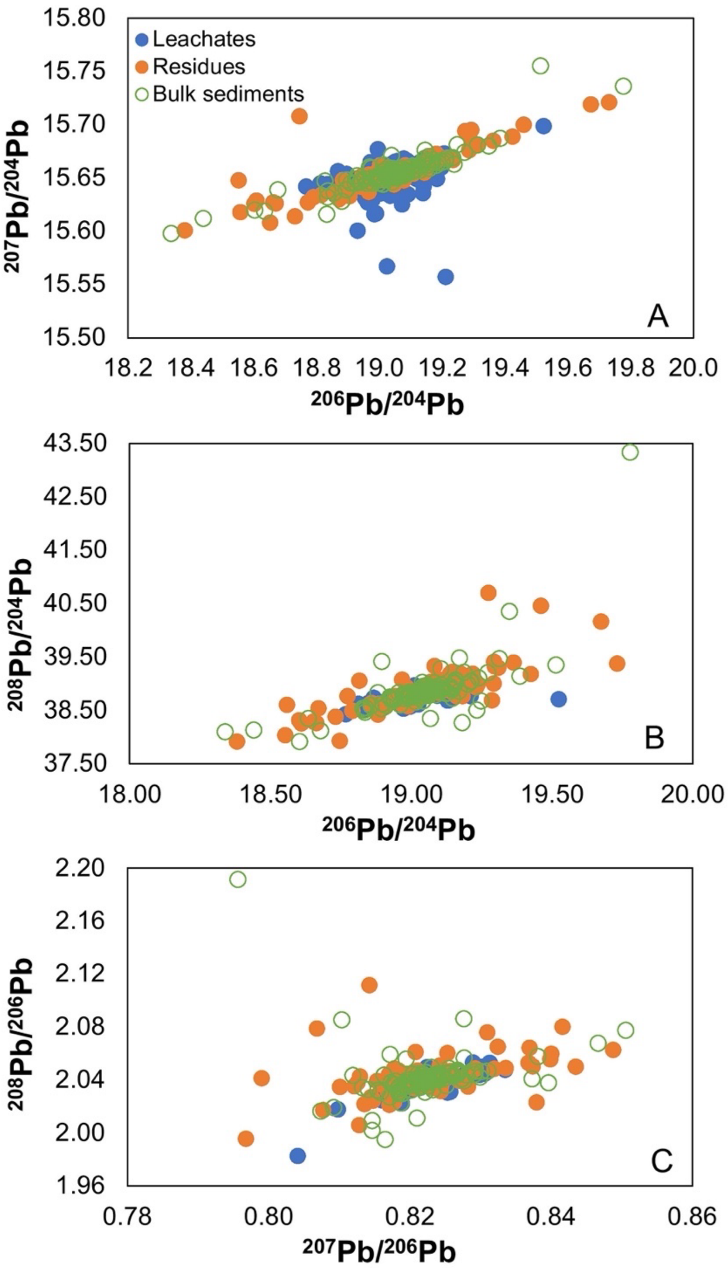

Panel A is Galveston Bay surface sediment leachates, residues, and bulk digests plotted in 207Pb/204Pb vs. 206Pb/204Pb space. Panel B is Galveston Bay surface sediment leachates, residues, and bulk digests plotted in 208Pb/204Pb vs. 206Pb/204Pb space. Panel C is Galveston Bay surface sediment leachates, residues, and bulk digests plotted in 208Pb/206Pb vs. 207Pb/206Pb space.

Figure 7. Pb isotope compositions of Galveston Bay sediment leachates, residues, and bulk sediment digests.

Spatial and temporal variations of leachates, residues, and bulk digests of surface sediments over time are shown in Fig. 11. Among the leachates, bay stations in Lower Galveston Bay (1-5, 10-11, 14) have more radiogenic Pb isotope ratios than do those from the bay stations in Upper Galveston Bay (7-9, 12-13). Specifically, the lower bay station sediment leachates range from ^{206}Pb/^{204}Pb = 18.858 ± 0.003 – 19.207 ±0.003, ^{207}Pb/^{204}Pb = 15.636 ±0.002 – 15.673 ± 0.003, and ^{208}Pb/^{204}Pb = 38.616 ± 0.006 – 38.952 ± 0.009. Upper bay station sediment leachates are less radiogenic with values between ^{206}Pb/^{204}Pb = 18.813 ± 0.002 – 19.020 ± 0.005, ^{207}Pb/^{204}Pb = 15.626 ± 0.003 – 15.662 ± 0.002, and ^{208}Pb/^{204}Pb = 38.569 ± 0.005 – 38.778 ± 0.006. The opposite trend is observed in residue Pb isotope compositions, though it is less pronounced. Lower bay station residues are between ^{206}Pb/^{204}Pb = 18.662 ± 0.002 – 19.673 ± 0.004, ^{207}Pb/^{204}Pb = 15.614 ± 0.002 – 15.719 ± 0.003, and ^{208}Pb/^{204}Pb = 38.268 ± 0.004 – 40.459 ± 0.006. The upper bay station residues have Pb isotope ratios ranging from ^{206}Pb/^{204}Pb = 18.899 ± 0.002 – 19.731 ± 0.001, ^{207}Pb/^{204}Pb = 15.641 ± 0.001 – 15.721 ± 0.001 and ^{208}Pb/^{204}Pb = 38.601 ± 0.003 – 39.400 ± 0.003.

Galveston Bay core sediment Pb isotope ratios

The Pb isotope compositions and concentrations of E3 core sediments are presented in Table 8 and Fig. 8. The E3 core sediments have Pb isotope compositions for ^{206}Pb/^{204}Pb between 19.211 – 19.313 ± 0.003, ^{207}Pb/^{204}Pb between 15.656 – 15.684 ± 0.002, ^{208}Pb/^{204}Pb between 38.976 – 39.468 ± 0.005, ^{208}Pb/^{206}Pb between 2.04460 – 2.06131 ± 0.00138 and ^{207}Pb/^{206}Pb between 0.82304 – 0.82542 ± 0.00003. The E3 core sediment leachates, residues and bulk digests become less radiogenic as core depth decreases, particularly following 1940 (core depth 31 cm). E3 core leachates have ^{206}Pb/^{204}Pb of 19.057 – 19.184, E3 core residues have ^{206}Pb/^{204}Pb 19.108 – 19.309, and E3 core bulk sediments have ^{206}Pb/^{204}Pb 19.027 – 19.313 between 1880 and 1946. From the mid-1940s to the present, the ^{206}Pb/^{204}Pb values become less radiogenic with leachate ^{206}Pb/^{204}Pb between 18.956 and 19.211, residue ^{206}Pb/^{204}Pb between 19.018 and 19.181, and bulk sediment ^{206}Pb/^{204}Pb between 19.001 and 19.201 (Fig. 8). The E3-5 leachate representing the approximate year 2002 is enriched in thorogenic ^{208}Pb (^{208}Pb/^{204}Pb = 38.976) as compared to other E3 core leachates (^{208}Pb/^{204}Pb $\leq$ 38.939) and has an elevated Pb concentration of 14.03 μg/g, which is higher than all other leachate Pb concentrations by 9 μg/g. The E3-7 (approximately 1994) leachate has a distinctly high ^{206}Pb/^{204}Pb of 19.211 and low ^{207}Pb/^{204}Pb of 15.557 compared to its counterparts, which have ^{206}Pb/^{204}Pb $\leq$ 19.090 and ^{207}Pb/^{204}Pb $\geq$ 15.617. Temporal Pb concentration trends in E3 core sediments are mirrored in literature studies of Galveston Bay cores and regulatory agency datasets (TCEQ, 2020; Al Mukiami et al., 2018; Santschi et al., 2001). Based on the agreement between the findings of this study, historical TCEQ data and literature data, the following conclusions are evident: 1) gasoline consumption and industrial activity resulted in increased anthropogenic Pb emissions into Galveston Bay between the early and late 20th century and 2) Pb concentrations in Galveston Bay decreased from the late 20th century into the 21st century likely in response to reduced anthropogenic emissions and regulatory efforts (Al Mukaimi et al., 2018; Bollhofer and Rosman, 2001; Lester and Gonzalez, 2011; Santschi et al., 2001).

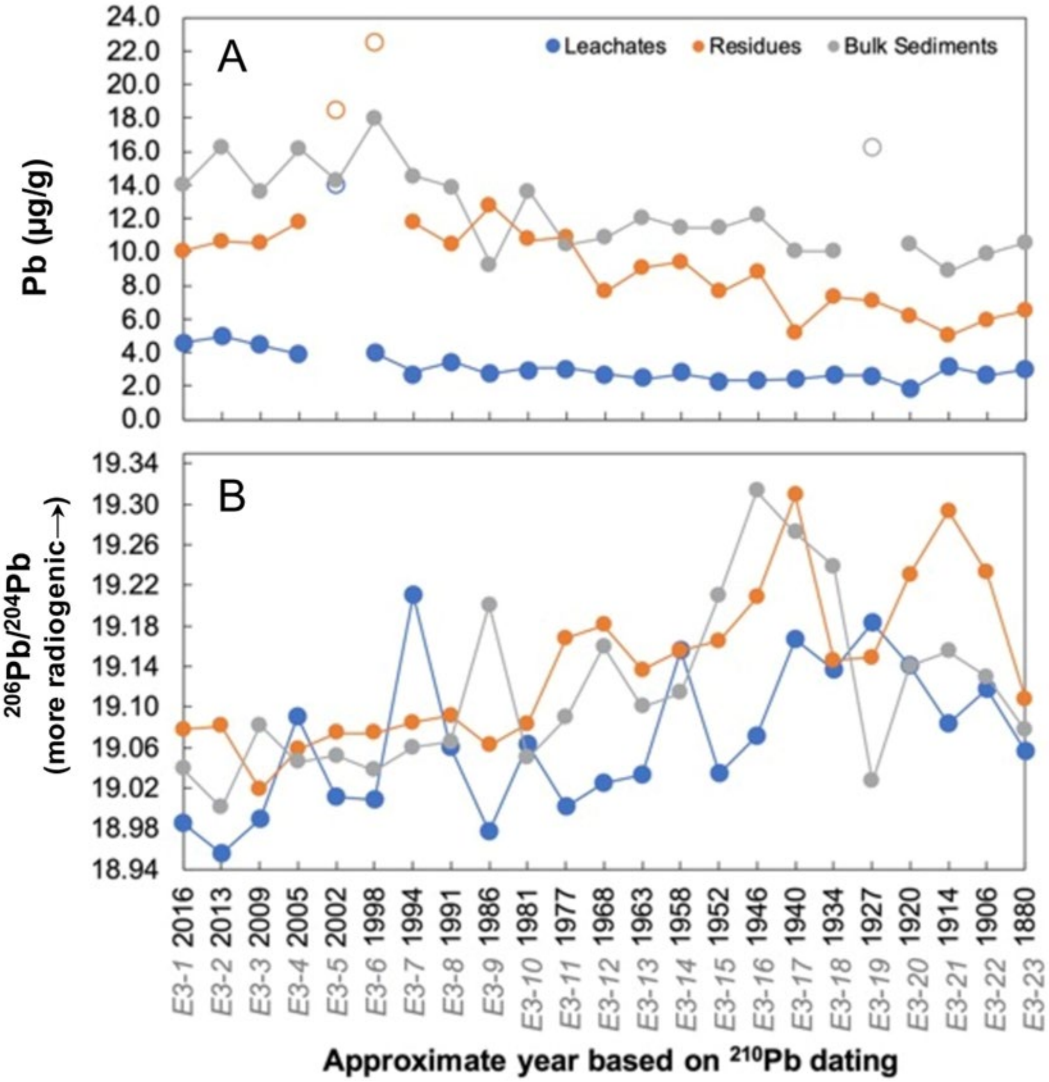

Figure 8. Galveston Bay core sediment Pb (a) concentrations and (b) isotope ratios between the years 1880 and 2016. Note that the x-axis is the same for both panels.

Galveston Bay Water Heavy Metal Concentrations

Galveston Bay water sample elemental concentrations are presented in Table 11 and range from 0 – 0.01 nanograms per milliliter (ng/mL) for Cd, 0.07 – 2.4 ng/mL for Cu, 0.09 – 24 ng/mL for Fe, 0.09 – 52 ng/mL for Mn, 0.04 – 2.3 ng/mL for Ni, 0 – 0.06 ng/mL for Pb, and 0 – 5.5 ng/mL for Zn. The surface water metal concentrations range as follows, Cd 0 – 0.02 ng/mL, Cu 0.44 – 2.4 ng/mL, Fe 0.15 – 24 ng/mL, Mn 0.12 – 52 ng/mL, Ni 0.43 – 2.3 ng/mL, Pb 0 – 0.06 ng/mL, and Zn 0.07 – 5.5 ng/mL. The bottom water metal concentrations range as follows, Cd 0 – 0.02 ng/mL, Cu 0.07 – 1.9 ng/mL, Fe 0.09 – 12 ng/mL, Mn 0.09 – 6.6 ng/mL, Ni 0.04 – 2.3 ng/mL, Pb 0 – 0.02 ng/mL, and Zn 0 – 0.93 ng/mL. The mean ± SD metal concentrations in the water samples is Cd 0.01 ± 0.004 ng/mL (surface 0.01 ± 0.004 ng/mL, bottom 0.01 ± 0.004 ng/mL), Cu 1.4 ± 0.38 ng/mL (surface 1.4 ± 0.42 ng/mL, bottom 1.3 ± 0.33 ng/mL), Fe 2.1 ± 4.0 ng/mL (surface 2.9 ± 5.0 ng/mL, bottom 1.3 ± 2.4 ng/mL), Mn 2.3 ± 7.3 ng/mL (surface 3.5 ± 10.0 ng/mL, bottom 0.94 ± 1.2 ng/mL), Ni 1.2 ± 0.41 ng/mL (surface 1.2 ± 0.42 ng/mL, bottom 1.3 ± 0.41 ng/mL), Pb 0.01 ± 0.01 ng/mL (surface 0.01 ± 0.004 ng/mL, bottom 0.01 ± 0.01 ng/mL), and Zn 0.38 ± 0.72 ng/mL (surface 0.52 ± 0.98 ng/mL, bottom 0.23 ± 0.13 ng/mL).

Table 11. Galveston Bay water metal concentration data. Metal concentration units are ng/mL. Dash indicates no sample/measurement taken.

Sample Date	**Station Number**	**Surface/ Bottom**	**Salinity (*psu)**	**Fe**	**Zn**	**Ni**	**Cu**	**Cd**	**Pb**	**Mn**
6/5/17	1	Bottom	22.5	0.38	0.19	0.83	1.12	0.015	0.007	3.27
6/5/17	2	Bottom	19.0	0.36	0.20	1.25	1.31	0.013	0.011	0.76
6/5/17	3	Bottom	17.0	0.12	0.32	1.53	1.69	0.011	0.012	0.37
6/5/17	4	Bottom	15.2	0.10	0.19	1.42	1.33	0.012	0.008	0.74
6/5/17	5A	Bottom	15.3	0.16	0.25	1.04	1.19	0.007	0.005	0.63
6/5/17	6	Bottom	16.8	0.09	0.15	1.16	1.27	0.014	0.005	0.36
6/8/17	6	Bottom	19.4	0.26	0.14	1.16	1.28	0.012	0.005	0.90
6/8/17	7	Bottom	14.1	0.62	0.21	1.45	1.36	0.008	0.008	0.51
6/8/17	8	Bottom	10.4	0.15	0.14	1.76	1.27	0.006	0.005	0.43
6/8/17	9	Bottom	7.5	0.29	0.16	1.98	1.18	0.005	0.008	0.58
6/8/17	10	Bottom	18.9	0.18	0.20	1.29	1.36	0.010	0.007	0.95
9/9/17	1	Bottom	8.7	3.05	0.25	0.77	1.12	0.006	0.005	0.71
9/9/17	2	Bottom	3.2	7.05	0.30	0.91	1.32	0.006	0.012	0.59
9/9/17	3	Bottom	2.7	7.97	0.29	1.07	1.38	0.005	0.010	0.71
9/16/17	3	Bottom	15.1	1.54	0.16	1.07	1.27	0.005	0.004	0.24
9/16/17	5A	Bottom	2.4	2.44	0.11	1.18	1.20	0.003	0.004	0.28
9/16/17	7	Bottom	2.5	3.93	0.19	1.34	1.31	0.003	0.009	0.24
9/16/17	8	Bottom	1.0	6.30	0.14	1.55	1.30	0.002	0.012	0.17
9/16/17	9	Bottom	0.2	12.31	0.13	1.91	1.14	0.002	0.018	0.47

Sample Date	Station Number	Surface/ Bottom	Salinity (*psu)	Fe	Zn	Ni	Cu	Cd	Pb	Mn
11/4/17	1	Bottom	25.3	0.23	0.25	0.68	0.87	0.016	0.008	1.90
11/4/17	3	Bottom	18.3	0.22	0.37	0.97	1.06	0.014	0.008	0.46
11/4/17	5A	Bottom	11.8	0.30	0.29	1.20	1.16	0.013	0.006	1.58
11/4/17	9	Bottom	9.5	0.28	0.22	1.31	1.26	0.012	0.005	0.41
11/4/17	11	Bottom	20.2	0.17	0.21	0.83	0.89	0.015	0.005	0.91
11/4/17	12	Bottom	11.2	0.20	0.27	1.28	1.31	0.010	0.005	0.30
11/4/17	13	Bottom	12.5	0.19	0.33	1.27	1.42	0.014	0.006	0.55
11/4/17	14	Bottom	15.9	0.24	0.35	1.07	1.20	0.015	0.007	0.78
3/24/18	3	Bottom	18.0	0.38	0.28	1.10	1.64	0.011	0.008	1.01
3/24/18	5B	Bottom	14.2	0.25	0.21	1.27	1.57	0.009	0.005	1.36
3/24/18	9	Bottom	0.3	1.56	0.28	2.33	1.37	0.004	0.014	0.09
3/24/18	11	Bottom	21.2	0.29	0.22	0.96	1.21	0.012	0.005	0.41
3/24/18	12	Bottom	2.5	0.54	0.22	1.94	1.68	0.004	0.007	0.23
3/24/18	13	Bottom	8.3	0.35	0.26	1.60	1.87	0.005	0.007	0.33
3/24/18	14	Bottom	14.3	0.31	0.30	1.31	1.73	0.007	0.008	0.41
3/24/18	15	Bottom	25.6	0.48	0.30	0.70	1.02	0.014	0.006	4.57
6/16/18	1	Bottom	29.6	0.39	0.15	0.68	0.85	0.011	0.011	2.17
6/16/18	3	Bottom	26.7	0.13	0.25	0.88	1.15	0.011	0.010	0.78
6/16/18	5B	Bottom	33.1	0.42	0.08	0.46	0.44	0.010	0.010	0.72
6/16/18	9	Bottom	9.9	0.23	0.14	1.73	1.68	0.007	0.008	1.65
6/16/18	11	Bottom	33.3	0.30	0.11	0.42	0.43	0.010	0.010	0.48
6/16/18	12	Bottom	14.0	0.16	0.19	1.54	1.80	0.010	0.010	1.02
6/16/18	13	Bottom	18.6	0.18	0.34	1.41	1.63	0.009	0.013	0.95
6/16/18	14	Bottom	23.7	0.14	0.20	1.10	1.37	0.008	0.012	0.71

Sample Date	Station Number	Surface/ Bottom	Salinity (*psu)	Fe	Zn	Ni	Cu	Cd	Pb	Mn
9/22/18	3	Bottom	17.9	0.26	0.41	1.07	1.46	0.011	0.016	0.66
9/22/18	5B	Bottom	20.2	-	-	-	-	-	-	-
9/22/18	9	Bottom	12.6	0.39	0.17	1.32	1.21	0.010	0.009	1.13
9/22/18	11	Bottom	26.4	0.21	0.20	0.68	1.01	0.012	0.009	0.69
9/22/18	12	Bottom	15.6	0.24	0.26	1.23	1.41	0.011	0.013	0.91
9/22/18	13	Bottom	16.1	0.28	0.36	1.24	1.72	0.014	0.017	0.43
9/22/18	14	Bottom	16.9	0.30	0.42	1.13	1.55	0.010	0.019	1.12
11/3/18	1	Bottom	26.2	0.37	0.25	1.00	1.19	0.012	0.008	0.86
11/3/18	3	Bottom	10.8	0.27	0.42	1.41	1.49	0.009	0.009	0.32
11/3/18	5B	Bottom	9.8	0.40	0.30	1.40	1.34	0.009	0.008	6.28
11/3/18	9	Bottom	0.2	10.52	0.31	1.75	1.27	0.004	0.022	0.40
11/3/18	11	Bottom	28.3	0.21	0.18	0.69	0.72	0.010	0.006	0.32
11/3/18	12	Bottom	0.2	4.73	0.15	1.80	1.20	0.002	0.009	0.33
11/3/18	13	Bottom	5.3	1.90	0.93	1.69	1.54	0.009	0.011	0.40
11/3/18	14	Bottom	8.4	0.46	0.51	1.55	1.36	0.009	0.009	0.49
3/23/19	1	Bottom	18.2	0.73	0.11	0.81	0.87	0.006	0.012	6.59
3/23/19	3	Bottom	12.9	-	-	-	-	-	-	-
3/23/19	5B	Bottom	12.9	0.47	0.17	0.98	1.42	0.008	0.011	0.60
3/23/19	9	Bottom	1.7	5.16	0.20	1.75	1.59	0.007	0.012	2.01
3/23/19	11	Bottom	21.0	0.66	0.05	0.54	0.80	0.008	0.010	1.36
3/23/19	12	Bottom	7.6	0.50	0.24	1.26	1.71	0.008	0.005	0.71
3/23/19	13	Bottom	10.1	0.38	0.24	1.13	1.77	0.008	0.005	0.91
3/23/19	14	Bottom	12.5	0.46	0.26	1.00	1.53	0.007	0.011	0.55

Sample Date	Station Number	Surface/ Bottom	Salinity (*psu)	Fe	Zn	Ni	Cu	Cd	Pb	Mn
6/19/19	1	Bottom	13.7	0.32	0.13	0.93	1.13	0.006	0.008	1.07
6/19/19	3	Bottom	8.3	0.41	0.21	1.25	1.48	0.004	0.007	0.20
6/19/19	5A	Bottom	-	-	-	-	-	-	-	-
6/19/19	5B	Bottom	-	-	-	-	-	-	-	-
6/19/19	9	Bottom	0.2	4.21	0.11	1.78	1.16	0.003	0.007	0.17
6/19/19	11	Bottom	20.7	0.32	0.11	0.65	0.75	0.009	0.007	0.31
6/19/19	12	Bottom	0.4	1.28	0.00	0.04	0.07	0.000	0.004	0.47
6/19/19	13	Bottom	1.8	0.72	0.17	1.55	1.45	0.002	0.004	0.11
9/9/17	1	Surface	7.3	3.08	0.25	0.78	1.13	0.007	0.006	0.88
9/9/17	2	Surface	3.2	6.50	0.27	0.92	1.36	0.006	0.012	0.57
9/9/17	3	Surface	2.8	6.94	0.37	1.03	1.39	0.004	0.011	0.68
9/16/17	3	Surface	6.1	1.58	0.20	1.09	1.29	0.005	0.004	0.24
9/16/17	5A	Surface	2.4	2.92	0.11	1.22	1.20	0.003	0.005	0.34
9/16/17	7	Surface	1.9	4.48	0.16	1.40	1.23	0.003	0.010	0.30
9/16/17	8	Surface	0.7	7.50	0.13	1.59	1.33	0.003	0.016	0.22
9/16/17	9	Surface	0.2	13.44	0.13	1.86	1.21	0.003	0.022	0.39
11/4/17	1	Surface	25.3	0.24	0.36	0.69	0.87	0.017	0.008	1.37
11/4/17	3	Surface	18.3	0.24	0.43	0.97	1.18	0.015	0.008	0.45
11/4/17	5A	Surface	11.8	0.34	0.30	1.21	1.24	0.013	0.006	5.35
11/4/17	9	Surface	9.5	0.29	0.23	1.30	1.32	0.013	0.005	0.63
11/4/17	11	Surface	20.1	0.18	0.28	0.83	0.87	0.015	0.008	0.66
11/4/17	12	Surface	11.2	0.25	0.36	1.28	1.35	0.010	0.006	0.32
11/4/17	13	Surface	12.5	0.20	0.30	1.24	1.38	0.011	0.006	0.26

Sample Date	**Station Number**	**Surface/ Bottom**	**Salinity (*psu)**	**Fe**	**Zn**	**Ni**	**Cu**	**Cd**	**Pb**	**Mn**
11/4/17	14	Surface	15.5	0.24	0.41	1.13	1.12	0.013	0.008	0.74
3/24/18	3	Surface	18.0	0.34	0.31	1.11	1.59	0.011	0.008	1.04
3/24/18	5A	Surface	14.2	0.27	0.21	1.28	1.64	0.009	0.005	0.68
3/24/18	9	Surface	0.3	2.29	0.25	2.33	1.41	0.004	0.017	0.19
3/24/18	11	Surface	19.2	0.38	0.35	1.08	1.39	0.011	0.006	0.48
3/24/18	12	Surface	2.5	0.62	0.20	1.95	1.55	0.004	0.007	0.13
3/24/18	13	Surface	8.3	0.35	0.28	1.60	1.97	0.006	0.007	0.42
3/24/18	14	Surface	14.3	0.41	0.30	1.34	1.80	0.007	0.008	0.49
3/24/18	15	Surface	23.8	0.57	0.74	0.83	1.21	0.014	0.011	4.27
6/16/18	1	Surface	29.6	0.39	0.11	0.67	0.82	0.011	0.011	2.84
6/16/18	3	Surface	26.5	0.17	0.42	0.88	1.26	0.012	0.011	0.64
6/16/18	5B	Surface	33.1	0.29	0.09	0.45	0.48	0.010	0.016	0.58
6/16/18	9	Surface	9.9	0.25	0.16	1.69	1.71	0.005	0.008	2.72
6/16/18	11	Surface	33.3	0.32	0.15	0.43	0.44	0.010	0.010	0.78
6/16/18	12	Surface	14.0	0.17	0.19	1.52	1.82	0.008	0.010	0.32
6/16/18	13	Surface	18.6	0.17	0.31	1.41	1.69	0.009	0.012	0.64
6/16/18	14	Surface	22.5	0.15	0.22	1.11	1.43	0.008	0.012	0.56
9/22/18	3	Surface	17.9	0.27	0.39	1.07	1.53	0.011	0.017	0.70
9/22/18	5B	Surface	-	-	-	-	-	-	-	-
9/22/18	9	Surface	12.6	0.40	0.18	1.41	1.41	0.011	0.011	0.98
9/22/18	11	Surface	22.8	0.20	0.20	0.76	1.07	0.012	0.011	0.53
9/22/18	12	Surface	15.6	0.25	0.24	1.24	1.26	0.012	0.013	0.63
9/22/18	13	Surface	16.1	0.30	0.36	1.20	1.74	0.013	0.017	0.49
9/22/18	14	Surface	16.9	0.35	0.41	1.19	1.64	0.012	0.020	1.18

Sample Date	Station Number	Surface/ Bottom	Salinity (*psu)	Fe	Zn	Ni	Cu	Cd	Pb	Mn
11/3/18	1	Surface	17.6	0.43	0.41	1.01	1.23	0.012	0.009	1.07
11/3/18	3	Surface	10.7	0.24	0.42	1.43	1.52	0.009	0.009	0.34
11/3/18	5B	Surface	9.8	0.43	0.32	1.40	1.36	0.009	0.008	4.85
11/3/18	9	Surface	0.2	12.11	0.20	1.74	1.19	0.003	0.022	1.58
11/3/18	11	Surface	16.1	0.20	0.28	1.09	1.12	0.010	0.006	0.26
11/3/18	12	Surface	0.2	4.84	0.15	1.79	1.19	0.002	0.010	0.27
11/3/18	13	Surface	5.2	1.93	0.96	1.69	1.58	0.009	0.011	0.41
11/3/18	14	Surface	8.3	0.47	0.47	1.56	1.40	0.009	0.009	0.52
3/23/19	1	Surface	17.5	0.87	0.13	0.82	0.96	0.007	0.013	8.11
3/23/19	3	Surface	12.9	0.48	0.17	0.99	1.58	0.009	0.011	0.53
3/23/19	5B	Surface	-	0.47	0.17	0.98	1.42	0.008	0.011	0.60
3/23/19	9	Surface	1.4	4.78	0.20	1.69	1.54	0.007	0.011	1.08
3/23/19	11	Surface	19.8	0.64	0.07	0.65	0.93	0.008	0.010	1.09
3/23/19	12	Surface	7.6	0.49	0.23	1.25	1.74	0.008	0.005	0.90
3/23/19	13	Surface	10.1	0.40	0.23	1.15	1.84	0.008	0.005	0.61
3/23/19	14	Surface	12.4	0.41	0.22	1.04	1.61	0.007	0.010	0.52
6/19/19	1	Surface	13.7	0.34	0.15	0.98	1.27	0.007	0.007	0.73
6/19/19	3	Surface	8.3	0.41	0.21	1.26	1.52	0.004	0.007	0.18
6/19/19	5A	Surface	4.2	0.48	0.16	1.38	1.34	0.003	0.004	0.36
6/19/19	5B	Surface	10.5	0.39	0.15	1.08	1.32	0.002	0.006	0.19
6/19/19	9	Surface	0.2	4.39	0.13	1.72	1.13	0.003	0.007	0.21
6/19/19	11	Surface	20.8	0.32	0.09	0.64	0.78	0.009	0.007	0.30
6/19/19	12	Surface	0.4	-	-	-	-	-	-	-

Sample Date	Station Number	Surface/ Bottom	Salinity (*psu)	Fe	Zn	Ni	Cu	Cd	Pb	Mn
6/19/19	13	Surface	1.8	0.70	0.14	1.58	1.44	0.003	0.004	0.12
6/15/19	101	Surface	1.3	5.34	0.58	1.23	2.07	0.001	0.020	0.88
6/15/19	102	Surface	0.8	6.48	0.63	1.13	2.18	0.001	0.023	0.71
6/15/19	103	Surface	0.3	10.59	0.63	0.89	2.10	0.001	0.027	0.69
6/15/19	201	Surface	5.9	2.71	4.82	2.00	2.44	0.016	0.016	29.92
6/15/19	202	Surface	3.6	4.84	5.53	2.18	2.41	0.011	0.023	52.25
6/15/19	203	Surface	4.7	4.85	4.39	2.01	2.40	0.012	0.022	46.12
6/15/19	301	Surface	1.9	24.18	2.35	1.76	2.41	0.007	0.061	40.35
6/15/19	302	Surface	1.2	22.95	2.16	1.67	2.32	0.005	0.039	23.82
6/16/19	401	Surface	6.6	1.74	0.41	1.21	1.31	0.004	0.006	0.65
6/16/19	402	Surface	3.3	20.66	0.32	1.16	1.24	0.003	0.022	2.47
6/16/19	403	Surface	6.5	-	-	-	-	-	-	-
6/16/19	501	Surface	0.2	4.21	0.15	1.83	1.11	0.003	0.004	0.58
6/16/19	502	Surface	0.2	4.87	0.16	1.84	1.09	0.003	0.005	0.98
6/16/19	503	Surface	0.2	5.15	0.18	1.82	1.12	0.003	0.005	1.00

*psu = practical salinity units

Spatial variability in water heavy metal concentrations

Salinity driven flocculation controls the spatial distribution of dissolved heavy metal concentrations in Galveston Bay waters. Low salinity regions have higher dissolved heavy metal loads than high salinity regions (Table 12). Cadmium is the exception to this as it readily forms chloride complexes, which can result in higher dissolved Cd concentrations with increasing salinity (Wen et al., 1999). Bay stations near the Gulf of Mexico (Stations 1, 4, 6, 10, 11, and 15) have mean ± SD salinity of 21.2 ± 6.1 psu and mean ± SD Cd, Cu, Fe, Mn, Ni, Pb, and Zn concentrations of 0.011 ± 0.003 ng/mL, 1.01 ± 0.24 ng/mL, 0.51 ± 0.68 ng/mL, 1.57 ± 1.85 ng/mL, 0.83 ± 0.23 ng/mL, 0.008 ± 0.002 ng/mL, and 0.21 ± 0.13 ng/mL. Endmember stations (Stations 101, 102, 103, 201, 202, 203, 301, 302, 401, 402, 501, 502, and 503) have mean ± SD salinity of 2.6 ± 2.5 psu and mean ± SD metal concentrations of Cd 0.005 ± 0.005 ng/mL, Cu 1.73 ± 0.75 ng/mL, Fe 8.47 ± 8.05 ng/mL, Mn 14.32 ± 19.79 ng/mL, Ni 1.48 ± 0.58 ng/mL, Pb 0.019 ± 0.016 ng/mL, and Zn 1.59 ± 1.95 ng/mL. Waters from bay stations within Galveston Bay proper (Stations 2-3, 5A, 5B, 7-9, 12-14) have mean ± SD salinity of 10.7 ± 7.5 psu and mean ± SD dissolved metal concentrations between the endmember and Gulf of Mexico adjacent bay stations as follows, Cd 0.007 ± 0.004 ng/mL, Cu 1.32 ± 0.44 ng/mL, Fe 1.48 ± 2.79 ng/mL, Mn 0.67 ± 0.99 ng/mL, Ni 1.24 ± 0.48 ng/mL, Pb 0.009 ± 0.005 ng/mL, and Zn 0.25 ± 0.15 ng/mL.

Table 12. Summary of water heavy metal concentrations at high, moderate, and low salinity stations in Galveston Bay.

	High salinity stations		**Moderate salinity stations**		**Low salinity stations**	
	Average	*Standard deviation*	*Average*	*Standard deviation*	*Average*	*Standard deviation*
Salinity (psu)	21.15	6.11	10.71	7.48	2.62	2.46
Cd (ng/mL)	0.011	0.003	0.007	0.004	0.005	0.005
Cu (ng/mL)	1.01	0.24	1.32	0.44	1.73	0.75
Fe (ng/mL)	0.51	0.68	1.48	2.79	8.47	8.05
Mn (ng/mL)	1.57	1.85	0.67	0.99	14.32	19.79
Ni (ng/mL)	0.83	0.23	1.24	0.48	1.48	0.58
Pb (ng/mL)	0.008	0.002	0.009	0.005	0.019	0.016
Zn (ng/mL)	0.21	0.13	0.25	0.15	1.59	1.95

Temporal variability in water heavy metal concentrations

Trinity River discharge <250 m^3/s constitutes dry conditions and Trinity River discharge >250 m^3/s indicates wet conditions. Using this categorization, dry conditions occur during the November 2017, June 2018, and September 2018 sampling events and wet conditions prevail during June 2017, September 2017, March 2018, November 2018, March 2019, and June 2019 (Table 7). In wet conditions the mean ± SD salinity is 9.0 ± 7.8 psu and the mean ± SD dissolved metal concentrations are Cd 0.007± 0.004 ng/mL, Cu 1.40 ± 0.38 ng/mL, Fe 2.92 ± 4.62 ng/mL, Mn 2.82 ± 8.66 ng/mL, Ni 1.32 ± 0.42 ng/mL, Pb 0.010 ± 0.008 ng/mL, and Zn 0.43 ± 0.86 ng/mL. In dry conditions the mean ± SD salinity is 19.0 ± 7.1 psu and the mean ± SD dissolved metal concentrations are Cd 0.011 ± 0.003 ng/mL, Cu 1.24 ± 0.37 ng/mL, Fe 0.25 ± 0.08 ng/mL, Mn 0.99 ± 0.89 ng/mL, Ni 1.07 ± 0.33 ng/mL, Pb 0.010 ± 0.004 ng/mL, and Zn 0.27 ± 0.10 ng/mL.

Galveston Bay Oyster Tissue Heavy Metal Concentrations

Table 13 shows the oyster tissue Pb, Cd, Zn, and Hg concentrations. According to river gage data from the USGS (gage number 08067000), the average Trinity River discharge was approximately 109 cubic meters per second (m^3/s) in December 2019-January 2020 and 207 m^3/s in September 2020 (USGS Water Data for the Nation tool). Metal concentrations within these sedentary oysters reflect a compilation of metal fluxes over time. The December 2019 and January 2020 oysters represent the dry conditions that prevailed during the two to three months prior to sampling. The September 2020 oysters are representative of the wet period three to six months prior to sample collection. Consequently, oyster tissue samples from December 2019 and January 2020 are referred to as “dry” samples, while oyster tissue samples from September 2020 are referred to as “wet” samples.

Table 13. Galveston Bay oyster tissue heavy metal concentrations.

Sample ID	Area*	Wet/Dry	Cd (*µg/g)	Pb (µg/g)	Zn (µg/g)	Hg (µg/g)
93	Upper GB/Trinity Bay	Dry	0.47	0.08	580.04	*b.d.*
169	Upper GB/San Jacinto River	Dry	2.36	0.46	2228.03	0.05
396	Lower GB	Dry	0.77	0.10	630.95	0.04
405	East Bay	Dry	3.39	0.32	2398.21	0.06
563	West Bay	Dry	2.35	0.61	2431.03	0.09
110	Upper GB/Trinity Bay	Wet	3.29	0.66	2139.12	0.05
168	Upper GB/San Jacinto River	Wet	3.10	0.61	4114.22	0.07
435	Lower GB	Wet	2.98	0.75	5090.44	0.05
350	East Bay	Wet	4.51	0.46	1961.51	0.07
576	West Bay	Wet	3.06	0.76	1804.58	0.08

*GB = Galveston Bay; b.d. = below detection; µg/g = micrograms per gram

Mean ± SD metal concentrations for the samples are 2.63 ± 1.22 µg/g for Cd, 0.48 ± 0.25 µg/g for Pb, 2,337.81 ± 1,383.46 µg/g for Zn, and 0.06 ± 0.02 µg/g for Hg. Mercury content in the dry season Trinity Bay oyster sample (sample ID 93) is below the analytical detection limit and thus excluded from the mean. Metal concentrations within the oysters do not covary and have weak linear correlations ($R^2 < 0.49$), indicating that different metals are differentially sourced to and/or utilized by Galveston Bay oysters.

Spatial variability in Galveston Bay oyster tissue heavy metal concentrations

The spatial distributions of oyster tissue metal concentrations indicate that oysters in Lower Galveston Bay (Area 3) and Upper Galveston Bay/Trinity Bay (Area 1) are generally more pristine, containing lower metal concentrations than oysters elsewhere in Galveston Bay (Fig. 9; exception of wet season oyster Lower Galveston Bay Zn concentrations and wet season Pb concentrations). The lowest Pb (0.37 ± 0.41 µg/g), Hg (below detection), Cd (1.88 ± 2.00 µg/g), and Zn (1,359.58 ± 1,102.44 µg/g) concentrations were observed in Upper Galveston/Trinity Bay. Lower Galveston Bay also had low Hg (average of 0.04 ± 0.005 µg/g) and low (Cd 1.87 ± 1.56 µg/g). In contrast, West Bay had the highest Pb concentrations (0.68 ± 0.11 µg/g) and Hg concentrations (0.08 ± 0.005 µg/g); East Bay had the highest Cd concentrations (3.95 ± 0.79 µg/g); and Upper Galveston Bay/San Jacinto River area had the highest Zn concentrations (3,171.12 ± 1,333.74 µg/g).

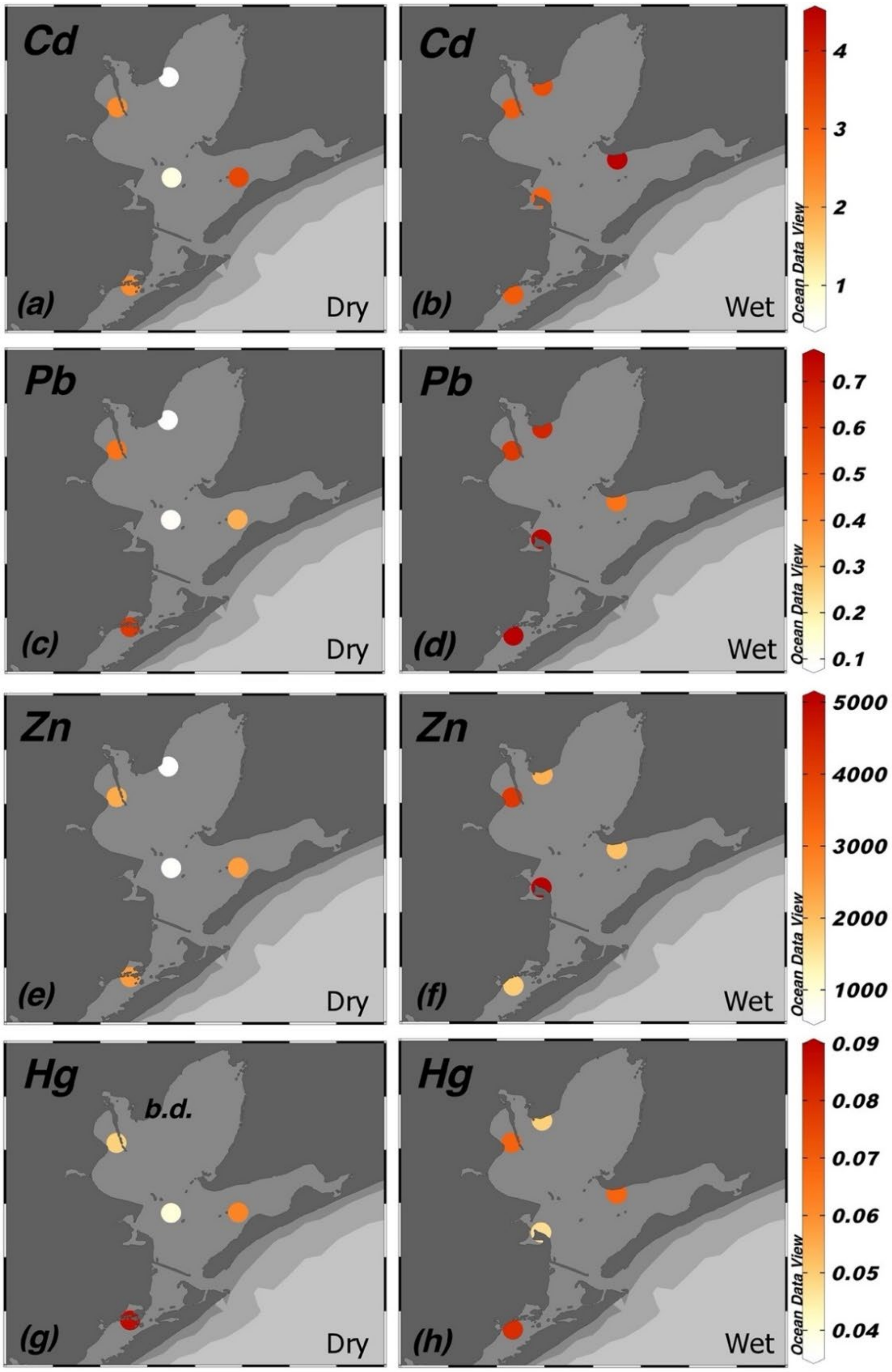

b.d. = below detection.

Figure 9. Spatiotemporal variation in Galveston Bay oyster tissue metal concentrations (µg/g). Left side panels a, c, e, g contain dry condition samples. Right side panels b, d, f, h contain wet condition samples.

Temporal variability in Galveston Bay oyster tissue heavy metal concentrations

Oyster tissues collected during wet conditions have higher metal concentrations than oysters collected during dry conditions. The dry oysters have Cd concentrations between 0.47 – 3.39 µg/g (average of 1.87 µg/g), Pb concentrations of 0.08 – 0.61 µg/g (average of 0.31 µg/g), and Zn concentrations of 580.04 – 2,431.03 µg/g (average of 1,653.65 µg/g). The Cd, Pb and Zn in wet season oysters ranges from 2.98 – 4.51 µg/g (average of 3.39 µg/g), 0.46 – 0.76 µg/g (average of 0.65 µg/g) and 1,804.58 – 5,090.44 µg/g (average of 3,021.98 µg/g), respectively. Mercury deviates from this temporal trend with both wet and dry oysters containing a mean ± SD of 0.06 ± 0.02 µg/g Hg (no seasonal distinction). Given that Hg is primarily introduced to aquatic environments from atmospheric deposition, it stands to reason that Hg levels could remain stable while Cd, Pb and Zn levels vary temporally in response to other source inputs (Apeti et al., 2012; Muir et al., 2005; U.S. EPA, 1997; United States Geological Survey,1997).

Galveston Bay Oyster Tissue Pb Isotope Ratios

Table 14 tabulates the Pb isotope compositions measured in Galveston Bay oyster tissues. The Pb isotope compositions measured in Galveston Bay oyster tissues range from $^{206}Pb/^{204}Pb$ = 18.949 ± 0.001 – 19.084 ± 0.003, $^{207}Pb/^{204}Pb$ = 15.654 ± 0.002 – 15.678 ± 0.002, and $^{208}Pb/^{204}Pb$ = 38.753 ± 0.012 – 38.992 ± 0.007. Oyster tissue Pb contents range from 0.08 µg/g to 0.76 µg/g with a mean ± SD concentration of 0.48 ± 0.25 µg/g. Two Galveston Bay oyster tissue sample aliquots were digested separately for Pb concentration (HNO_3 digestion) and Pb isotope ratio (HNO_3, HF, H_2O_2 digestion) analyses; thus, a truly direct comparison cannot be assumed. However, assuming true sample homogenization during sample preparation, the Pb isotopic composition of a sample does not depend on the Pb content within that sample. This is corroborated by good agreement between measured Pb isotope ratios of the NIST 1566b SRM in this study and previous work (Lopez, 2021b). For this reason, a preliminary comparison between Galveston Bay oyster tissue Pb isotope ratios and concentrations is made here. Correlation coefficient values between the $^{206}Pb/^{204}Pb$, $^{207}Pb/^{204}Pb$, and $^{208}Pb/^{204}Pb$ ratios of the oyster tissues range between 0.17 and 0.40. Weak linear correlations (R^2 between 0.38 – 0.44) exist between oyster tissue Pb concentrations and Pb isotope ratios, indicating that Pb isotope ratio variation does not correspond with Pb concentration change in the oyster tissues. The lack of consistent linear correlations between Pb isotope ratios indicates that the oyster tissues do not fit into a single binary mixing model with two main Pb sources. Rather it is likely that more than two Pb sources contribute to the samples, which was also true for Galveston Bay sediment.

Table 14. Galveston Bay oyster tissue Pb isotope ratios.

Sample ID	Area*	Wet/Dry	$^{206}Pb/^{204}Pb$	error	$^{207}Pb/^{204}Pb$	error	$^{208}Pb/^{204}Pb$	error

93	Upper GB/ Trinity Bay	Dry	19.010	0.002	15.678	0.002	38.863	0.005
169	Upper GB/San Jacinto River	Dry	19.082	0.002	15.672	0.002	38.852	0.004
396	Lower GB	Dry	19.080	0.004	15.674	0.003	38.926	0.009
405	East Bay	Dry	19.084	0.003	15.677	0.003	38.992	0.007
563	West Bay	Dry	18.949	0.001	15.667	0.001	38.834	0.003
110	Upper GB/ Trinity Bay	Wet	19.001	0.003	15.654	0.002	38.844	0.006
168	Upper GB/San Jacinto River	Wet	18.982	0.006	15.669	0.005	38.753	0.012
435	Lower GB	Wet	18.988	0.005	15.671	0.004	38.806	0.01
350	East Bay	Wet	19.057	0.005	15.667	0.005	38.813	0.012
576	West Bay	Wet	18.950	0.004	15.668	0.003	38.826	0.008

*GB = Galveston Bay

Spatial variability in Galveston Bay oyster tissue Pb isotope ratios

There are more radiogenic Pb isotope compositions of the oyster tissues in Upper Galveston Bay/San Jacinto River, Upper Galveston Bay/Trinity Bay, Lower Galveston Bay, and East Bay (i.e., areas 1-4) compared to those from West Bay (area 5; Fig. 10). Specifically, the areas 1-4 oysters range from ^{206}Pb/^{204}Pb = 18.982 ± 0.006 – 19.084 ± 0.003, ^{207}Pb/^{204}Pb = 15.654 ± 0.002 – 15.678 ± 0.002, and ^{208}Pb/^{204}Pb = 38.753 ± 0.012 – 38.992 ± 0.007, while West Bay oysters have well-constrained values between ^{206}Pb/^{204}Pb = 18.949 ± 0.001 – 18.950 ± 0.004, ^{207}Pb/^{204}Pb = 15.667 ± 0.001 – 15.668 ± 0.003, and ^{208}Pb/^{204}Pb = 38.826 ± 0.003 – 38.834 ± 0.008.

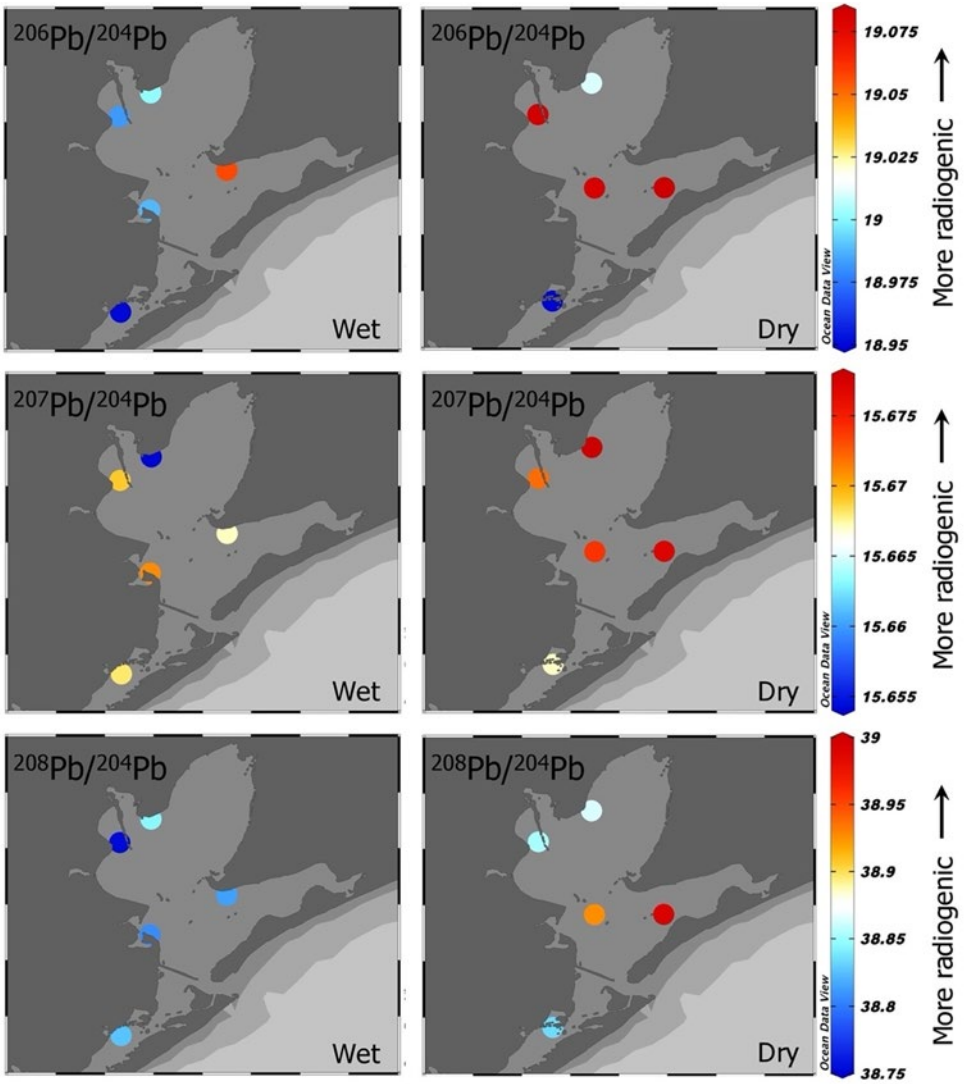

Left side panels contain Pb isotopic data for oyster samples collected in wet conditions. Right side panels show Pb isotope ratios for oyster samples collected in dry conditions. Warmer colors indicate more radiogenic Pb isotope ratios.

Figure 10. Spatiotemporal variation in Galveston Bay oyster tissue 206Pb/204Pb, 207Pb/204Pb and 208Pb/204Pb ratios.

Temporal variability in Galveston Bay oyster tissue Pb isotope ratios

Temporally, Galveston Bay oyster tissue Pb isotope compositions vary between the dry and wet sampling events (Fig. 10). Samples collected in dry conditions have more radiogenic Pb isotope compositions and lower Pb concentrations than samples collected in wet conditions. The dry condition oysters have 206Pb/204Pb ratios of 18.949 ± 0.001 – 19.084 ± 0.003, 207Pb/204Pb ratios of 15.667 ± 0.001 – 15.678 ± 0.002, 208Pb/204Pb ratios of 38.384 ± 0.003 – 38.992 ± 0.007 and a mean ± SD Pb content of 0.26 ± 0.13 µg/g. The wet condition oyster Pb isotope ratios are between 18.950 ± 0.004 – 19.057 ± 0.005 (206Pb/204Pb), 15.654 ± 0.002 – 15.671 ± 0.004 (207Pb/204Pb), 38.753 ± 0.012 – 38.844 ± 0.006 (208Pb/204Pb).

Discussion

Galveston Bay Sediments

Discussion of spatiotemporal variation in sediment heavy metal concentrations

Independent t-tests were done in IBM SPSS 26.0 on the Galveston Bay bulk sediment heavy metal concentration data to evaluate 1) whether the spatial trend of higher bay and shoreline station metal contents east of the HSC versus west of the HSC is statistically significant for each metal measured, 2) whether the spatial trend of lower Trinity River endmember station metal contents versus higher endmember stations metal contents is statistically significant for each metal measured and 3) if the mean metal concentrations are different between wet and dry conditions (Ross and Willson, 2017; Gaur and Gaur, 2006). P values less than 0.05 are statistically significant. There is a significant difference in mean metal concentrations between bay and shoreline stations located to the east of the HSC and bay and shoreline stations located to the west of the HSC ($p < 0.01$). There is a significant difference in mean Cd, Pb, Ni, and Zn concentrations between Trinity River endmember stations and bay and the other endmember stations ($p < 0.04$). Independent t-tests results indicate that the differences in metal concentration means between wet and dry conditions are only statistically significant for Pb ($p < 0.04$).

Low metal concentrations at western stations are surprising, since industrial metal sources are significantly greater in the west near Houston than in the more natural eastern Galveston Bay. However, Trinity River is the primary source of freshwater to Galveston Bay and so the northeast corner of Galveston Bay carries the lowest salinity (Du et al., 2019a-b; Guthrie et al., 2012). High riverine concentrations of dissolved metals are flocculated at salinity <5 in this region, driving the elevated metal concentrations in eastern Galveston Bay sediments (Wen et al., 1999). This is confirmed by the fact that metal concentrations at low-salinity Trinity River endmember stations 501-503 are some of the lowest in the study (Table 4, Fig. 5). Thus, the Trinity River does not supply the high sedimentary metal loads to Galveston Bay; instead, the high heavy metal contents in eastern Galveston Bay are the result of adsorbed metals on sediment surfaces during estuarine flocculation. Additionally, it is possible that under certain hydrodynamic conditions, some metal-rich sediments from the San Jacinto River/Buffalo Bayou are transported east of the HSC and are physically trapped there; a good example is the sediments deposited by Hurricane Harvey at Stations 5-12 that account for the observed higher metal contents in these areas (Dellapenna et al., 2021 *in review*).

Heavy metal toxicity in Galveston Bay sediments

The National Ocean and Atmospheric Administration (NOAA) Screening Quick Reference Tables (SQuiRTs) provide T20 and T50 toxicity thresholds for Cd, Ni, Pb, and Zn in marine sediment (Buchman, 2008). The T20 and T50 values are the concentrations of a given element above which there is a 20% or 50% probability of observing benthic toxicity. The measured heavy metal concentrations values for Galveston Bay sediment leachates and digests were compared to the NOAA SQuiRTs T20 and T50 values to assess toxicity in the bay (Table 15). In the leachates 1.3% of samples exceed T20 and T50 limits for Zn. Bulk sediment T20 threshold exceedances are as follows, 1.0% of samples are above Cd and Cu limits and 6.0% of samples are higher than the Ni and Zn limits.

The TCEQ Texas Risk Reduction Program[1] provides sediment benchmarks for assessing heavy metal toxicity in marine sediments. The measured heavy metal concentrations values for Galveston Bay sediment leachates and digests were compared to the TCEQ Texas Risk Reduction Program saltwater benchmark (“TCEQ 1”) and saltwater benthic protective concentration level (“TCEQ 2”) values to assess toxicity in the bay (Table 15). In the leachates 1.3% of samples exceed TCEQ 1 and TCEQ 2 limits for Zn. Two percent of bulk sediment samples exceed TCEQ 1 threshold for Cu and Zn, whereas 1.0% of samples are higher than the Ni limit. Bulk sediment TCEQ 2 exceedances are as follows, 2.0% of samples exceed the Cu limit and 1.0% of samples exceed the Zn limit.

The low levels of toxicity observed in Galveston Bay sediments, especially sediments near the Gulf of Mexico, indicate that minor amounts of toxic metals (Zn > Cu, Ni > Cd) enter into the Gulf of Mexico as estuarine sediments are exported from the bay into the open ocean. This is particularly poignant for the sediment leachates which represent metals that are most readily accessible to biota in Galveston Bay.

---

[1] www.tceq.texas.gov/remediation/trrp

Table 15. Galveston Bay bulk sediment toxicity screening using NOAA SQuiRTs, TCEQ sediment saltwater benchmark (TCEQ 1), and TCEQ sediment saltwater benthic protective concentration level (TCEQ 2) values.

	Cd	**Cu**	**Ni**	**Pb**	**Zn**
Leachates					
% above T_{20}	-	-	-	-	1.3
% above T_{50}	-	-	-	-	1.3
% above TCEQ 1	-	1.3	-	-	1.3
% above TCEQ 2	-	1.3	-	-	1.3
Bulk sediments					
% above T_{20}	1.0	1.0	6.0	-	6.0
% above T_{50}	-	-	-	-	-
% above TCEQ 1	-	2.0	1.0	-	2.0
% above TCEQ 2	-	2.0	-	-	1.0
NOAA SQuiRTs					
T_{20} (µg/g)	0.38	32	15	30	94
T_{50} (µg/g)	1.4	94	47	94	245
TCEQ values					
TCEQ 1 (µg/g)	1.2	34	21	47	150
TCEQ 2 (µg/g)	5.4	152	36	132	280

Percentages calculated by dividing the number of samples exceeding the T_{20} and T_{50} limits, respectively, divided by the total number of measurements then multiplying by 100. Dashes indicate no exceedances.

Discussion of spatiotemporal variation in sediment Pb isotope ratios

The bay station bulk sediment Pb isotope ratios are variable and do not follow a clear spatial pattern (Fig. 11). Because bulk digests represent the combination of sediment leachate and residue components, they display more overlap between stations making regional differences more difficult to visualize. Temporally, there are no clear patterns in sediment leachate, residue, or bulk digest Pb isotope ratios. Rather sporadic shifts in Pb input to the study area, which may be natural (i.e., changes in riverine discharge) and/or anthropogenic (i.e., pollutant releases), can account for the variable Pb isotope ratios in sediment leachates, residues, and bulk sediments. For example, Hurricane Harvey moved across southeast Texas from August 26-30, 2017, depositing record-breaking rainfall totals, which resulted in massive freshwater fluxes through Galveston Bay (Steichen et al., 2020). A thick sediment layer was deposited across the bay following severe Harvey flooding, which may have redistributed sediments at more than under normal bay conditions resulting in unique Pb isotope ratios during this time (Dellapenna et al., 2021 in review).

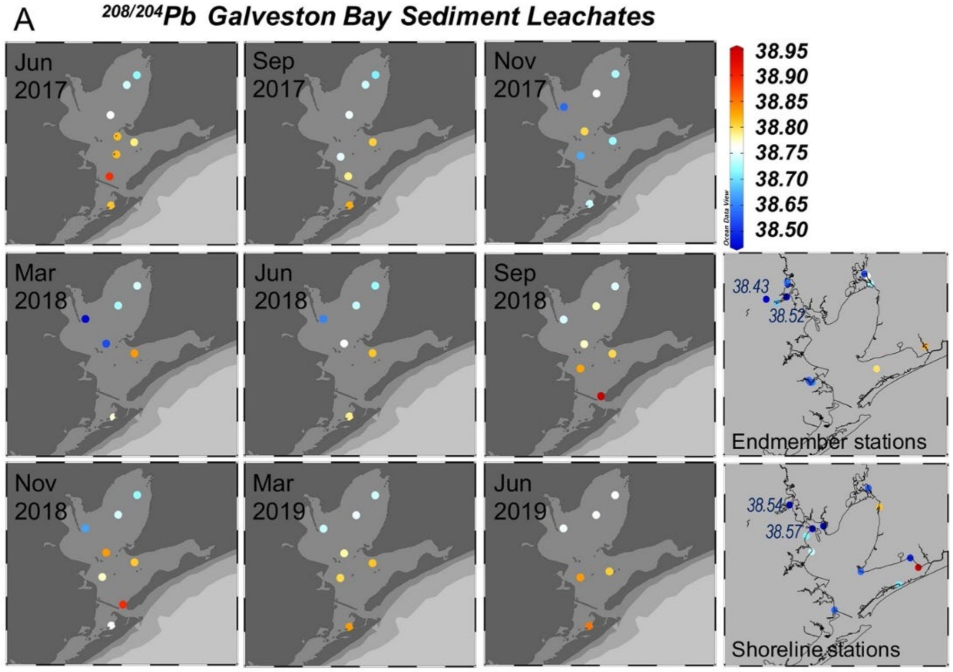

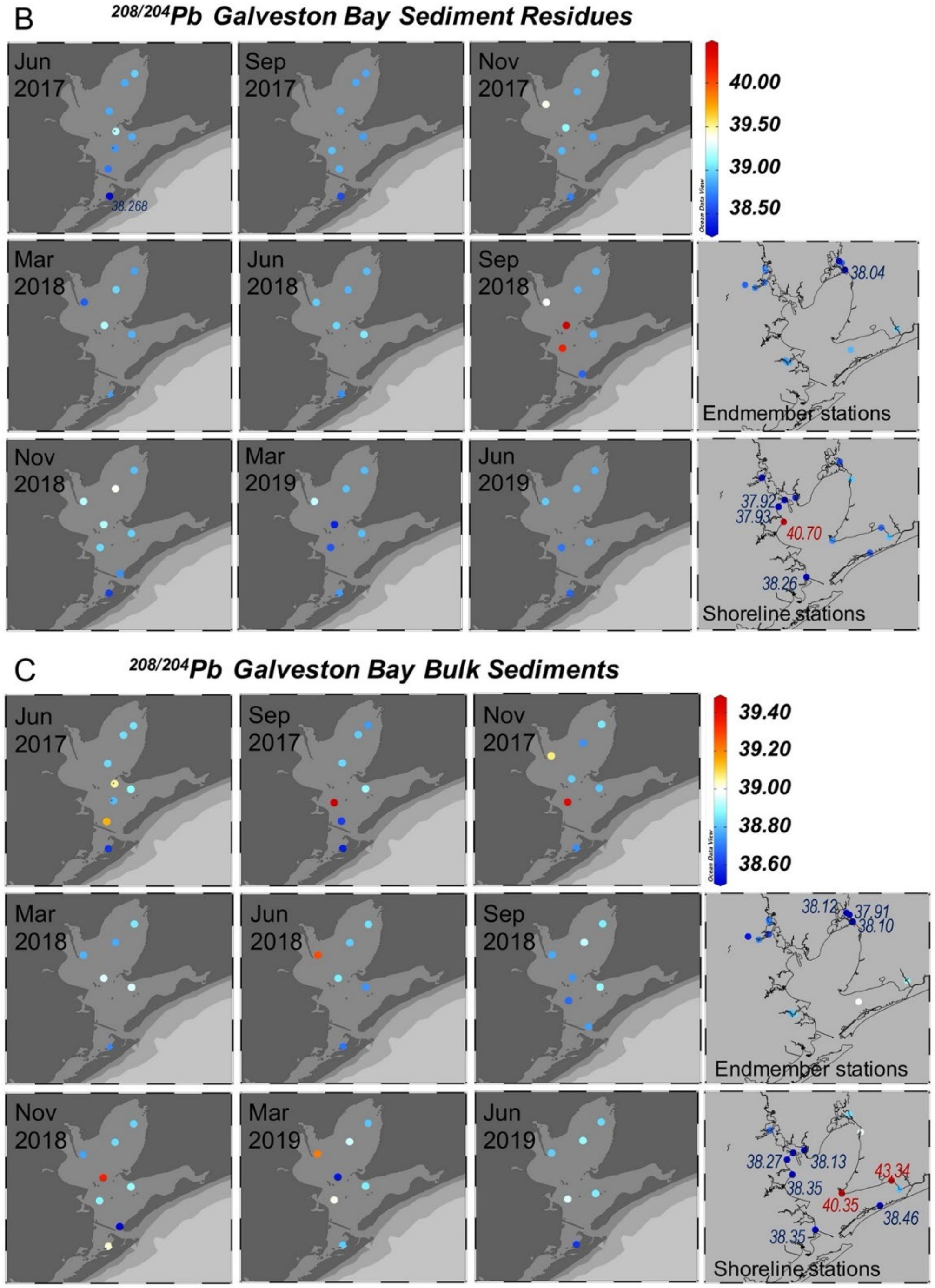

Cooler colors indicate less radiogenic (lower ^{208}Pb/^{204}Pb) ratios, and warmer colors indicate more radiogenic (higher ^{208}Pb/^{204}Pb) ratios.

Figure 11. Spatiotemporal variation of Galveston Bay sediment (a) leachates, (b) residues and (c) bulk sediments 208Pb/204Pb ratios.

Heavy metal sources in Galveston Bay sediments (Pb isotope modeling)

Previous studies have reported industrial heavy metal inputs to Galveston Bay from vehicle exhaust, surface runoff, spills and leaks from vessels traversing the bay and atmospheric deposition (Al Mukaimi et al. 2018; Harmon et al., 2003; Morse et al. 1993). Chemical production and petrochemical activities within the HSC have been determined to be the main culprits of anthropogenic metals in Galveston Bay and the Gulf of Mexico (Apeti et al., 2012). A few cases of Galveston Bay heavy metal point sources have been identified including a former Chlor-Alkali plant and paper mill (Al Mukaimi et al. 2018; Hieke et al. 2016). Unpublished data indicates that sediments adjacent to the paper mill had elevated Cd, Cu, and Pb concentrations denoting that the paper mill may have contributed metals to the bay in addition to dioxins (Presley et al. 1990).

Here, the sources of Pb (and by proxy other heavy metals) in Galveston Bay sediments is explored using a Pb isotope modeling approach. Further investigation into the sources of heavy metals in Galveston Bay sediments using enrichment factors, principal components analysis, and cluster analysis was done by Lopez (2021). Briefly, Lopez (2021) determined that Ni in Galveston Bay sediments is primarily derived from natural sources (i.e., continental weathering of crustal rocks) whereas Cd, Pb and Zn are mainly derived from anthropogenic (i.e., pollutant) sources. The source of Cu to Galveston Bay sediments is the least clear. Some metrics suggest that Cu is naturally sourced, however an anthropogenic source of Cu in Galveston Bay is considered more likely given the increasing prevalence of Cu as a pollutant in anthropogenically influenced aquatic systems (Lopez, 2021; Herut and Sandler, 2006; Presley et al., 1990; Sholkovitz, 1989).

Pb isotope modeling – MixSIAR

Lead in sediments is a mixture between natural and anthropogenic Pb (Komarek et al., 2008; Hansmann and Koppel, 2000). Linear arrays defined by three isotopes can be interpreted as mixing between two endmembers at either end of the linear trend (Marcantonio et al., 2000). In cases where more than two or three endmembers exist, linear mixing arrays may be insufficient for parsing Pb source contributions to an area. Pb isotope mixing models can then be used to quantitatively assess Pb sources recorded within a sediment sample mixture. Commonly used Pb isotope binary or ternary mixing models are useful for constraining Pb sources in well determined systems where only two or three of sources are plausible (Alyazichi et al., 2016; Bird, 2011; Marcantonio et al., 2000). The Pb isotope data in this study indicate that more than three sources of Pb exist within Galveston Bay sediments (Fig. 7). More complex models that incorporate more than three Pb sources can offer a clearer understanding of the potential Pb source inputs to a study area. In the mixing space defined by two isotopic ratios, sources can be considered vertices of a polygon in which mixtures reside. Monte Carlo simulations of a mixing polygon can quantitatively evaluate the mixing space geometry and estimate the relative contributions of each source to a mixture that lays within the mixing polygon (Upadhayhay et al., 2017). MixSIAR is a software package that creates and implements Bayesian mixing models to analyze Pb isotopes and estimate the proportions of source contributions to a sample mixture (Stock et al., 2018). MixSIAR is the framework in which Bayesian statistics is used to create a mixing model that incorporates means and standard deviations of user data and prior study system information. Markov Chain Monte Carlo (MCMC) simulations are used to generate model fits, which result in probable Pb source proportion estimates based upon the data and probability densities. Pb source proportion estimates that are not probabilistically consistent with the data are rejected and modeled sample mixtures must be close to the input sample mixtures in order for the MCMC chains to reach convergence. The model outputs posterior distributions, which are probability distributions for each Pb source in the designated study area. Further details regarding the MixSIAR model may be found in Longman et al. (2018).

There is a degree of independence between $^{206}Pb/^{204}Pb$, $^{207}Pb/^{204}Pb$ and $^{208}Pb/^{204}Pb$ ratios because each is derived from a difference decay chain. It is recommended that the three ^{204}Pb ratios ($^{206}Pb/^{204}Pb$, $^{207}Pb/^{204}Pb$ and $^{208}Pb/^{204}Pb$) are used in MixSIAR in order to capture as much isotope ratio variability as possible in the modeling process (Longman et al., 2018). To maximize the discriminatory performance of the MixSIAR model, Pb source datasets that are isotopically similar, not statistically significantly different, and categorically plausible should be grouped *a priori* or *a posteriori*. A database of potential Pb source isotope data was compiled from the academic literature before using MixSIAR. The nature of the Galveston Bay and literature Pb source isotope data were further assessed for statistically defined normal distributions. Specifically, Shapiro-Wilk and Kolmogorov-Smirnov tests were done to assess the normality of each Pb isotope ratio in the datasets, and then Mardia, Henze-Zirkler and Royston statistical tests were completed to assess multivariate normality of the ^{204}Pb three-isotope system in the datasets. Results from the statistical tests indicate that the Pb isotope ratios of the datasets do not display univariate or multivariate normality across the board. Thus, the MixSIAR model approach using means and standard deviations is well suited for the data in this study. The MCMC chains must reach convergence by the end of a model run to ensure meaningful results. Data convergence is assessed using two post-model run diagnostics, the Gelman-Rubin and Geweke tests (Longman et al., 2018; Cowles and Carlin, 1996). Gelman-Rubin test statistic values near 1 signal that the MCMC chains have reached convergence. The Geweke diagnostic tests for equality of the means of the first and last part of a Markov chain and generates z-scores for each MCMC chain. Low Geweke z-scores, typically between ±2, indicate convergence. Running longer MCMC chains increases the likelihood of achieving model convergence, all models in this study used “extreme” MCMC chains (the longest MCMC chain option in MixSIAR). The model run results presented here have reached convergence as indicated by the Gelman-Rubin and/or Geweke tests for each model. Model uncertainty is summarized at the 95% credible interval. The 95% credible interval exists where the probability that the mean model output is within the interval defined by the lower (2.5%) and upper (97.5%) bounds is 95%.

Figure 12 contains two dimensional scatter plots of Galveston Bay and literature Pb isotope ratios were used to characterize mixing geometry and identify potential Pb sources in Galveston Bay that should be included in MixSIAR, the means and standard deviation error bars of the literature Pb source endmembers are shown in these figures (Rabinowitz, 2005; Bollhoffer and Rosman, 2001; Brandon and Smith, 1994; Kesler et al., 1994; Brandon and Lambert, 1993; James and Henry, 1993; Sun, 1980; Chow and Earl, 1972). The Pb found in natural systems ultimately originates from crustal rocks. Continental weathering of bedrocks contributes natural Pb to the environment. The mining and refining of Pb-bearing ores, which are subsequently used for industrial Pb applications, supplies anthropogenic Pb to the environment. Atlantic marine sediments are an amalgamation of eroded crustal material that provide a sample of the average continental crust (White, 2015; Sun, 1980). Granitoids from the North American Cordillera, the White Creek batholith in the Southern Canadian Cordillera, and the southeastern portion of the North American Craton in Texas and Mexico also provide samples of crustal source material (Brandon and Smith, 1994; Brandon and Lambert, 1993; James and Henry, 1993). Collectively, these data serve as a proxy for the presence of naturally weathered detrital Pb in Galveston Bay. Rabinowitz (2005) analyzed soils from five historic U.S. Pb smelting and refining facilities documented to have processed Pb ores originating from Missouri, northeast Washington, Utah, Montana, Colorado, and Mexico. The Pb isotopic signal from Rabinowitz (2005) provides an estimate of anthropogenic Pb used in the U.S. throughout the 20th century. Lead from MVT ores accounted for 40 – 90% of U.S. Pb production between the 1960s and 1980s (Potra et al., 2018). These MVT ores have a wide range of Pb isotopic ratios and are characterized by atypically radiogenic Pb as compared to other Pb ore deposits worldwide (Marcantonio et al., 2002; Sangster et al., 2000). MVT ores were used in the manufacturing of gasoline consumed in the U.S. (Landmeyer et al., 2003). Previous work established that MVT ores from Central Appalachia are less radiogenic than other MVT ores and have Pb isotope ratios similar to U.S. atmospheric particulate Pb (Potra et al., 2018b). This finding supports the conclusion that the Pb used in gasoline additives during the mid to late 20th century is in part derived from MVT ores from Central Appalachia. Accordingly, the Pb in U.S. and Central American aerosols has been interpreted as a proxy for vehicle exhaust from burning of gasoline (Potra et al., 2018; Bollhofer and Rosman, 2001; Wu and Boyle, 1997). The MVT Pb ores and U.S. and Central American aerosols represent industrial and automobile Pb emissions in the Galveston Bay area. North American coal derived Pb in Galveston Bay can be directly linked to the use of coal power in Texas. According to the U.S. Energy Information Administration, Texas consumes more energy than any other state in the country, with coal power supplying an estimated 37% of that energy demand (Stillwell et al., 2011; "Texas State Energy Profile Overview." U.S. Energy Information Administration). The North American coal signal seen in this dataset captures the prevalence of coal and demonstrates that coal continues to be a source of Pb to natural environments despite recent shifts toward cleaner burning energy sources such as natural gas. The sources of Pb identified in Galveston Bay sediments and the corresponding MixSIAR model estimates for Pb source contributions to Galveston Bay sediment leachates, residues, and bulk digests are listed in Table 16.

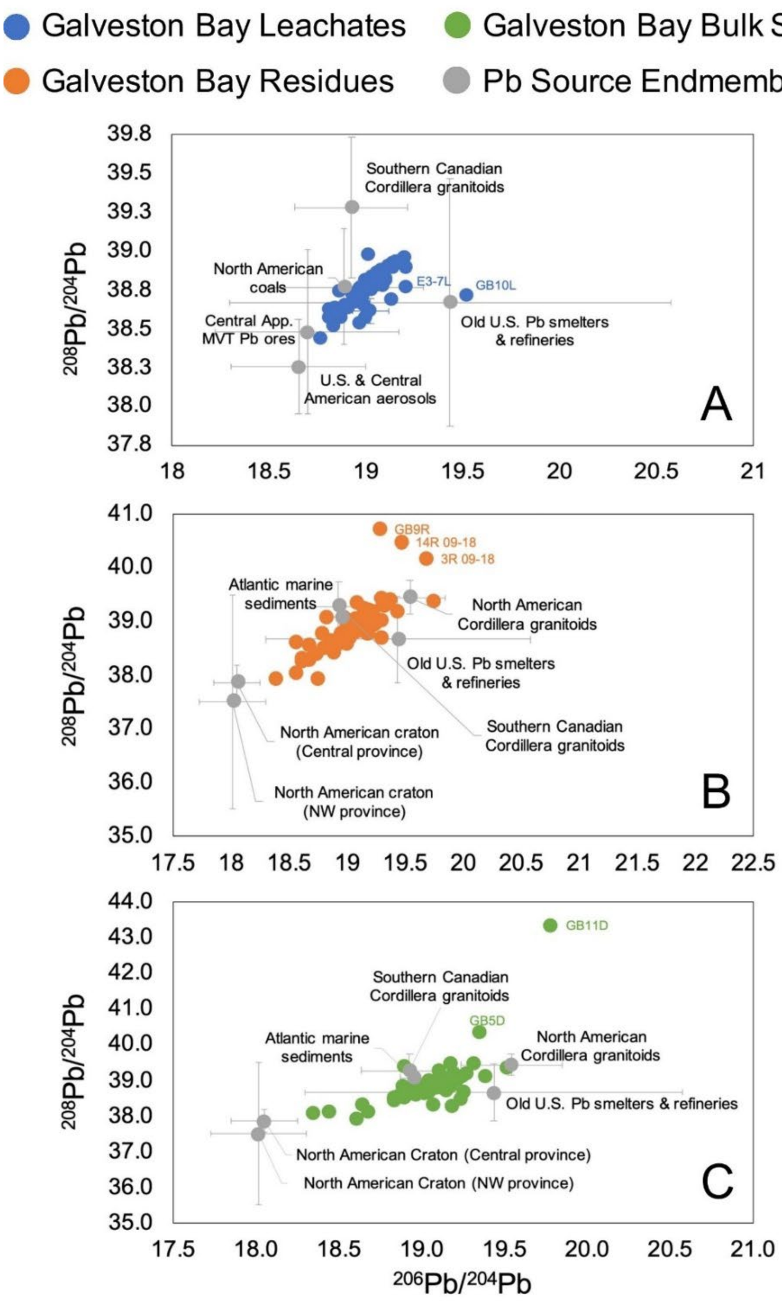

Figure 12. Mixing geometry for Galveston Bay (a) sediment leachates, (b) sediment residues and (c) bulk sediments alongside literature Pb sources used in MixSIAR models.

Table 16. MixSIAR model results summary.

Pb Source	Mean (%)	2.5%	97.5%	Source type
Galveston Bay sediment leachates (whole study area)				

Pb Source	**Mean (%)**	**2.5%**	**97.5%**	**Source type**
Old US Pb smelters & refineries	22.0	0.6	64.7	Anthropogenic
Central Appalachian MVT Pb ores	20.4	0.9	60.5	Anthropogenic
US & Central American aerosols	20.8	0.5	62.2	Anthropogenic
North American coals	20.6	0.8	60.8	Anthropogenic
Southern Canadian Cordillera granitoids	16.2	0.4	54.9	Natural
Galveston Bay sediment leachates (upper Galveston Bay)				
Old US Pb smelters & refineries	20.1	0.0	92.0	Anthropogenic
Central Appalachian MVT Pb ores	28.9	0.0	98.8	Anthropogenic
US & Central American aerosols	20.3	0.0	91.6	Anthropogenic
North American coals	28.4	0.0	97.8	Anthropogenic
Southern Canadian Cordillera granitoids	2.4	0.0	12.3	Natural
Galveston Bay sediment leachates (lower Galveston Bay)				
Old US Pb smelters & refineries	47.9	0.0	100.0	Anthropogenic
Central Appalachian MVT Pb ores	3.7	0.0	35.6	Anthropogenic
US & Central American aerosols	44.6	0.0	100.0	Anthropogenic
North American coals	3.7	0.0	35.9	Anthropogenic
Southern Canadian Cordillera granitoids	0.1	0.0	0.8	Natural
Galveston Bay sediment residues (whole study area)				
Old US Pb smelters & refineries	16.6	0.5	37.1	Anthropogenic
Southern Canadian Cordillera granitoids	16.8	0.4	37.0	Natural
North American Cordillera granitoids	7.7	0.3	19.6	Natural
North American Craton intermediate & felsic rocks	51.3	0.9	53.4	Natural
Atlantic marine sediments	7.6	0.3	19.5	Natural
Galveston Bay sediment residues (upper Galveston Bay)				
Old US Pb smelters & refineries	16.9	0.2	36.7	Anthropogenic

Pb Source	**Mean (%)**	**2.5%**	**97.5%**	**Source type**
Southern Canadian Cordillera granitoids	17.1	0.2	36.5	Natural
North American Cordillera granitoids	6.6	0.1	17.3	Natural
North American Craton intermediate & felsic rocks	52.8	0.3	54.8	Natural
Atlantic marine sediments	6.6	0.1	17.0	Natural
Galveston Bay sediment residues (lower Galveston Bay)				
Old US Pb smelters & refineries	15.6	0.2	33.3	Anthropogenic
Southern Canadian Cordillera granitoids	15.6	0.2	33.0	Natural
North American Cordillera granitoids	6.4	0.1	16.2	Natural
North American Craton intermediate & felsic rocks	56.1	0.4	58.1	Natural
Atlantic marine sediments	6.3	0.1	16.4	Natural
Galveston Bay sediment bulk digests (whole study area)				
Old US Pb smelters & refineries	25.5	5.7	47.9	Anthropogenic
Southern Canadian Cordillera granitoids	14.3	0.5	36.3	Natural
North American Cordillera granitoids	23.1	1.3	44.7	Natural
North American Craton intermediate & felsic rocks	17.7	0.4	21.2	Natural
Atlantic marine sediments	19.4	1.3	40.0	Natural

Data are presented as mean percent contribution with lower (2.5%) and upper (97.5%) bounds representing 95% credible intervals

Pb sources in Galveston Bay sediment leachates

The Pb sources and their estimated proportions in Galveston Bay sediment leachates are crustal rocks (southern Canadian Cordillera granitoids) 16.2%, Central Appalachian MVT ores 20.4%, ores processed at historic U.S. smelters and refineries 22.0%, U.S. and Central American aerosols 20.9%, and North American coals 20.6% (Fig. 12a, Table 16, Rabinowitz, 2005; Bollhoffer and Rosman, 2001; Kesler et al., 1994; Brandon and Lambert, 1993; Chow and Earl, 1972). The Gelman-Rubin test statistic values are near 1 supporting the conclusion that this model reached convergence. Typically, 5% of variables are expected to fall outside of the MixSIAR Geweke diagnostic z-score threshold ±1.96. In this model, between 10% and 18% of variables have z-scores outside of ±1.96. Based on the Gelman-Rubin diagnostic this model is considered converged, however the output is interpreted with caution (Gelman at al., 2013). Data points GB10L and E3-7L deviate the most from other Galveston Bay leachates and are considered separately for additional insight. The E3-7L point has a $^{207}Pb/^{204}Pb$ of 15.557 that forms the lower bound of $^{207}Pb/^{204}Pb$ values observed for the remaining study area sediments, which typically have $^{207}Pb/^{204}Pb \geq 15.617$. The point E3-7L ($^{207}Pb/^{206}Pb$ = 0.80982 ±0.00002 and $^{208}Pb/^{206}Pb$ = 2.01807 ±0.00008) falls on a mixing line between average continental crust (average $^{207}Pb/^{206}Pb$ and $^{208}Pb/^{206}Pb$ of 0.82351 and 2.06451 based on values in Zartman et al., 1981 and Asmerom and Jacobsen, 1993) and U.S. Pb ores from the Eastern Tennessee mining district (average $^{207}Pb/^{206}Pb$ and $^{208}Pb/^{206}Pb$ of 0.80621 and 2.00840 based on ratios published in Sangster et al., 2000) in $^{208}Pb/^{206}Pb$ versus $^{207}Pb/^{206}Pb$ space. The E3-7L point may reflect a discrete period in which gasoline made with Pb from the Eastern Tennessee mining district was used in the Houston-Galveston area, making it a discrete regional Pb source. The GB10L data point has a distinctly radiogenic Pb isotope composition ($^{206}Pb/^{204}Pb$ = 19.523, $^{207}Pb/^{204}Pb$ = 15.699, $^{208}Pb/^{204}Pb$ = 38.710, $^{208}Pb/^{206}Pb$ = 1.98280, and $^{207}Pb/^{206}Pb$ = 0.80412) that cannot be clearly attributed to previously identified Pb sources in the literature, signifying that the Pb in this sample may the result of contamination or a hitherto uncharacterized Pb source(s).

Pb sources in Galveston Bay sediment residues and bulk sediments

The same Pb sources contribute Pb to the Galveston Bay sediment residues and bulk sediments. The Pb sources and their mean estimated proportions in Galveston Bay sediment residues are crustal rocks from the southern Canadian Cordillera 16.8%, the North American Cordillera 7.7%, the North American Craton 51.3%, marine sediments from the Atlantic Ocean 7.6%, and ores historically smelted and refined in the U.S. 16.6% (Fig. 12b, Table 16, Rabinowitz, 2005; Brandon and Smith, 1994; Brandon and Lambert, 1993; James and Henry, 1993; Sun, 1980). The points GB9R, 3R 09-18 (Station 3 residue from September 2018), and 14R 09-18 (Station 14 residue from September 2018) have distinctly high $^{208}Pb/^{204}Pb$ values of 40.704, 39.326, and 40.459, respectively, that push these points outside of the range of other Galveston Bay sediments (Fig. 12). The high ^{208}Pb cannot be attributed to any literature Pb sources. Consequently, these three points are not included in the MixSIAR model and are assessed separately. The Station GB9 sediments are from El Jardin Beach and are strikingly different (e.g., light tan color, large quartz and feldspar grains) from Galveston Bay sediment samples (e.g., dark gray, fine-grained muds and clays). It may be that Station GB9 sediments are allochthonous and represent imported beach infill rather than naturally occurring sediment aggregates from the Galveston Bay watershed. It is also plausible that a Pb discharge stemming from human activity (e.g., outboard motor use) at El Jardin Beach could contribute to the unique ^{208}Pb isotope signal. Stations 3 and 14 are located in the HSC within 8 km of each other. Considering that the elevated Station 3 and 14 ratios occur in September 2018 only, it is likely that a discrete Pb discharge came from shipping vessel traffic in the bay. The Missouri MVT Pb ores source has notably high $^{208}Pb/^{204}Pb$ ratios ranging from 39.283 to 41.694 that are closer in range to the GB9R, 3R 09-18, and 14R 09-18 $^{208}Pb/^{204}Pb$ ratios (39.326 – 40.704; Sverjensky, 1981). It is possible that Missouri MVT Pb ores contribute at least in part to GB9R, 3R 09-18 and 14R 09-18 in addition to other unknown Pb inputs.

Bulk sediments Pb sources and their respective mean contributions to the bay are Atlantic Ocean marine sediments 19.4 %, ores historically smelted and refined in the U.S. 25.5%, and crustal rocks from the southern Canadian Cordillera 14.3%, the North American Cordillera 23.1%, and the North American Craton 17.7%, (Fig. 12c, Table 16, Rabinowitz, 2005; Brandon and Smith, 1994; Brandon and Lambert, 1993; James and Henry, 1993; Sun, 1980). All Galveston Bay sediment bulk digests have ^{208}Pb/^{204}Pb values $\leq$ 39.480 except GB5D and GB11D, which have ^{208}Pb/^{204}Pb ratios of 40.352 and 43.340 respectively. Stations GB5 and GB11 are located on the northern edge of East Bay southeast and are the only two stations to feature sediments containing tan sand intermixed with dark brown-gray mud. The exceptional Pb isotope values seen at GB11 indicate the presence of a heretofore unknown source of thorogenic Pb stemming from the northeastern rim of East Bay. No source with a similar Pb isotopic composition to GB11D has been identified in the literature, making it difficult to contextualize this data point. For this reason, GB11D is not included in the MixSIAR model. Further analyses on the sediments from GB11 are necessary to characterize and assess the Pb at this site.

Outliers in MixSIAR models

Station GB9 is located at El Jardin Beach, Texas and Station GB10 is at Sylvan Beach, Texas, both of which are pedestrian beach parks maintained and frequented by humans. Swimming is allowed at both El Jardin Beach and Sylvan Beach. The Sylvan Beach and El Jardin Beach sediments stand out from the other shoreline, endmember, and bay station sediment samples. Upon visual inspection they are rich in quartz and feldspar and contain fine-to-coarse beige and tan sand grains, which clearly differ from the dark brown-gray muds, silts and clays found throughout Galveston Bay. Station GB11 sediment is a mixture of tan sand and dark gray mud that was taken from a public access recreational and swimming area within the Anahuac National Wildlife Refuge. Based on the anthropogenic settings and clear visual difference between the GB9, GB10 and GB11 sediments and other bay sediments, it is plausible that the unique Pb isotope ratios observed at this station stem from unique sediment fluxes likely associated with heavy human activities.

Regional distributions of Pb sources in Galveston Bay

Spatiotemporal patterns in Galveston Bay sediment Pb concentrations cannot be explained by the Pb isotope ratios in the Galveston Bay sediment samples. As described above the Galveston Bay leachate Pb isotope ratios are slightly more radiogenic at Lower Galveston Bay stations (1-5, 10-11, 14) than at Upper Galveston Bay stations (7-9, 12-13), while the opposite is observed in the Galveston Bay residue Pb isotope compositions. This observation is not mirrored by sediment Pb concentrations, which instead reflect an east-west trend along the HSC. The upper versus lower Galveston Bay Pb isotope ratios trends in sediment leachates and residues were used to model the regional distribution of Pb in the bay (Table 16 italicized subsections). The Galveston Bay sediment leachate regional distribution MixSIAR model indicates that upper bay stations receive more Pb from the North American coals and Central Appalachia MVT Pb ores sources (28.4% and 28.9%) than U.S. and Central American aerosols, soils from U.S. Pb smelters and refineries, and crustal rocks (20.3%, 20.1%, and 2.4%). Conversely, the lower bay station leachates Pb is dominated by U.S. and Central American aerosols and historic U.S. Pb smelters and refineries sources (44.6% and 47.9%). The Galveston Bay sediment residue MixSIAR model output indicates that stations in upper and lower bay stations generally receive Pb from the same sources despite slightly variant Pb isotope compositions in the residue fractions. Or in other words, the Pb source isotope signals in the residue fraction are not heterogenous enough for the model to distinguish upper bay Pb sources from lower bay Pb sources. In all sediment fractions the E3 core samples lie within the range of the Galveston Bay surface sediments and fall within the same mixing envelopes as surface sediments indicating that the sources of core sediment Pb are not different than surface sediment Pb. *A posteriori* groupings of the Pb sources into anthropogenic versus natural reveals that the Galveston Bay sediment leachates are dominated by anthropogenic Pb while the sediment residues and bulk sediments are dominated by natural Pb inputs. Anthropogenic Pb sources supply approximately 83.8%, 16.6% and 25.5% of Pb to the leachates, residues, and bulk sediments respectively. Natural sources account for 16.2% of the total Pb in the leachates, 83.4% of the total Pb in the residues, and 74.5% of the total Pb in the bulk sediments.

Sediment leaching artifacts

The presence of anthropogenic Pb in the residual sediment fraction leaves open the possibility that the sequential leaching method used in this study did not fully leach surface adsorbed Pb from the sediment sample grain surfaces, thus the residual fraction as operationally defined here, does not represent the true natural Pb isotopic signal. The 0.02M HH- CH_3COOH leach used here is one of many proposed leaching agents for marine sediments (Graney et al., 1995; Sholkovitz, 1989; Horowitz, 1985). Previous work has shown that the 0.02M HH-CH_3COOH may not thoroughly access surface adsorbed heavy metals (Graney et al., 1995; Sholkovitz, 1989; Chester and Hughes, 1967). For example, Graney et al. (1995) demonstrated that different Pb concentrations and isotope ratios were measured in the same sediments when leached with CH_3COOH versus HCl, HNO_3-HCl and HNO_3 leaching solutions. It is also plausible that leaching artifacts are being observed. This idea has been explored in several previous studies, which have found that re-adsorption of leached metals back onto sediment grains often occurs during sequential leaching procedures, including when using the 0.02M HH-CH_3COOH leach method (Piper and Wandless, 1992; Nirel and Morel, 1990; Sholkovitz, 1989).

Galveston Bay Waters

Discussion of spatiotemporal variation in water heavy metal concentrations

Salinity is the primary spatiotemporal control on water (dissolved fraction) heavy metal concentrations. Dissolved heavy metal loads are higher in low salinity regions. Conversely, dissolved heavy metal loads are lower in high salinity regions. Cadmium displays the inverse trend as it readily forms chloride complexes, which can result in higher dissolved Cd concentrations with increasing salinity (Wen et al., 1999). A one-way analysis of variance (ANOVA) was done using IBM SPSS 26.0 to evaluate the statistical significance of dissolved heavy metal concentration variation between areas of high salinity (bay stations near the Gulf of Mexico), intermediate salinity (main bay stations) and low salinity (endmember stations). When homogeneity of variance can be assumed based on Levene's test, regular ANOVA and Tukey post hoc tests were performed as appropriate (Gaur and Gaur, 2006). In cases where the data violate the assumption of homogeneity of variances based on Levene's test, Welch's ANOVA and Games-Howell post hoc tests were performed as appropriate (Gaur and Gaur, 2006). Significant differences ($p \leq 0.05$) between the mean metal concentrations between the high salinity, intermediate salinity and low salinity areas were identified by the ANOVA with the following exceptions: the Cd and Pb concentrations are not statistically different between low salinity endmember stations and intermediate salinity main bay stations and Zn concentrations are not statistically different between intermediate salinity main bay stations and high salinity bay stations near the Gulf of Mexico (Fig. 13).

Trinity River discharge <250 m^3/s constitutes dry conditions and Trinity River discharge >250 m^3/s indicates wet conditions. Independent t-tests were done in IBM SPSS 26.0 to compare the means between the wet/dry dissolved metal concentrations and determine if the difference between the means of each group is statistically significant (Ross and Willson, 2017; Gaur and Gaur, 2006). The endmember stations were sampled once during wet conditions, thus no temporal comparison between wet/dry conditions can be made. At the main bay stations there is a significant difference ($p \leq 0.05$) in mean Cd, Fe, and Ni concentrations between wet and dry conditions whereas there is no significant difference in the mean Cu, Mn, Pb, and Zn concentrations between wet and dry conditions. At the bay stations near the Gulf of Mexico only dissolved Cu concentrations are statistically significant different between wet and dry sampling events, all other metal concentrations are not significantly statistically different (Fig. 13).

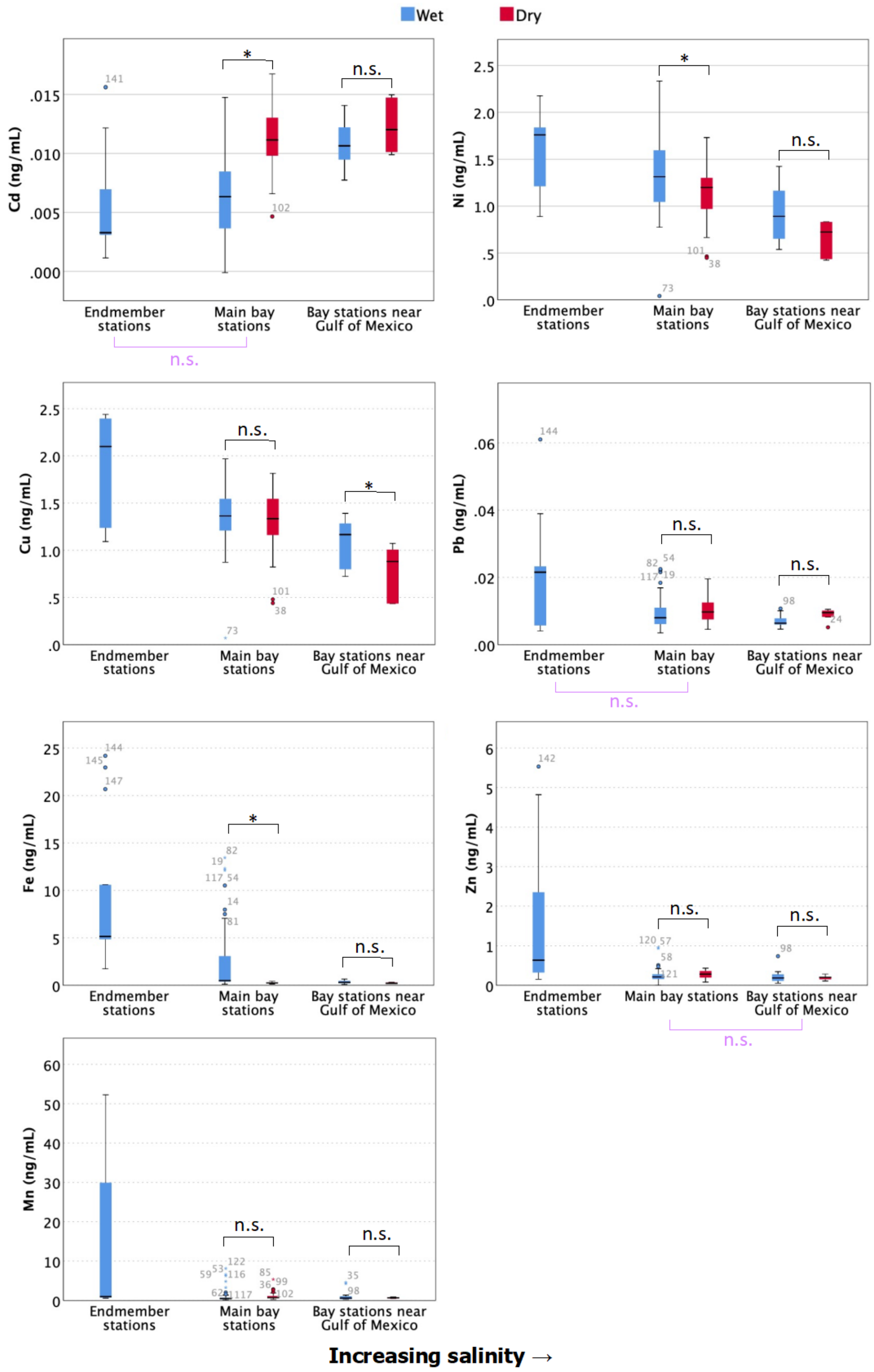
🟦 Wet
🟥 Dry
Cd (ng/mL)
.015
.010
.005
.000
141
102
*
n.s.
Ni (ng/mL)
2.5
2.0
1.5
1.0
.5
.0
101
38
73
Cu (ng/mL)
Pb (ng/mL)
.06
.04
.02
.00
144
82 54
117 19
98
24
Fe (ng/mL)
25
20
15
10
5
0
145 144
147
82
19
117 54
14
81
Zn (ng/mL)
6
5
4
3
2
1
0
142
120 57
58
121
98
Mn (ng/mL)
60
50
40
30
20
10
0
59 53 122 116
62 117
85 99
36 102
35
98
Endmember stations
Main bay stations
Bay stations near Gulf of Mexico
Increasing salinity →

Regular outliers (red or blue colored circles) are samples with concentrations greater than 1.5 times the interquartile range. Extreme outliers (red or blue colored asterisks) are samples with concentrations greater than 3 times the interquartile range. Statistical differences between means of each wet/dry group are indicated by black brackets. Statistical differences between metal concentration means of high salinity, intermediate salinity and low salinity areas are indicated by purple brackets. Bracket with asterisk = the means of each group are significantly different. Bracket with n.s. = the means of each group are not significantly different

Figure 13. Box and whisker plots showing spatiotemporal trends in Galveston Bay water heavy metal concentrations. Wet condition samples are shown in blue, dry condition samples are shown in red.

Heavy metal toxicity in Galveston Bay waters

The Galveston Bay dissolved fraction water samples analyzed in this study have heavy metal concentration ranges as follows, Cd 0 – 0.02 ng/mL, Cu 0.07 – 2.4 ng/mL, Fe 0.09 – 24 ng/mL, Mn 0.09 – 52 ng/mL, Ni 0.04 – 2.3 ng/mL, Pb 0 – 0.06 ng/mL, and Zn 0 – 5.5 ng/mL. The Galveston Bay samples were screened for toxicity using the NOAA SQuiRTs T_{20} and T_{50} toxicity thresholds as well as the saltwater chronic benchmark and "fish only" human health criteria values outlined in the TCEQ Risk Reduction Program and TCEQ Texas Surface Water Quality Standards (Buchman, 2008). A summary of the state and federal screening values used is given in Table 17. None of the Galveston Bay water samples in this study exceeded toxicity thresholds.

Table 17. Water heavy metal toxicity screening values from NOAA SQuiRTs, TCEQ Risk Reduction Program and TCEQ Surface Water Quality Standards.

	Cd	Cu	Fe	Pb	Ni	Mn	Zn
TCEQ							
Saltwater Chronic Benchmark (ng/mL)	8.75	3.6	-	5.3	13.1	-	84.2
Human Health Criteria "Fish Only" (ng/mL)	-	-	-	3.83	1140	-	-
NOAA							
Freshwater Acute (ng/mL)	2.0	13	-	65	470	2300	120
Freshwater Chronic (ng/mL)	0.3	9.0	1000	2.5	52	80	120
Saltwater Acute (ng/mL)	40	4.8	300	210	74	-	90
Saltwater Chronic (ng/mL)	8.8	3.1	50	8.1	8.2	100	81

Galveston Bay Oyster Tissues

Discussion of spatiotemporal variation in oyster tissue heavy metal concentrations

A one-way ANOVA was done using IBM SPSS 26.0 to evaluate the statistical significance of heavy metal concentration variation between the five areas (Arantes et al., 2016; Alfonso et al., 2013; Vazquez-Sauceda et al., 2011). The data violate the assumption of homogeneity of variances based on Levene's test, therefore Welch's ANOVA and Games-Howell post hoc tests were performed as appropriate (Gaur and Gaur, 2006). No significant differences between the mean Cd, Pb and Zn concentrations between the five sampling areas were identified by Welch's ANOVA ($p \geq 0.48$), subsequently no post hoc testing was done. Note that Hg is not included in the ANOVA as only one Upper Galveston Bay/Trinity Bay data point exists (Hg concentrations below detection in Upper Galveston Bay/Trinity Bay in December 2019-January 2020 sampling event).

This spatial distribution of oyster tissue metal contents follows previously reported metal patterns in Galveston Bay oysters in which the highest metal concentrations are located near industrial areas (Jiann and Presley, 1997). The Upper Galveston Bay/San Jacinto River (Area 2) oyster tissue samples are located near the convergence of the San Jacinto River and Galveston Bay and are in close proximity to the heavily industrialized HSC. The West Bay oyster samples were gathered near where Highland Bayou enters West Bay just south of Texas City, Texas. Texas City hosts a large-scale industrial complex including petrochemical manufacturing and petroleum refining facilities. This suggests that heavy metal discharges into the vicinity of the Upper Galveston Bay and West Bay sampling sites likely explain the elevated metal levels seen in the oyster tissues at these locations. However, note that the highest heavy metal concentrations in Galveston Bay bulk sediments are in eastern bay areas. While oyster tissue metal concentrations are elevated in East Bay, particularly for Cd, to mimic the sediment spatial trend, oyster tissue metal concentrations are very low in Upper Galveston/Trinity Bay, despite that sediment metal concentrations were some of the highest at those sites. Importantly, oysters are known to take up both particulate and dissolved metals, which may play a role in any correlations (or lack thereof) between sediment and oyster metal distributions (Griscom and Fisher, 2004).

Independent t-tests were done in IBM SPSS 26.0 to compare the means between the wet/dry metal concentrations and determine if the difference between the means of each group is statistically significant (Ross and Willson, 2017; Gaur and Gaur, 2006). There is a significant difference in mean Cd and Pb Galveston Bay oyster tissue concentrations between wet and dry condition sampling events ($p \leq 0.04$). In all five sampling areas, the primary control on oyster tissue heavy metal concentrations is their categorization as wet or dry based on riverine discharge. This trend diverges from the Galveston Bay sediments for which spatial location east or west of the HSC is the primary controlling factor.

While the seasonal oyster sampling periods as wet and dry is described to be consistent with the temporal pattern controlling sediment metal distributions, the oysters' living tissue responds to other factors over seasonal timescales including temperature, oyster life cycle, etc. In prior studies of Galveston Bay, Chesapeake Bay, and estuarine systems in Cornwall, England and the Fujian province of China, higher oyster tissue metal concentrations have been observed in warmer summer months (analogous to the September 2020 "wet" samples) versus cooler months winter (analogous to the December 2019 and January 2020 "dry" samples) (Weng and Wang, 2015; Jiann and Presley, 1997; Riedel et al. 1995; Sanders et al. 1991; Wright et al. 1985; Boyden and Phillips 1981). However, the opposite temperature trend has been observed in other bivalves around the globe (Otchere, 2019 and references therein). Thus, temperature is not likely the major controlling factor in oyster tissue temporal metal variations.

Instead, at least in Galveston Bay, oyster tissue metal concentrations vary with riverine discharge. Oyster tissue metal concentrations are higher during high river flow (wet) conditions and lower during low river flow (dry) conditions. Higher dissolved metal loads as well as increased flocculation of dissolved metals to sediments occur as riverine discharge increases. Accordingly, since both dissolved and particulate metals can be taken up by oysters, it follows that increased amounts of dissolved and sediment-bound metals would correlate with an increase in oyster tissue metal levels. The same metal abundance correlation with riverine discharge is seen in the Galveston Bay sediments and indicates that riverine input to Galveston Bay is a controlling factor in heavy metal distributions over time.

Other studies have proposed biotic (e.g., phytoplankton production, organism weight, reproductive stage, depuration) and abiotic (e.g., temperature, salinity) influences on bivalve metal concentration variability; however, there is no consensus on which factors are most influential (Otchere, 2019; Alfonso et al., 2013; Bendell and Feng, 2009; Joiris et al., 1998). In Galveston Bay, oyster tissue Pb, Cd, and Zn concentrations have been observed to reduce by half of their initial values within as short as three to nine months, indicating that metals may naturally be removed from oyster tissues if given enough time (Jiann and Presley, 1997). Eight to nine months exist between the sampling points in this study, indicating that sufficient time has passed to show concentration oscillations in response to environmental metal loadings, which might not be expected for biological tissues on shorter timescales. However, any deeper interpretation of the spatial and temporal metal concentration trends that could be controlling this dataset is precluded by only having two samples. Corroboration of the patterns discussed here against future sampling events is recommended to more accurately characterize the spatiotemporal variability in Galveston Bay oyster tissue metal concentrations, especially regarding biotic controlling factors.

Heavy metal toxicity in Galveston Bay oyster tissues

Galveston Bay oysters are a common source of food in Texas and throughout the Gulf of Mexico region (Ropicki et al., 2018a-b; "Oyster reefs in Galveston Bay," Galveston

Bay Estuary Program); thus, one of the primary study goals was to determine how many Galveston Bay oysters would need to be consumed by humans to reach metal toxicity thresholds. The oysters analyzed in this study have a mean ± SD Cd concentration of 2.63 ± 1.22 µg/g, Pb concentration of 0.48 ± 0.25 µg/g, Zn concentration of 2,340 ± 1,380 µg/g, and Hg concentration of 0.06 ± 0.02 µg/g. The U.S. Environmental Protection Agency (EPA) daily oral reference doses (maximum dose of a toxic metal that is considered acceptable per kg of body weight) for Cd, Pb, and Zn are 1 µg/kg, 3.5 µg/kg and 300 µg/kg, respectively (Kusin et al., 2018). Mercury is more difficult to assign because it exists across several chemical forms that each have different toxicity. Methyl Hg is extremely bioaccumulative and widely considered the most toxic form of Hg due to its high affinity for protein thiol groups (Murphy et al., 2008; U.S. EPA, 1997); per the EPA recommendation, the total Hg within the Galveston Bay oyster samples are conservatively assumed to be present as methyl Hg when estimating toxicity (Sajwan et al., 2008). The methyl Hg EPA daily oral reference dose is 0.1 µg/kg (US EPA, 2010). Thus, given an average adult male body weight of 70 kg and an average adult female body weight of 60 kg, toxicity thresholds for daily metal consumption can be calculated as 60 to 70 µg of Cd, 210 to 245 µg of Pb, 18,000 to 21,000 µg of Zn, and 6 to 7 µg of Hg (Alfonso et al., 2013; Sajwan et al., 2008). Then, it can be calculated that dry Galveston Bay oyster tissue mass of 23 – 27 g (Cd), 438 – 510 g (Pb), 8 – 9 g (Zn), and 100 – 117 g (Hg) must be consumed in a day to reach the respective EPA metal daily consumption limits. Oyster tissue weights (dry weights) in this study ranged from 0.1 – 5.4 g with a mean dry tissue weight of 3.4 g. Thus, the average human would reach the EPA Zn threshold by consuming two to three average size oysters from Galveston Bay in one day. The Cd EPA limit could be reached by a human consuming seven to eight average size oysters from Galveston Bay daily, and approximately 30 and 129 average Galveston Bay oysters would need to be consumed in one day to reach the EPA daily intake limits for Hg and Pb, respectively. These results thus indicate that Galveston Bay oyster toxicity is Zn > Cd > Hg > Pb using EPA limits.

The Texas Department of State Health Services (DSHS) uses a different method to assess oyster toxicity: they have set daily health assessment comparison values based on the EPA oral reference doses and U.S. Department of Health and Human Services Agency for Toxic Substances and Disease Registry (ATSDR) minimal risk levels. These values can be used to screen Galveston Bay fish and shellfish directly for metal toxicity (DSHS, 2019). The DSHS screening values are 0.233 µg/g for Cd, 0.6 µg/g for Pb, 700 µg/g for Zn and 0.7 µg/g for Hg (DSHS, 2019; DSHS, 2007). Consumption of samples with metal concentrations exceeding the DSHS health assessment comparison values are anticipated to result in negative health impacts (DSHS, 2019). All of the Galveston Bay oysters exceed the DSHS Cd limit, 80% of the Galveston Bay oyster samples exceed the DSHS Zn limit, and 50% of the Galveston Bay oyster samples exceed the DSHS Pb limit. For Zn, all samples except the Upper Bay/Trinity Bay and Lower Galveston Bay samples collected in dry conditions exceed the DSHS limit. All wet season oysters, except those from East Bay, exceed the Pb DSHS limit, and the dry season West Bay oysters surpass the DSHS Pb threshold. None of the samples are above the DSHS Hg limits. Thus, these results indicate that Galveston Bay oyster toxicity is Cd > Zn > Pb > Hg using TX DSHS thresholds.

Both the EPA and DSHS metrics indicate that Cd and Zn have the highest potential for toxicity in Galveston Bay oysters as a human food source. The Galveston Bay oysters are not likely toxic for Pb by EPA standards; however, there is potential Pb toxicity in wet season Galveston oysters by DSHS standards. Provided that most humans consume oysters sporadically and in limited quantities, it is unlikely that Galveston Bay oyster consumption would result in significant toxic effects from Pb or Hg. Cadmium toxicity in humans is linked to neurotoxicity, renal disfunction, cancer (predominantly lung and renal), infertility, skeletal demineralization, and increased likelihood of cardiovascular mortality (Rahimzadeh et al., 2017). Though Zn is a biologically essential element, it can become toxic at high concentrations (Plum et al., 2010). Humans with Zn toxicity may experience copper deficiencies, impaired immune response and brain damage (Plum et al., 2010). Based on this study, metal toxicity associated with the consumption of Galveston Bay oysters warrants deeper investigation by regulatory authorities, particularly with respect to the potential negative human health impacts of ingesting elevated amounts of Cd and Zn, as these metals are known to bioaccumulate and biomagnify (Tchounwou et al., 2012; Wright and Welbourn, 2002).

Discussion of spatiotemporal variation in oyster tissue Pb isotope ratios

To evaluate the statistical significance of Pb isotope ratio variation between the five areas, one-way ANOVA was done in IBM SPSS 26.0 (Arantes et al., 2016; Alfonso et al., 2013; Vazquez-Sauceda et al., 2011). The data violate the assumption of homogeneity of variances based on Levene's test, therefore Welch's ANOVA and Games-Howell post hoc tests were performed as appropriate (Gaur and Gaur, 2006). There was a statistically significant difference in the mean ^{206}Pb/^{204}Pb ratio versus the mean ^{207}Pb/^{204}Pb and ^{208}Pb/^{204}Pb ratios in the five study areas as determined by Welch's ANOVA ($p \leq 0.03$). However, the Games-Howell post hoc test showed that there was no significant difference between the mean ^{206}Pb/^{204}Pb ratios of the five individual bay areas ($p \geq 0.11$). Given that West Bay is noticeably less radiogenic than the other bay areas, the samples were clustered into two groups, West Bay versus other bay areas, and assessed for statistically significant differences. Independent t-tests (IBM SPSS 26.0) results indicate that the differences in Pb isotope ratio means between oysters from West Bay and the remaining bay areas are statistically significant for ^{206}Pb/^{204}Pb only ($p = 0.001$, Fig. 10). This finding aligns with the one-way ANOVA results, which highlight a significant difference in the mean ^{206}Pb/^{204}Pb ratios between bay areas.

There is a significant difference in mean ^{208}Pb/^{204}Pb ratios between oyster tissues samples in wet conditions and dry conditions based on an independent t-test done using IBM SPSS 26.0 ($p \leq 0.03$; Fig. 10). The shift toward more radiogenic Pb isotope ratios during the dry sampling event may reflect higher contributions of anthropogenic Pb to Galveston Bay oysters during December 2019 and January 2020. Across all sampling areas, the primary control on oyster tissue Pb isotope compositions is their categorization as wet or dry based on riverine discharge. This trend diverges from the Galveston Bay sediments for which there is no clear temporal control on sediment leachate, residue, or bulk digest Pb isotope compositions.

Comparison of oyster tissue heavy metal concentrations with sediment and water heavy metal concentrations

Previous studies have compared sediment and water heavy metal levels to oyster tissue heavy metals levels in order to assess metal contaminant uptake from sediments or waters by oysters (Vazquez-Sauceda et al., 2011; Sajwan et al., 2008; Boening, 1999). Leachates represent metals adsorbed to sediment grain surfaces, which may be bioavailable to organisms depending on metal speciation within the system (Berger et al., 2008). Here, Galveston Bay oyster tissue metal concentrations are compared to metal concentrations in both sediment leachates and bulk sediment digestions. The oyster samples were acquired from different locations and timepoints than the sediment samples, making direct correlations between these datasets challenging; however, nearby stations are used as a first effort at this analysis (Fig. 14). Stations 7-9, 12, GB2, GB3 and GB4 are closest to the Upper Bay/Trinity Bay (Area 1) oyster samples; stations 13, GB8, GB9 and GB10 are closest to the Upper Bay/San Jacinto River (Area 2) oyster samples; stations 2-4, 10-11, 14 and GB7 are closest to the Lower Galveston Bay (Area 3) oyster samples; stations 5A, 5B, GB5, GB6, GB11, GB 12 and 401 are closest to the East Bay (Area 4) oyster samples; and stations 1 and 15 are closest to the West Bay (Area 5) samples (Fig. 14). Galveston Bay dissolved water heavy metal concentrations and oyster tissue heavy metal concentrations were compared as follows, stations 7-9, 12 were compared to Area 1; station 13 was compared to Area 2; stations 2-4, 10-11, and 14 were compared to Area 3; stations 5A, 5B, and 401 were compared to Area 4; and stations 1 and 15 were compared to Area 5. Galveston Bay sediment heavy metal concentrations and oyster tissue heavy metal concentrations were compared as follows, stations 7-9, 12, GB2, GB3 and GB4 were compared to Area 1; 13, GB8, GB9 and GB10 were compared to Area 2; stations 2-4, 10-11, 14 and GB7 were compared to Area 3; stations 5A, 5B, GB5, GB6, GB11, GB 12 and 401 were compared to Area 4; and stations 1 and 15 were compared to Area 5.

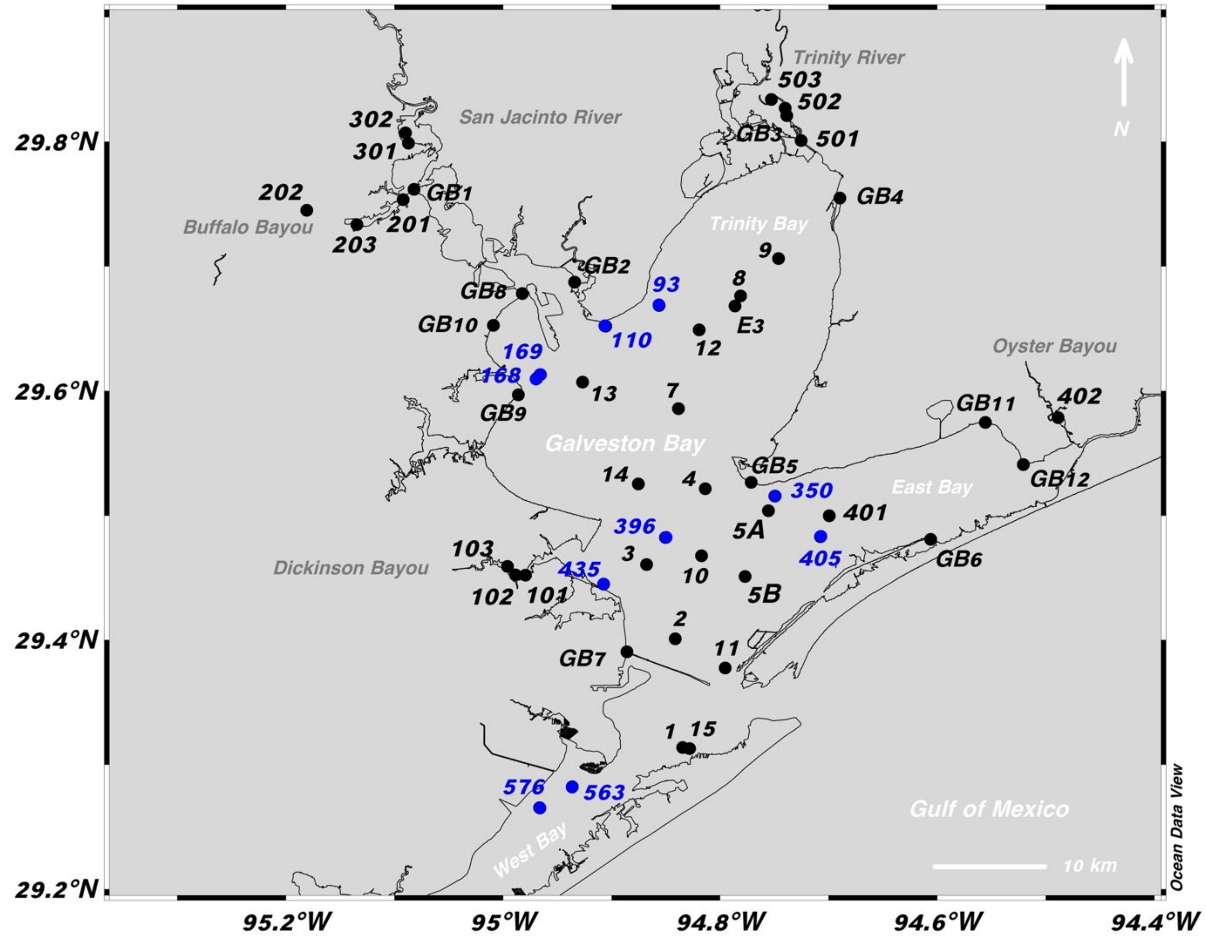

Sediment and water samples collected at stations shown in black. Oyster samples collected at stations shown in blue.

Figure 14. Galveston Bay sample location map.

When the mean ± SD sediment and oyster tissue metal concentrations are compared, the strongest relationship is the negative linear correlation between oyster tissue Zn and bulk sediment Zn contents, with an R^2 of 0.92 (Fig. 15, dashed black line). This negative relationship is surprising, since at face value it would suggest that low environmental sediment Zn concentrations cause elevated oyster tissue Zn concentrations. Previous work, including studies from Galveston Bay, have shown that Zn easily bioaccumulates in oyster tissue relative to sediments such that oyster tissue Zn contents are often considerably higher than the ambient sediment Zn concentrations (Sajwan et al., 2008; Shulkin et al., 2003; Jiann and Presley, 1997; Park and Presley, 1997). Shulkin et al. (2003) observed that the Zn content in oyster tissues increases more slowly at higher ambient sediment Zn levels. This phenomenon has been attributed to the physiological control of Zn accumulation by oysters, which is plausible given that Zn is a biologically essential element that is metabolically controlled (Sajwan et al., 2008; de Freitas Rebelo et al., 2003; Shulkin et al., 2003; Amiard-Triquet et al., 1986; Phillips and Yim, 1981).

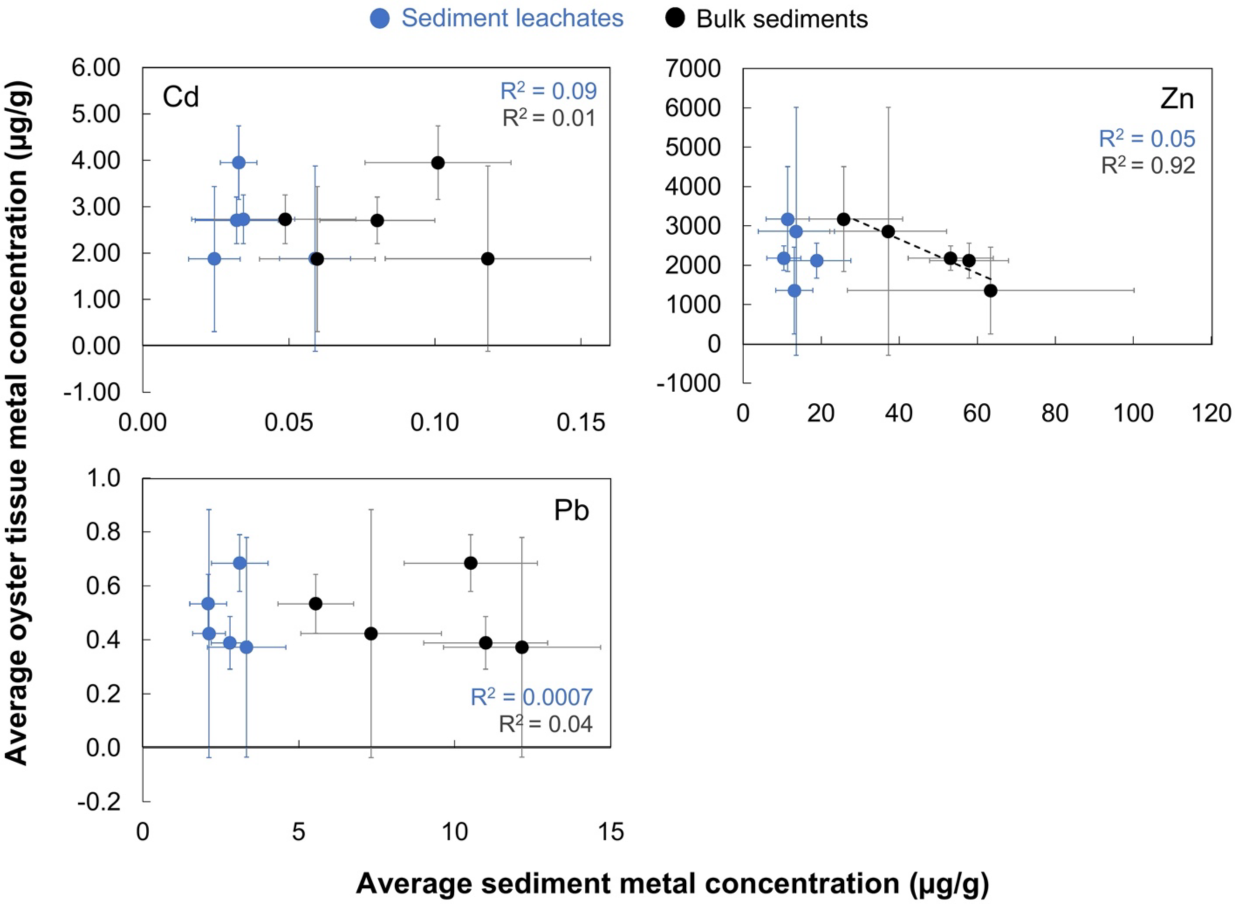

X-axis error bars are the sediment metal concentration data errors. Y-axis error bars shown are the standard deviation of the oyster tissue metal concentrations. The sediment Cd concentration data error is ±14%, the sediment Pb concentration data error is ±2%, and the sediment Zn concentration data error is ±4%. Linear correlation coefficients (R^2) listed on each panel. Blue symbols designate sediment leachates. Black symbols represent bulk sediments. Dashed lines shown where linear correlations exist.

Figure 15. Average Galveston Bay sediment Cd, Zn, and Pb concentrations versus average Galveston Bay oyster tissue Zn concentrations in Areas 1-5.

No other linear relationships between sediment and oyster metal concentrations are observed. When the mean ± SD water (dissolved fraction) and oyster tissue metal concentrations are compared, no linear correlations are observed ($R^2 < 0.66$, Fig. 16). The lack of linear relationships between sediment/water metal contents and oyster metal contents is not uncommon in the literature and may result from differing sediment and oyster sample locations and timepoints, the large errors associated with the spatiotemporal averages compared (Figs. 15-16) and/or other biotic and abiotic factors that regulate metal exchange between oysters and sediments (Vazquez-Sauceda et al., 2011; Sajwan et al., 2008; Griscom and Fisher, 2004; de Freitas Rebelo et al., 2003). For example, previous work has shown that oyster tissue metal bioavailability can be impacted by oyster physiology (i.e., size, age), salinity and freshwater inflows, seasonal effects and dredging activity (Birch and Hogg, 2011 and references therein).

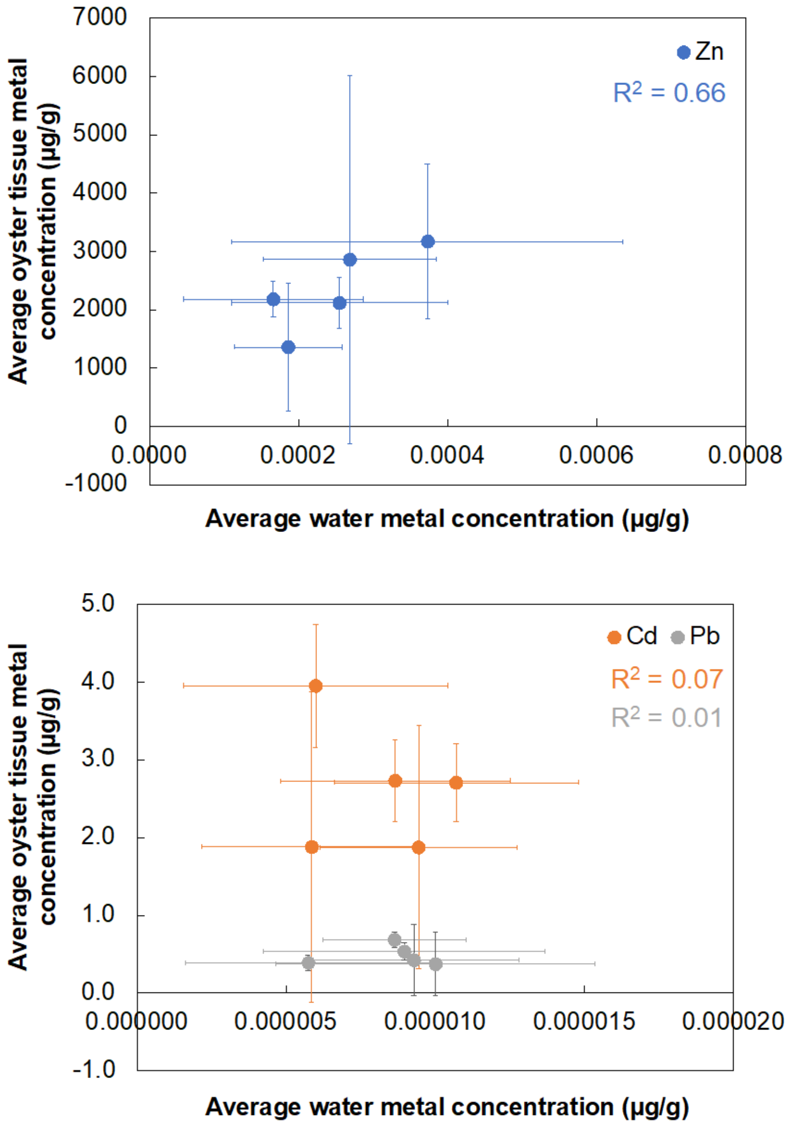

X-axis error bars are the standard deviation of the water metal concentrations. Y-axis error bars shown are the standard deviation of the oyster tissue metal concentrations.

Figure 16. Average Galveston Baywater (dissolved) Cd, Zn, and Pb concentrations versus average Galveston Bay oyster tissue Zn concentrations in Areas 1-5.

Future work assessing the relative importance of dissolved versus sedimentary metals as pathways of Galveston Bay oyster uptake should minimally include oyster tissues, filtered water and sediment samples collected from the same location and time over multiple sampling events, which would allow direct spatial and temporal comparison of metal contents between the oysters, waters, and sediments (Birch and Hogg, 2011; Apeti et al., 2005a-b; Shulkin et al., 2003). Additionally, specific biological parameters such as oyster sex, age and reproductive stage should be included to address biotic factors (Birch and Hogg, 2011; Griscom and Fisher, 2004; de Freitas Rebelo et al., 2003). Other physiochemical parameters, notably salinity and temperature, should also be included at the time of sampling to address abiotic factors (Birch and Hogg, 2011; Griscom and Fisher, 2004; de Freitas Rebelo et al., 2003). Collectively, these data parameters would yield a more robust understanding of Galveston Bay oyster tissue metal exchange with ambient waters and sediments.

Heavy metal sources in Galveston Bay oysters (Pb isotope modeling)

Lead in the environment is a mixture between Pb of natural and anthropogenic origins (Komarek et al., 2008; Hansmann and Koppel, 2000). Lead isotope ratios of environmental samples can be used to differentiate these sources between known “isotopic endmembers;” e.g. linear arrays defined by three isotopes are interpreted as mixing between two endmembers at either end of the linear trend (Marcantonio et al., 2000). In cases where more than two or three endmembers exist, linear mixing arrays may be insufficient for parsing Pb source contributions to an area. The oyster tissue Pb isotope data in this study do not display linear relationships, indicating that more than three sources of Pb exist within these samples.

Previous work has demonstrated that Pb isotopic fractionation is largely undetectable in biological, chemical, and physical processes (Zhu et al., 2000; O’Nions et al., 1998; Flegal and Smith, 1995; Doe, 1970). For this reason, trophic discrimination factors, which are used to correct for isotopic fractionation associated with dietary processes, are not included in the models presented here. This study uses MixSIAR models to assess Pb sources in the Galveston Bay oyster tissues. The model outputs are posterior distributions, which are probability distributions for each Pb source in the designated study area.

Fig. 17 shows the mixing geometry and Pb sources in Galveston Bay that are included in MixSIAR (Rabinowitz, 2005; Millot et al., 2004; Brandon and Lambert, 1993; Sun, 1980; Chow and Earl, 1972). The sources of Pb identified in Galveston Bay oyster tissues and the corresponding MixSIAR model estimates for Pb source contributions to Galveston Bay oysters are listed in Table 18. Lead source contributions were estimated for each of the 10 individual Galveston Bay oyster tissue samples (independent model fits for each sample data point, Stock and Semmens, 2016). The model outputs (mean Pb source contribution estimates, standard deviation of the mean Pb source contribution estimates and credible intervals) for each individual sample were then grouped and averaged to assess the overall Pb source contributions to all samples. This model approach is better suited to this small dataset with no clear covariate structure (i.e., only two sample points are available in each area, samples do not clearly vary by area) (Stock and Semmens, 2016). Though there is a significant difference in mean ^{208}Pb/^{204}Pb ratios between oyster tissues samples in wet conditions and dry conditions based on an independent t-test ($p \leq 0.03$; Fig. 10), the MixSIAR model could not constrain seasonal (wet/dry) difference in Pb source inputs to the oysters. This is due to 1) similar Pb isotope ratios in both wet and dry samples (i.e., the Pb isotopic ratios in the wet samples are not distinct enough from the Pb isotopic ratios in the dry samples for MixSIAR) and 2) the limited sample size within the dataset (i.e., there is one wet season sampling event and one dry season sampling event, multiple wet and dry season sampling events are needed for MixSIAR to adequately constrain wet/dry season differences).

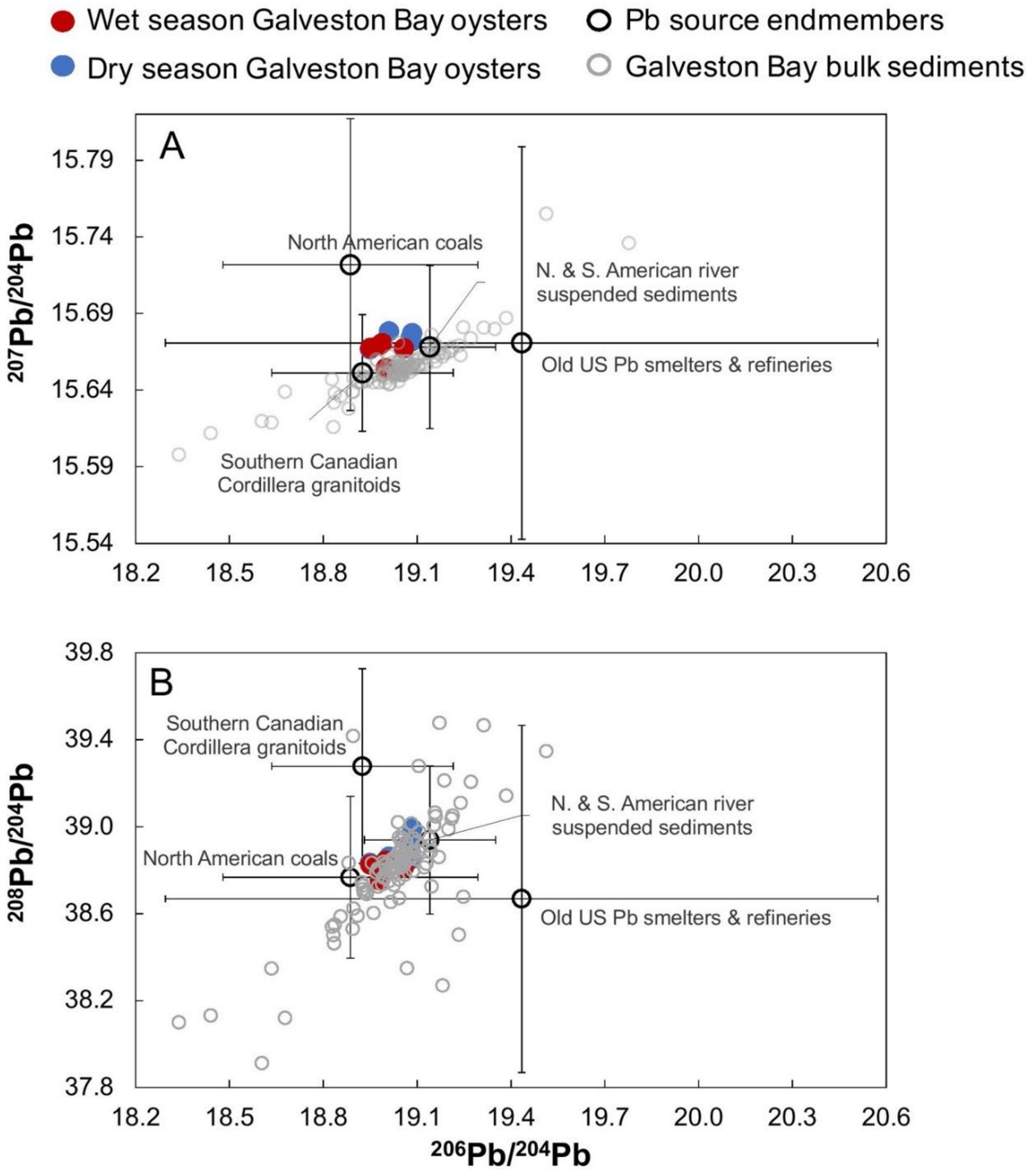

Panel A is a ^{207}Pb/^{204}Pb vs. ^{206}Pb/^{204}Pb scatter plot and Panel B is a ^{208}Pb/^{204}Pb vs. ^{206}Pb/^{204}Pb scatter plot. Both plots show the mixing geometry for Galveston Bay oyster tissues (red and blue filled circles), Galveston Bay bulk sediments (open gray circles) and literature Pb source endmembers (black open circles) used in MixSIAR models. Endmember error bars are standard deviations of published values. Literature data sources are Rabinowitz (2005), Millot et al. (2004), Brandon and Lambert (1993), Chow and Earl (1972).

Figure 17. Pb isotope ratios and mixing geometry of Pb sources in Galveston Bay oysters and sediments.

Table 18. MixSIAR model estimates of Pb source contributions to Galveston Bay oyster tissues.

Pb Source	Mean %	SD	2.5%	97.5%
North American coals	15.6%	0.14	0.6%	53.0%
Old US Pb smelters & refineries	4.4%	0.06	0.1%	20.0%
North & South American river suspended particulate matter	55.2%	0.23	10.7%	92.9%
Southern Canadian Cordillera granitoids	24.7%	0.19	1.4%	70.3%

Data are presented as mean percent contribution and the standard deviation (SD) of the mean percent contribution with lower (2.5%) and upper (97.5%) bounds representing 95% credible intervals.

The Pb sources and their estimated proportions in Galveston Bay oyster tissues are crustal rocks (southern Canadian Cordillera granitoids) 24.7%, suspended particulate matter in North and South American rivers 55.2%, Pb ores processed at historic U.S. smelters and refineries 4.4%, and North American coals 15.6% (Table 18), Rabinowitz, 2005 Millot et al., 2004; Brandon and Lambert, 1993; Chow and Earl, 1972). Regional and seasonal (wet/dry) differences in Pb source contributions could not be distinguished. Natural Pb sources account for about 80% of the total Pb in the oyster samples and anthropogenic sources account for the remaining 20%. This finding highlights the presence of anthropogenic Pb in Galveston Bay oysters, which has implications for larger ecological food chain within Galveston Bay as Pb, and other heavy metals, bioaccumulate and biomagnify between trophic levels (Tchounwou et al., 2012; Wright and Welbourn, 2002).

The Pb sources identified in Galveston Bay oysters using Pb isotope data agrees with the Galveston Bay sediment Pb source tracing. The MixSIAR modeling indicates that southern Canadian Cordillera granitoids, North American coals, and old U.S. Pb ore smelters and refineries are endmember Pb sources in both the Galveston Bay sediments and oyster tissues (Fig. 17). Anthropogenic sources supply approximately 83.8% and 25.5% of Pb to the Galveston Bay sediment leachates and bulk sediments, respectively. In contrast, natural sources account for 16.2% of the total Pb in the sediment leachates and 74.5% of the total Pb in the bulk sediments. The overall oyster Pb source modeling agrees with the bulk sediment Pb source modeling, with natural sources contributing an estimated 80% of the total Pb in Galveston Bay oysters.

The overlapping Pb isotope ratios of the Galveston Bay sediments and oysters in addition to the MixSIAR modeling results indicate that particulate metals are likely a pathway of metal uptake for Galveston Bay oysters. Measuring the Pb isotope ratios of the Galveston Bay water samples could further elucidate the relative importance of dissolved versus particulate (sedimentary) metals for oysters in Galveston Bay.

Galveston Bay water Pb isotope ratios significantly different from those of Galveston Bay sediments and oysters would imply that waters do not supply the majority of metals to Galveston Bay oysters. However, Galveston Bay water Pb isotope ratios that overlap with the Pb isotope compositions of Galveston Bay sediments and oysters may not be sufficient for assessing the roles of dissolved and particulate metals as sources of metals in Galveston Bay oyster tissues, given the large range of biotic and spatiotemporal physical effects related to natural metal distributions in oysters, sediments, and aqueous environmental samples.

Discussion

Summary

The watershed of Galveston Bay encapsulates some of the highest density of petrochemical facilities in the US. This study investigates heavy metal cycling in Galveston Bay sediments and oysters. The results of this study offer a detailed assessment of Galveston Bay heavy metal geochemistry and provide new insight into heavy metal sources, fluxes, and toxicity in this anthropogenic estuary. Additionally, this study offers the first Pb isotope dataset for Galveston Bay and serves as a testbed for future work in this region.

Galveston Bay sediments are potentially toxic for Cd, Cu, Ni, and Zn based on TCEQ and NOAA toxicity thresholds. Areas east of the HSC (Trinity Bay and near the entrance of East Bay) have higher metal concentrations than areas to the west of the HSC. The elevated metal contents in eastern Galveston Bay are driven by high flocculation of dissolved metals in low salinity regions. Thus, riverine discharge largely influences Galveston Bay sediment metal concentration variation over time. Metal concentrations are highest during periods of elevated river discharge and subsequent flocculation of dissolved metal loads to bay sediments. Despite low Pb concentrations, Pb isotope ratios reveal that a large percentage of Pb in Galveston Bay is anthropogenic in origin. The HH-CH_3COOH sediment leaching procedure used here shows distinct Pb isotopic differences between sediment leachates and residues, which are used to assess anthropogenic and natural Pb sources in Galveston Bay sediments. The Pb isotope modeling demonstrates that sediment leachates are dominated by anthropogenic Pb (i.e., U.S. Pb ores, North American coals) while the sediment residues and bulk sediments are dominated by natural Pb inputs (i.e., continental weathering of crustal rocks in North America).

Salinity is the primary spatiotemporal control on water (dissolved fraction) heavy metal concentrations. Dissolved heavy metal loads are higher in low salinity regions. Conversely, dissolved heavy metal loads are lower in high salinity regions. Dissolved heavy metal concentrations in Galveston Bay waters are influenced by riverine discharge over time. Higher dissolved metal concentrations exist during wet periods (Trinity River discharge >250 m^3/s) and lower dissolved metal concentrations exist during dry periods (Trinity River discharge <250 m^3/s). Cadmium displays the inverse trend as it readily forms chloride complexes, which can result in higher dissolved Cd concentrations with increasing salinity (Wen et al., 1999). Thus, dissolved Cd concentrations tend to be higher in high salinity areas and during dry conditions when bay-wide salinities are generally higher.

The oysters from Lower Galveston Bay and Trinity Bay have lower heavy metal concentrations than oysters in Upper Galveston Bay near the San Jacinto River, East Bay, and West Bay. Anthropogenic metal inputs likely influence the oyster metal loadings in these regions shaping the geographic distribution of oyster tissue metal contents observed. As with the sediments in Galveston Bay, oyster tissue metal concentrations vary in response to riverine inflow to Galveston Bay over time such that wet condition oyster tissues have higher Cd, Pb and Zn concentrations than dry condition oyster tissues. Galveston Bay oysters are likely toxic to humans for Cd and Zn and to a lesser extent Pb based on federal and state screening values. Lead isotope modeling results indicate that about 50% of the Pb in Galveston Bay oyster tissues is naturally derived and about 50% is anthropogenically derived.

Collectively, this report provides a comprehensive understanding of heavy metal contaminant cycling in Galveston Bay. These data clearly demonstrate that Galveston Bay sediment and water heavy metal concentrations are shaped by riverine input and flocculation dynamics rather than anthropogenic activities. Deeper study of oyster tissue metal contents including biotic and abiotic factors (i.e., age, sex, water temperature, turbidity) is needed to characterize the spatiotemporal controls on oyster tissue heavy metal concentrations in Galveston Bay. Lead isotope tracing reinforces the presence of gasoline-derived and industrial ore-derived Pb in Galveston Bay and identifies coal as another anthropogenic metal contaminants source in the bay. Sediments may supply Zn to oysters based on linear correlations between Galveston Bay sediment and oyster tissue metal concentrations. Moreover, Galveston Bay sediment and oyster tissue Pb isotope compositions largely overlap demonstrating that oysters can incorporate metals from ambient sediments. No correlation between water (dissolved fraction) heavy metal contents and oyster tissue heavy metal contents was observed. Future work using oyster tissue, filtered water and sediment samples collected from the same location and time over multiple sampling events is needed to allow direct spatial and temporal comparison of metal contents between the oysters, waters, and sediments, which would yield a more robust understanding of Galveston Bay oyster tissue metal exchange with ambient waters and sediments. This study highlights the importance of estuaries in regulating heavy metal exchange between terrestrial and marine environments and serves as a testbed for future heavy metal contaminant studies in estuarine systems worldwide as well as a resource for ongoing contaminant reduction, remediation, and mitigation efforts in Galveston Bay.

References

Al Mukaimi M.E., Kaiser K., Williams J.R., Dellapenna T.M., Louchouarn P., and Santschi P.H. (2018) Centennial record of anthropogenic impacts in Galveston Bay: evidence from trace metals (Hg, Pb, Ni, Zn) and lignin oxidation products Environmental Pollution 237:887-899.

Alfonso J.A., Handt H., Mora A., Vasquez Y., Azocar J., and Marcano E. (2013) Temporal distribution of heavy metal concentrations in oysters Crassostrea rhizophorae from the central Venezuelan coast Marine Pollution Bulletin 73(1):394:398.

Alyazichi, Y.M., Jones, B. G., and McLean, E. (2016) Lead isotope Fingerprinting used as a tracer of lead pollution in marine sediments from Botany Bay and Port Hacking estuaries, southern Sydney, Australia *Regional Studies in Marine Science* 7:136-141.

Amiard-Triquet C., Berthet B., Metayer C., and Amiard J.C. (1986) Contribution to the ecotoxicological study of cadmium, copper and zinc in the mussel Mytilus edulis *Marine Biology* 92:7-13.

Apeti D.A., Johnson E., and Robinson L. (2005a) A model for bioaccumulation of metals in Crassostrea virginica from Apalachicola Bay, Florida *American Journal of Environmental Sciences* 1(3):239-248.

Apeti D.A., Robinson L., and Johnson E. (2005b) Relationship between heavy metal concentrations in American oyster (Crassostrea virginica) and metal levels in the water column and sediment in Apalachicola Bay, Florida *American Journal of Environmental Sciences* 1(3):179-186.

Apeti D.A., Lauenstein G.G., and Evans D.W. (2012) Recent status of total mercury and methyl mercury in the coastal waters of the northern Gulf of Mexico using oysters and sediments from NOAA’s mussel watch program *Marine Pollution Bulletin* 64:2399-2408.

Arantes F.P., Savassi L.A., Santos H.B., Gomes M.V.T., and Bazzoli N. (2016) Bioaccumulation of mercury, cadmium, zinc, chromium, and lead in muscle, liver, and spleen tissue of large commercially valuable catfish species from Brazil *Annals of the Brazilian Academy of Sciences* 88(1):137-147.

Asmerom Y. and Jacobsen S.B. (1993) The Pb isotopic evolution of the Earth: inference from river water suspended loads *Earth and Planetary Science Letters* 115:245-256.

Basak C., Marin E.E., and Kamenov G.D. (2011) Seawater Pb isotope extracted from Cenozoic marine sediments *Chemical Geology* 286(3-4):94-108.

Bendell L.I. and Feng C. (2009) Spatial and temporal variations in cadmium concentrations and burdens in the Pacific oyster (Crassostrea gigas) samples from the Pacific north-west *Marine Pollution Bulletin* 58:1137-1143.

Berger C. J. M., Lippiatt S.M., Lawrence M.G., and Bruland K.W. (2008) Application of a chemical leach technique for estimating labile particulate aluminum, iron, manganese in the Columbia River plume and coastal waters off Oregon and Washington *Journal of Geophysical Research* 113:1-16.

Bird G. (2011) Provenancing anthropogenic Pb within the fluvial environment: developments and challenges in the use of Pb isotopes *Environment International* 37:802-819.

Birch G.F. and Hogg T.D. (2011) Sediment quality guidelines for copper and zinc for filter-feeding estuarine oysters? *Environmental Pollution* 159:108-115.

Boening D.W. (1999) An evaluation of bivalves as biomonitors of heavy metals pollution in marine waters *Environmental Monitoring and Assessment* 55:459-470.

Bollhofer A. and Rosman K.J.R. (2001) Isotopic source signatures for atmospheric lead: The Northern Hemisphere *Geochimica et Cosmochimica Acta* 65(11):1727-1740.

Boyden C.R. and Phillips D.J.H. (1981) Seasonal variation and inherent variability of trace elements in oysters and their implications for indicator studies *Marine Ecological Programme Service* 5:29-40.

Brandon A.D. and Lambert R.S. (1993) Crustal melting in the Cordilleran Interior: The mid-cretaceous White Creek batholith in the Southern Canadian Cordillera *Journal of Petrology* 35:239-269.

Brandon A.D. and Smith A.D. (1994) Mesozoic granitoid magmatism in southeast British Columbia: implications for the origin of granitoid belts in the North American Cordillera *Journal of Geophysical Research* 99(B6):11879-11896.

Buchman M.F. (2008) National Oceanic and Atmospheric Administration Screening Quick Reference Tables, Report 08-1, Office of Response and Restoration National Oceanic and Atmospheric Administration Seattle, WA. 34 pp.

Chen M., Boyle E.A., Lee J-M., Nurhati I., Zurbrick C., Switzer A.D., and Carrasco G. (2016) Lead isotope exchange between dissolved and fluvial particulate matter: a laboratory study from the Johor River Estuary *Philosophical Transactions of the Royal Society A Mathematical, Physical and Engineering Sciences* 374:20160054.

Chen B., Liu J., Hu L., Liu M., Wang L., Zhang X., and Fan D. (2017) Spatio-temporal distribution and sources of Pb identified by stable isotopic ratios in sediments from Yangtze River Estuary and adjacent areas *Science of the Total Environment* 580:936-945.

Chester R. and Hughes M.J. (1967) A chemical technique for the separation of ferro-manganese minerals, carbonate minerals and adsorbed trace elements from pelagic sediments *Chemical Geology* 2:249-262.

Chow T. J. and Earl J.T. (1972) Lead isotope in North American coals *Science* 176(4034):510-511.

Conway T.M., Rosenberg A.D., Adkins J.F., and John S.G. (2013) A new method for precise determination of iron, zinc and cadmium stable isotope ratios in seawater by double-spike mass spectrometry *Analytica Chimica Acta* 793:44-52.

Cowles M.K. and Carlin, B.P. (1996) Markov Chain Monte Carlo convergence diagnostics: a comparative review *Journal of the American Statistical Association* 91:883-904.

Cundy A.B. and Croudace I.W. (2017) The fate of contaminants and stable Pb isotopes in a changing estuarine environment: 20 years on *Environmental Science and Technology* 51:9488-9497.

de Freitas Rebelo, M., do Amaral M.C.R., and Pfeiffer W.C. (2003) High Zn and Cd accumulation in the oyster Crassostrea rhizophorae, and its relevance as a sentinel species *Marine Pollution Bulletin* 46(10):1354-1358.

Dellapenna T.M., Hoelscher C.E., Hill L., Critides L., Bartlett V., Bell M., Al Mukaimi M.E., Du J., Park K., and Knap A. (2021) Hurricane Harvey delivered a massive load of mercury rich sediment to Galveston Bay, Texas, USA *Science of the Total Environment* Under Review.

Doe B.R. (1970) *Lead Isotopes* Springer-Verlag, Berlin Heidelberg. 138 pp.

Dorado S., Booe T., Steichen J., McInnes A.S., Windham R., Shepard A., Lucchese A.E.B., Preischel H., Pinckney J.L., Davis S.E., Roelke D.L. and Quigg A. (2015) Towards an understanding of the interactions between freshwater inflows and phytoplankton communities in a subtropical estuary in the Gulf of Mexico *PLoS ONE* 10(7): e0130931.

Du J., Park K., Dellapenna T.M., and Clay J.M. (2019a) Dramatic hydrodynamic and sedimentary responses in Galveston Bay and adjacent inner shelf to Hurricane Harvey *Science of the Total Environment* 653:554–564.

Du J., Park K., Dellapenna T.M., and Clay J.M. (2019b) Corrigendum to "Dramatic hydrodynamic and sedimentary responses in Galveston Bay and adjacent inner shelf to Hurricane Harvey" [Science of the Total Environment 653 (2019), 554–564] *Science of the Total Environment* 697: 134219.

Ewing S.A., Christensen J.N., Brown S.T., Vancuren R.A., Cliff S.S., and Depaolo D.J. (2010) Pb isotope as an indicator of the Asian contribution of particulate air pollution in urban California *Environmental Science and Technology* 44:8911-8916.

Flegal A.R. and Smith D.R. (1995) Measurements of environmental lead contamination and human exposure *Reviews of Environmental Contamination and Toxicology* 143:1-45.

Fitzsimmons J.N. and Boyle E.A. (2014) Assessment and comparison of Anopre and cross flow filtration methods for the determination of dissolved iron size fractionation into soluble and colloidal phases in seawater *Limnology and Oceanography: Methods* 12:244-261.

"Galveston Bay Report Card 2017" (2017) Houston Advanced Research Center and Galveston Bay Foundation. https://www.galvbaygrade.org/wpcontent/uploads/2017/08/ 2017_Galveston_Bay_Full_Report.pdf.

Galveston Bay Estuary Program "Oyster reefs in Galveston Bay" *Galveston Bay Status and Trends* Accessed January 6, 2021. www.galvbaydata.org/www.galvbaydata.org/Habitat/OysterReefs/tabid/836/Default.html

Garcon M., Chauvel C. France-Lanlord C., Limonta M., and Garzanti E. (2016) Removing the "heavy mineral effect" to obtain a new Pb isotope value for the upper crust *Geochemistry Geophysics Geosystems* 14(9):3324-3333.

Gaur A.S. and Gaur S.S. (2006) *Statistical methods for practice and research: A guide to data analysis using SPSS* Sage Publications. 172 pp.

Gelman A., Carlin J.B., Stern H.S., Dunson D.B., Vehtari A., and Rubin D.B. (2013) *Bayesian data analysis* Chapman and Hall/CRC. 675 pp.

Graney J.R., Halliday A.N., Keeler G.J., Nriagu J.O., Robbins J.A., and Norton S.A. (1995) Isotopic record of lead pollution in lake sediment from the northeastern United States *Geochimica et Cosmochimica Acta* 59(9):1715-1728.

Griscom S.B. and Fisher N.S. (2004) Bioavailability of sediment-bound metals to marine bivalve molluscs: An overview *Estuaries* 27(5):826-838.

Gomez-Caminero A., Howe P., Hughes M., Kenyon E., Lewis D.R., Moore M., Ng L., Aitio A., and Becking G. (2001) *Arsenic and arsenic compounds.* Geneva: World Health Organization

Guthrie C.G., Matsumoto J., and Solis R.S. (2012) Analysis of the Influence of Water Plan Strategies on Inflows and Salinity in Galveston Bay. Final report to the United States Army Corps of Engineers, Contract #R0100010015. Texas Water Development Board, Austin, TX.

Gutjahr M., Frank M., Stirling C.H., Klemm V., Ven de Flierdt T., and Halliday A.N. (2007) Reliable extraction of a deepwater trace metal isotope signal from Fe-Mn oxyhydroxide coatings of marine sediments *Chemical Geology* 242:351-370.

Hamelin B., Grousset F., and Sholkovitz E.R. (1990) Pb isotopes in surficial pelagic sediments from the North Atlantic *Geochimica et Cosmochimica Acta* 54:37-47.

Hansmann W. and Koppel V. (2000) Lead-isotopes as tracers of pollutants in soils *Chemical Geology* 171:123-144.

Harmon M., Pait A.S., and Hameedi M.J., (2003) Sediment Contamination, Toxicity, and Macroinvertebrate Infaunal Community in Galveston Bay. NOAA Technical Memorandum NOS NCCOS CCMA 122. Silver Spring, MD: NOAA, NOS, Center for Coastal Monitoring and Assessment.

Hem J.D. (1976) Geochemical controls on lead concentrations in stream water and sediments *Geochimica et Cosmochimica Acta* 40:599-609.

Herut B. and Sandler A. (2006) Normalization methods for pollutants in marine sediments: review and recommendations for the Mediterranean. Israel Oceanographic and Limnological Research Geological Survey of Israel IOLR Rep H 18.

Hieke A-S. C., Brinkmeyer R., Yeager K.M., Schindler K., Zhnag S., Xu C., Louchouarn P., and Santschi P.H. (2016) Widespread distribution of Dehalococcoides mccartyi in the Houston Ship Channel and Galveston Bay, Texas, sediments and the potential for reductive dechlorination of PCDD/F in an estuarine environment *Marine Biotechnology* 18: 630-644.

Honeyman B. and Santschi P.H. (1988) Metals in aquatic systems *Environmental Science and Technology* 22(8):862-871.

Horowitz A.J. (1985) *A primer on trace metal sediment-chemistry* United States Geological Survey Water-Supply Paper 2277.

Ip C.C.M., Li X-D., Zhang G., Wai O.W.H., and Li Y-S. (2007) Trace metal distribution in sediments of the Pearl River Estuary and the surrounding coastal area, South China *Environmental Pollution* 147:311-323.

James E.W. and Henry C.D. (1993a) Southeastern extent of the North American craton in Texas and northern Chihuahua as revealed by Pb isotopes *Geological Society of America Bulletin* 105:116-126.

Jensen L.T., Wyatt N.J., Landing W.M., and Fitzsimmons J.N. (2020) Assessment of the stability, sorption, and exchangeability of marine dissolved and colloidal metals *Marine Chemistry* 220:103754.

Jensen L.T., Wyatt N.J., Twining B.S., Rauschenberg S., Landing W.M., Sherrell R.M., and Fitzsimmons J.N. (2019) Biogeochemical cycling of dissolved zinc in the Western Arctic (Arctic GEOTRACES GN01) *Global Biogeochemical Cycles* 33:343-369.

Jiann K-T. and Presley B.J. (1997) Variations from trace metal concentrations in American oysters (Crassostrea virginica) collected from Galveston Bay, Texas *Estuaries* 20(4):710-724.

Johnson K.S., Boyle E.A., Bruland K.W., Coale K., Measures C., Moffett J., et al. (2007) Developing standards for dissolved iron in seawater *EOS Transactions America Geophysical Union* 88:131-132.

Joiris C.R., Azokwu M.I., Otchere F.A., and Ali I.B. (1998) Mercury in the bivalve Anadara (Senilia) senilis from Ghana and Nigeria *Science of the Total Environment* 224:181-188.

Kesler S.E., Appold M.S., Cummin G.L., and Krstic D. (1994) Lead isotope geochemistry of the Mississippi Valley-Type mineralization in the Central Applications *Economic Geology* 89:1492-1500.

Komarek M., Ettler V., Chrastny V., and Mihaljevic M. (2008) Lead isotopes in environmental sciences: a review *Environmental International* 34:562-577.

Koschinsky A. and Hein J.R. (2003) Uptake of elements from seawater by ferromanganese crusts: solid-phase associations and seawater speciation *Marine Geology* 198:331-351.

Kryc K.A., Murray R.W., and Murray D.W. (2003) Elemental fractionation of Si, Al, Ti, Fe, Ca, Mn, P, and Ba in five marine sedimentary reference materials: results from sequential extractions *Analytica Chimica Acta* 487(1):117-128.

Kusin F.M., Azani N.N.M., Hasan S.N.M.S., and Sulong N.A. (2018) Distribution of heavy metals and metalloid in surface sediments of heavily-mined area for bauxite ore in Pengerang, Malaysia and associated risk assessment *Catena* 165:454-464.

Lagerström M.E., Field M.P., Seguret M., Fischer L., Hann S., and Sherrell R.M. (2013) Automated on-line flow-injection ICP-MS determination of trace metals (Mn, Fe, Co, Ni, Cu and Zn) in open ocean seawater: application to the GEOTRACES program *Marine Chemistry* 155:71-80.

Lam P.J., Twining B.S., Jeandel C., Roychoudhury A., Resing J.A., Santschi P.H., and Anderson R.F. (2015) Methods from analyzing the concentration and speciation of major and trace elements in marine particles *Progress in Oceanography* 133:32-42.

Landmeyer J.E., Bradley P.M., and Bullen T.D. (2003) Stable lead isotopes reveal a natural source of high lead concentrations to gasoline-contaminated groundwater *Environmental Geology* 45:12-22.

Lester J. and Gonzalez L. (2011) The State of the Bay: A Characterization of the Galveston Bay Ecosystem. Third Edition. Texas Commission on Environmental Quality, Galveston Bay Estuary Program, Houston, Texas.

Lewis E.L. and Perkin R.G. (1981) The practical salinity scale 1978: conversion of existing data *Deep Sea Research Part A. Oceanographic Research Papers* 28(4):307-328.

Longman J., Veres D., Ersek V., Phillips D.L., Chauvel C., and Tamas C.G. (2018) Quantitative assessment of Pb sources in isotopic mixtures using a Bayesian mixing model *Scientific Reports* 8:6154 DOI:10.1038/s41598-018-24474-0.

Lopez A.M., Brandon A.D., Ramos F.C., Fitzsimmons J.N., Dellapenna T.M., and Adams H.A. (2021) Lead geochemistry of Galveston Bay, Texas sediments *Environmental Advances* 4: 100057.

Marcantonio F., Flowers G.C., and Templin N. (2000) Lead contamination in a wetland watershed: isotopes as fingerprints of pollution *Environmental Geology* 39:1070-1076.

Marcantonio F., Zimmerman A., Xu Y., and Canuel E. (2002) A Pb isotope record of mid-Atlantic U.S. atmospheric Pb emission in Chesapeake Bay sediments *Marine Chemistry* 77:123-132.

Millot R., Allegre C-J., Gaillardet J., and Roy S. (2004) Lead isotope systematics of major river sediments: a new estimate of the Pb isotope composition of the upper continental crust *Chemical Geology* 203:75-90.

Morse J.W., Presley B.J., and Taylor R.J. (1993) Trace metal chemistry of Galveston Bay: water, sediments, and biota *Marine Environmental Research* 36:1-37.

Muir, D., Wang X., Bright D., Lockhart L., and Kock G. (2005) Spatial and temporal trends of mercury and other metals in landlocked char from lakes in the Canadian Arctic archipelago *Science of the Total Environment* 351–352:464-478.

Murphy C.A., Rose K.A., del Carmen Alvarez M., and Fuiman L.A. (2008) Modeling larval fish behavior: scaling the sublethal effects of methylmercury to population-relevant endpoints *Aquatic Toxicology* 86:470-484.

Nielsen F. (2016) *Introduction to HPC with MPI for Data Science* Springer International Publishing. 282 pp.

Nirel P.M.V. and Morel F.M.M. (1990) Pitfalls of sequential extractions *Water Research* 8:1055-1056.

O'Nions R.K., Frank M., von Blanckenburg F., and Ling H.F. (1998) Secular variation of Nd and Pb isotopes in ferromanganese crusts from the Atlantic, Indian and Pacific Oceans *Earth and Planetary Science Letters* 155:15-28.

Ohnemus D.C. and Lam P.J. (2015) Cycling of lithogenic marine particles in the U.S. GEOTRACES North Atlantic transect *Deep-Sea Research II* 116:283-302.

Otchere F.A. (2019) A 50-year review on heavy metal pollution in the environment: bivalves as bio-monitors *African Journal of Environmental Science and Technology* 13(6):220-227.

Park J. and Presley B.J. (1997) Trace metal contamination of sediments and organisms from the Swan Lake area of Galveston Bay *Environmental Pollution* 98(2):209-221.

Pekowski A.D. (2017) Elevated modern sedimentation rates over the buried Trinity River incised valley suggests elevated, localized subsidence rates, Galveston Bay, TX, USA, Department of Oceanography, Texas A&M University, Master's thesis.

Phillips D.J.H. and Yim W.W.S. (1981) A comparative evaluation of oysters, mussels and sediments as indicators of trace metals in Hong Kong waters *Marine Ecology* 6:285-293.

Piper D.Z. and Wandless G.A. (1992) Hydroxylamine hydrochloride – acetic acid-soluble and -insoluble fractions of pelagic sediment: readsorption revisited *Environmental Science and Technology* 26:2489-2493.

Plum L.M., Rink L., and Haase H. (2010) The essential toxin: impact of zinc on human health *International Journal of Environmental Research and Public Health* 7(4):1342-1365.

Potra A., Ruhl L.S., and Samuelsen J.R. (2018) Legacy lead from past mining activity and gasoline additives: evidence from lead isotopes and trace element geochemical studies in the White River Basin, southern Ozark region, USA *Geosciences* 8(189):1-17.

Presley B.J., Taylor R.J., and Booth P.N. (1990) Trace metals in Gulf of Mexico oysters *Science of the Total Environment* 97-98:551-593.

Rabinowitz M.B. (2005) Lead isotopes in soils near five historic American lead smelters and refineries *Science of the Total Environment* 346:138-148.

Rahimzadeh M.R., Rahimzadeh M.R., Kazemi S., and Moghadamnia A-A. (2017) Cadmium toxicity and treatment: an update *Caspian Journal of Internal Medicine* 8(3):135-145.

Rauch J.N. and Pacyna J.M. (2009) Earth's global Ag, Al, Cr, Cu, Fe, Ni, Pb, and Zn cycles *Global Biogeochemical Cycles* 23:1-16.

Riedel G.F., Abbe G.R., and Sanders J.G. (1995) Silver and copper accumulation in two estuarine bivalves, the eastern Oyster (Crassostrea virginica) and the hooked mussel (Ischadium recurvum), in the Patuxent River Estuary, Maryland *Estuaries* 18:445-455.

Ropicki A., Dudensing R., and Hanselka D. (2018a) Economic contributions of the Texas oyster fishery *Texas A&M University Texas Sea Grant publication 502 (TAMU-SG-18-502).*

Ropicki A., Dudensing R., Hanselka D., Massey J., and O'Connell J. (2018b) Economic contributions of the Galveston Bay oyster fishery *Texas A&M University Texas Sea Grant publication 503 (TAMU-SG-18-503).*

Ross A. and Willson V.L. (2017) B*asic and advanced statistical tests: Writing results sections and creating tables and figures* Springer.

Sajwan K.S., Kumar K.S., Paramasivam S., Compton S.S., and Richardson J.P. (2008) Elemental status in sediment and American Oyster collected from savannah marsh/estuarine ecosystem: a preliminary assessment *Archives of Environmental Contamination and Toxicology* 54:245-258.

Saleh M.A. and Wilson B.L. (1999) Analysis of metal pollutants in the Houston Ship Channel by inductively coupled plasma/mass spectrometry *Ecotoxicology and Environmental Safety* 44: 113-117.

Sanders J.G., Riedel G.F., and Abbe G.R. (1991) Factors controlling the spatial and temporal variability of trace metal concentrations in Crassostrea virginica (Gmelin) In *Estuaries and Coasts: Spatial and Temporal Intercomparisons* Olson and Olson, Incorporated. pp. 335-339.

Sangster D.F., Outridge P.M., and Davis W.J. (2000) Stable lead isotope characteristics of lead ore deposits of environmental significance *Environmental Reviews* 8(2):115-147.

Santschi P.H., Presley B.J., Wade T.L., Garcia-Romero B., and Baskaran M. (2001) Historical contamination of PAHs, PCBs, DDTs, and heavy metals in Mississippi River Delta, Galveston Bay and Tamps Bay sediment cores *Marine Environmental Research* 52:51-79.

Sharma V.K., Rhudy K.B., Koenig R., Baggett A.T., Hollyfield S., and Vazquez F.G. (1999) Metals in sediments of Texas estuaries, USA *Journal of Environmental Science and Health Part A* 34(10):2061-2073*.*

Shiel A.E., Weis D., and Orians K.J. (2012) Tracing cadmium, zinc and lead sources in bivalves from the coast of western Canada and the USA using isotopes *Geochimica et Cosmochimica Acta* 76:175-190.

Sholkovitz E.R. (1989) Artifacts associated with the chemical leaching of sediments for rare-earth elements *Chemical Geology* 77:47-51.

Shulkin V.M., Presley B.J., and Kavun V.Ia. (2003) Metal concentrations in mussel Crenomytilus grayanus and oyster Crassostrea gigas in relation to contamination of ambient sediments *Environment International* 29:493-502.

Sohrin Y., Urushihara S., Nakatsuka S., Kono T., Higo E., Minami T., Norisuye K., and Umetani S. (2008) Multielemental determination of GEOTRACES key trace metals in seawater by ICPMS after preconcentration using an ethyldiaminetriacetic acid chelating resin *Analytical Chemistry* 80:6267-6273.

Steichen J.L., Labonté J.M., Windham R., Hala D., Kaiser K., Setta S., Faulkner P.C., Bacosa H., Yan G., Kamalanathan M., and Quigg A. (2020) Microbial, physical, and chemical changes in Galveston Bay following an extreme flooding event *Hurricane Harvey Frontiers in Marine Science* 7:186.

Stillwell A.S., King C.W., Webber M.E., Duncan I.J., and Hardberger A. (2011) The energy-water nexus in Texas. *Ecology and Society* 16(1):2.

Stock B.C. and Semmens B.X. (2016) MixSIAR GUI User Manual. Version 3.1. github.com/brianstock/MixSIAR/. doi:10.5281/zenodo.47719.

Stock B.C., Jackson A.L., Ward E.J., Parnell A.C., Phillips D.L, and Semmes B.X. (2018) Analyzing mixing systems using a new generation of Bayesian tracer mixing models *PeerJ* e5096: DOI 10.7717/peerj.5096.

Sun S-S. (1980) Lead isotopic study of young volcanic rocks from mid-ocean ridges, ocean islands and island arcs *Philosophical Transactions of the Royal Society of London. Series A, Mathematical and Physical Sciences* 297(1431):409-445.

Sun G-X., Wang X-J., and Hu Q-H. (2011) Using stable lead isotopes to trace heavy metal contamination sources in sediments Xiangjiang and Lishui Rivers in China *Environmental Pollution* 159:3406-3410.

Sverjensky D.A. (1981) The origin of a Mississippi Valley-Type deposit in the Viburnum Trend, southeast Missouri *Economic Geology* 76:1848-1872.

Tang D., Warnken K.W., and Santschi P.H. (2002) Distribution and partitioning of trace metals (Cd, Cu, Ni, Pb, Zn) in Galveston Bay waters *Marine Chemistry* 78:29-45.

Tchounwou P.B., Yedjou C.G., Patlolla A.K., and Sutton D.J. (2012) Heavy metals toxicity and the environment *Molecular Clinical Environmental Toxicology* 101:133-164.

Tessier A., Campbell P.G.C., and Bisson M. (1979) Sequential extraction procedure for the speciation of particulate trace metals *Analytical Chemistry* 51(7): 844-851.

Texas Commission on Environmental Quality Texas Risk Reduction Program. Austin, TX. www.tceq.texas.gov/remediation/trrp.

Texas Commission on Environmental Quality Surface Water Quality Monitoring Program. 2020. Austin, TX. Data provided by Houston Advanced Research Center.

Texas Department of State Health Services (2019) “Seafood evaluation in a portion of Upper Galveston Bay” Seafood and Aquatic Life Unit, Policy, Standards, and Quality Assurance Unit. Division for Regulatory Services. Austin, TX.

Texas Department of State Health Services (2012) “Public Health Assessment San Jacinto River Waste Pits Channelview, Harris County, Texas” Environmental and Injury Epidemiology and Toxicology Branch. Austin, TX.

Texas Department of State Health Services (2007) “Characterization of potential adverse health effects associated with consuming fish from the Donna Irrigation System Hidalgo County, TX” Seafood and Aquatic Life Group, Policy, Standards, and Quality Assurance Unit. Division for Regulatory Services and the Environmental and Injury Epidemiology and Toxicology Branch. Austin, TX.

“Texas State Energy Profile Overview” U.S. Energy Information Administration Independent Statistics and Analysis. www.eia.gov/state/?sid=TX.

Turner A. and Millward G.E. (2002) Suspended particles: their role in estuarine biogeochemical cycles *Estuarine, Coastal and Shelf Science* 55:857-883.

United States Environmental Protection Agency (2010) “Guidance for implementing the January 2001 methylmercury water quality criterion EPA-823-R-10-001” Office of Science and Technology. Washington, DC.

United States Environmental Protection Agency (1997) “Mercury Study Report to Congress. Vol. II: An Inventory of Anthropogenic Mercury Emissions in the United States EPA-452/R-97-004” Office of Air Quality Planning and Standards and Office of Research and Development. Washington, DC.

United States Geological Survey Water Data for the Nation online data repository. Accessible at www.waterdata.usgs.gov/nwis.

United States Geological Survey (1997) “Mercury contamination of aquatic ecosystems.” Retrieved from www.wi.water.usgs.gov/pubs/FS-216-95.

Upadhayhay H.R., Bode S., Griepentrog M., Huygens D., Bajracharya R.M., Blake W.H., Dercon G., Mabit L., Gibbs M., Semmens B.X., Stock B.C., Cornelis W., and Boeckx P. (2017) Methodological perspectives on the application of compound-specific stable isotope fingerprinting for sediment source apportionment *Journal of Soils and Sediments* 17:1537-1553.

Vazquez-Sauceda M.D.L.L., Aguirre-Guzman G., Sanchez-Martinez J.G., and Perez-Castaneda R. (2011) Cadmium, lead and zinc concentration in water, sediments and oyster (Crassostrea virginica) of San Andres Lagoon, Mexico *Bulletin of Environmental Contamination and Toxicology* 86:410-414.

Wen L-S., Santschi P., Gill G., and Paternostro C. (1999) Estuarine trace metal distributions in Galveston Bay: importance of colloidal forms in the speciation of the dissolved phase *Marine Chemistry* 63:185-212.

Wen L-S., Warnken K.W., and Santschi P.H. (2008) The role of organic carbon, iron, and aluminum oxyhydroxides as trace metal carriers: comparison between the Trinity River and the Trinity River Estuary (Galveston Bay, Texas) *Marine Chemistry* 112:20-37.

Weng N. and Wang W-X. (2015) Reproductive responses and detoxification of estuarine oyster Crassostrea hongkongensis under metal stress: a season study *Environmental Science and Technology* 49:3119-3127.

White W.M. (2015) *Isotope Geochemistry* Wiley-Blackwell. 496 pp.

Widory D., Liu X., and Dong S. (2010) Isotopes as tracers of lead and strontium in aerosols (TSP and $PM_{2.5}$) in Beijing *Atmospheric Environment* 44:3679-3687.

Wilson D.J., Piotrowski A.M. Galy A., and Clegg J.A. (2013) Reactivity of neodymium carriers in deep sea sediments: implications for boundary exchange and paleoceanography *Geochimica et Cosmochimica Acta* 109:197-221.

Wolff J.A. and Ramos F.C. (2003) Pb isotope variations among Bandelier Tuff feldspars: no evidence for a long-lived silicic magma chamber *Geology* 31(6):533-536.

Wright D.A., Mihursky J.A., and Phelps H.L. (1985) Trace metals in Chesapeake Bay oysters: intra-sample variability and its implications for biomonitoring *Marine Environmental Research* 16:181-197.

Wright D.A. and Welbourn P. (2002) *Environmental toxicology* Cambridge University Press. 658 pp.

Wu J. and Boyle E.A. (1997) Lead in the western North Atlantic Ocean: completed response to leaded gasoline phaseout *Geochimica et Cosmochimica Acta* 61(15):3279-3283.

Zartman R.E. and Haines S.M (1988) The plumbotectonic model for Pb isotopic systematics among major terrestrial reservoirs - a case for bi-directional transport *Geochimica et Cosmochimica Acta* 52:1327-1339.

Zhang W., Feng H., Chang J., Qu J., and Yu L. (2008) Lead (Pb) isotopes as a tracer of Pb origin in Yangtze River intertidal zone *Chemical Geology* 257:257-263.

Zhu X.K., O'Nions R.K., Guo Y., and Reynolds B.C. (2000) Secular variation of iron isotopes in North Atlantic deep water *Science* 287:2000-2002.

Zhu L., Tang J., Lee B., Zhang Y., and Zhang F. (2010) Lead concentrations and isotopes in aerosols from Xiamen, China *Marine Pollution Bulletin* 60:1946-1955.